Mining Cancer Cell Lines Databases: NCI-60, COSMIC, CCLE and Beyond

Aik Choon Tan, Ph.D.
Associate Professor of Bioinformatics
Division of Medical Oncology
Department of Medicine
aikchoon.tan@ucdenver.edu

10/30/2018

http://tanlab.ucdenver.edu/labHomePage/teaching/CANB7640

Outline

- Cancer Cell Lines
  - to study human cancer biology
  - preclinical model for drug discovery and development
- Cancer Cell Lines Resources
  - NCI-60
  - Catalog of Somatic Mutations in Cancer (COSMIC)
  - Cancer Cell Lines Encyclopedia (CCLE)
  - Genentech Cancer Cell Line Screening Initiative (gCSI)
- Beyond Cancer Cell Lines
  - Patient-derived tumor xenografts (PDX)
  - XactMice
  - Humanized Mice

HeLa

- First cancer cell lines
- Derived from cervical cancer patient (Henrietta Lacks) in 1951 at Johns Hopkins
- The cell line was found to be remarkably durable and prolific
  - Contamination of many other cell lines used in research

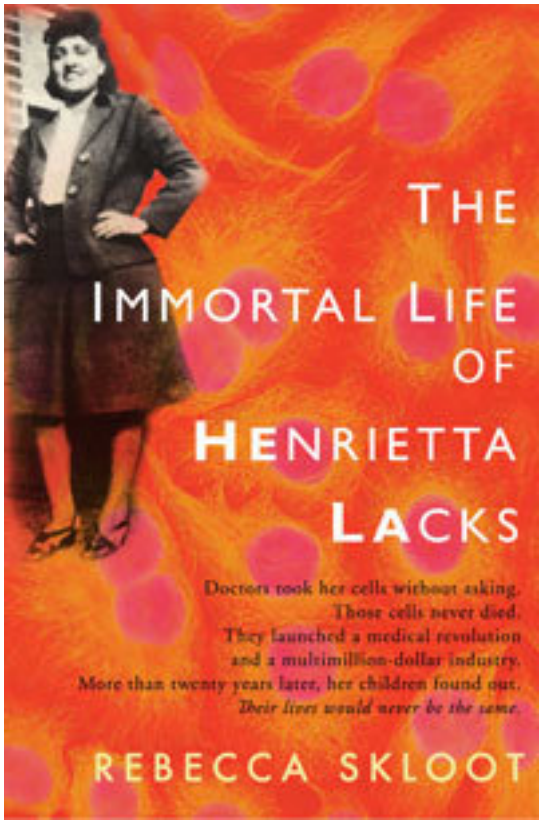

HeLa

HeLa cells were also the first human cells to be successfully cloned in 1955 by Theodore Puck and Philip I Marcus at the University of Colorado, Denver.

*A RAPID METHOD FOR VIABLE CELL TITRATION AND CLONE PRODUCTION WITH HeLa CELLS IN TISSUE CULTURE: THE USE OF X-IRRADIATED CELLS TO SUPPLY CONDITIONING FACTORS**

By Theodore T. Puck and Philip I. Marcus

DEPARTMENT OF BIOPHYSICS, FLORENCE R. SABIN LABORATORIES, UNIVERSITY OF COLORADO MEDICAL CENTER, DENVER

Communicated by O. H. Robertson, May 5, 1955

Studies of many aspects of the genetics and metabolism of animal cells are seriously handicapped by lack of a simple, effective technique for large-scale colony production from single cells. Thus it is not easily possible to develop a new population from the single-cell survivors isolated after the action of high-energy irradiation, virus invasion, or any of a variety of toxic drugs or nutritional stresses. This difficulty also makes almost impossible the preparation of mutant cell strains, a technique which has so enormously advanced studies of cell and virus genetics and biochemical transformations in microbial systems.[1] In addition, it is not possible to determine what fraction of any animal cell population is able to initiate multiplication, and therefore it becomes difficult to evaluate the mechanism of action of agents which change growth rates.

PNAS 1955 41 (7) 432-437

Cancer Cell Lines as Preclinical Models for Studying Human Cancers

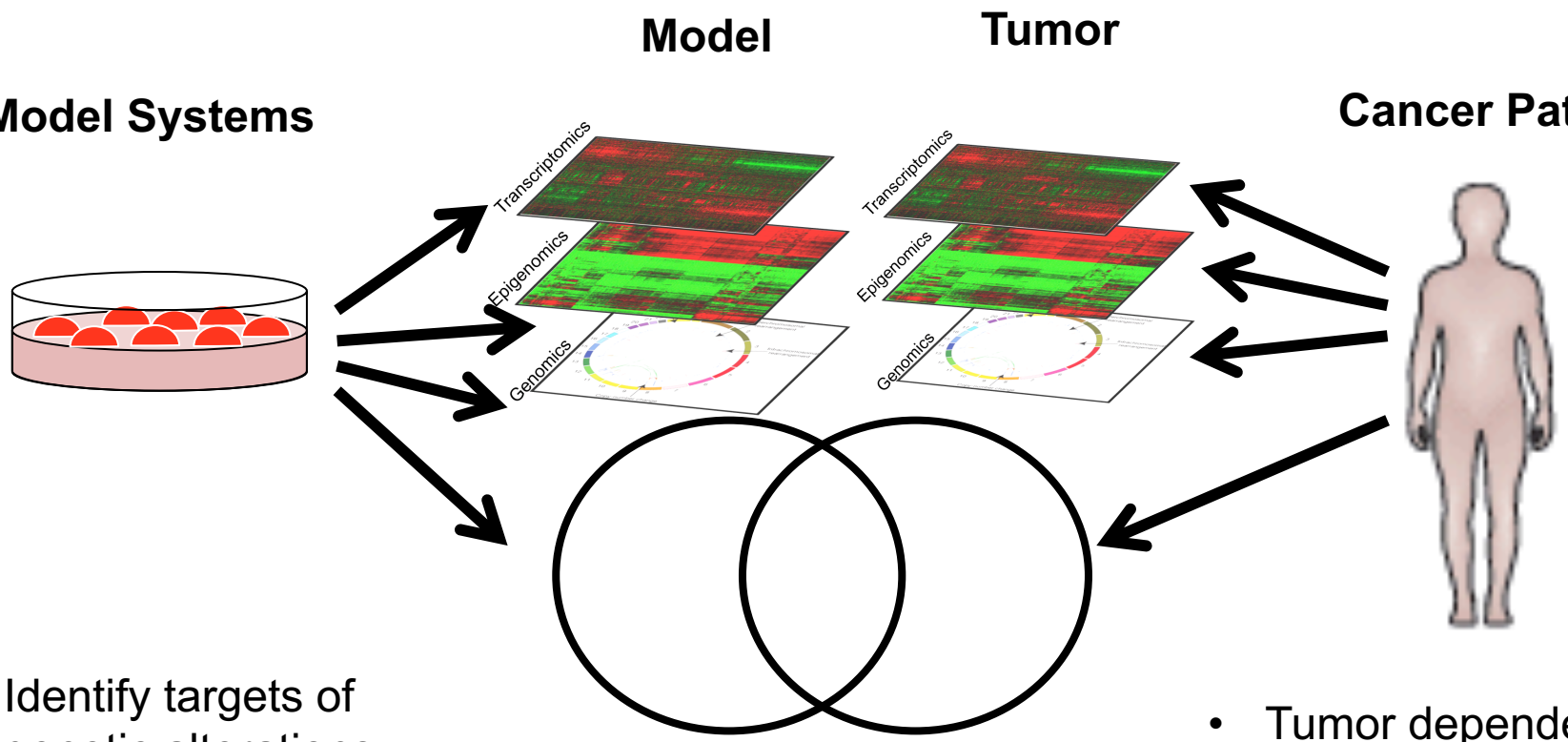

- Identify targets of genetic alterations
- Mechanistic studies
- Perturbagen data

Genetic/Molecular Information

- Tumor dependency
- Response to treatments
- Resistance mechanisms

Cancer Cell Lines Resources for Drug Development

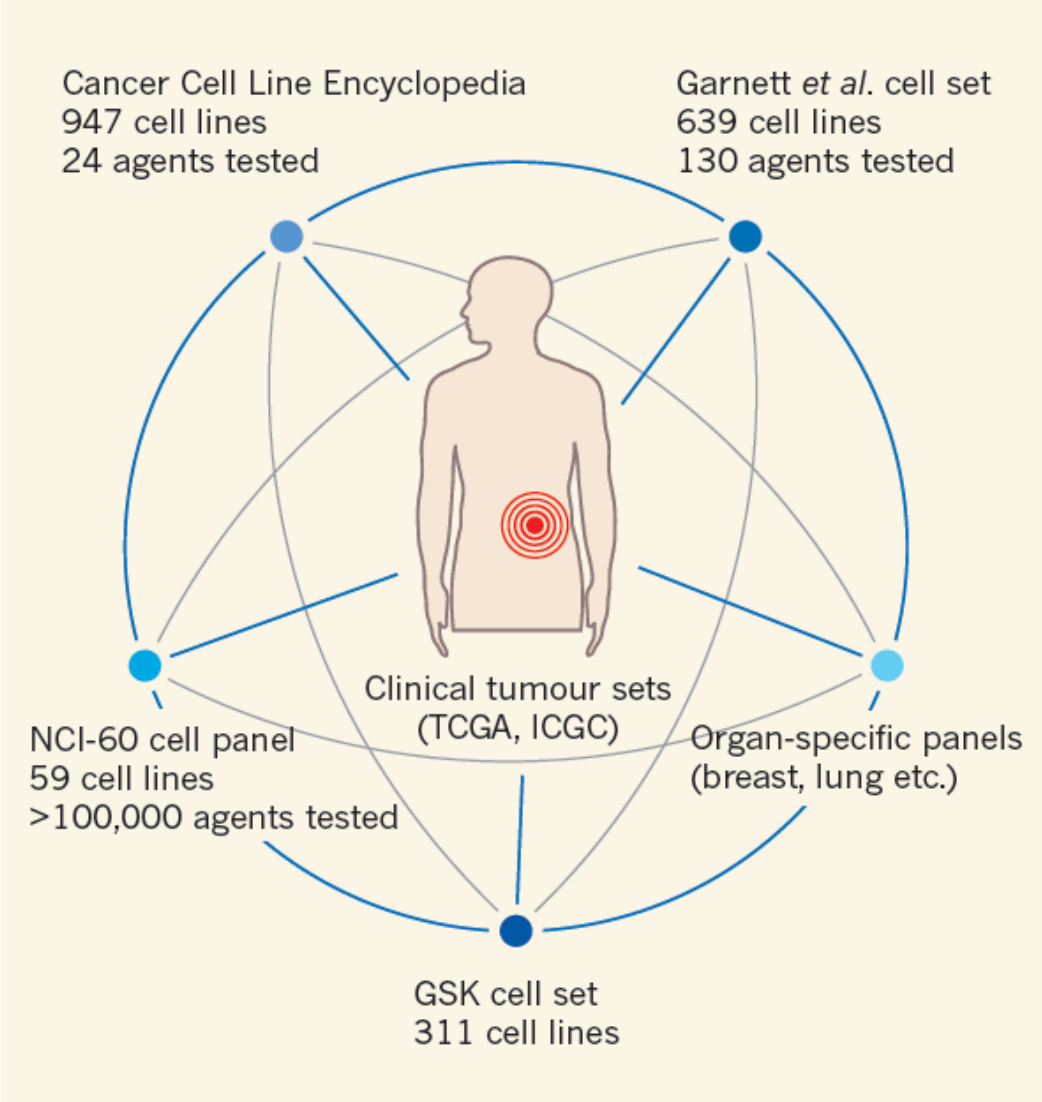

NCI-60

TIMELINE

The NCI60 human tumour cell line anticancer drug screen

Robert H. Shoemaker

Abstract | The US National Cancer Institute (NCI) 60 human tumour cell line anticancer drug screen (NCI60) was developed in the late 1980s as an *in vitro* drug-discovery tool intended to supplant the use of transplantable animal tumours in anticancer drug screening. This screening model was rapidly recognized as a rich source of information about the mechanisms of growth inhibition and tumour-cell kill. Recently, its role has changed to that of a service screen supporting the cancer research community. Here I review the development, use and productivity of the screen, highlighting several outcomes that have contributed to advances in cancer chemotherapy.

Timeline | **Major events in the development, implementation and use of the NCI60 cell lines**

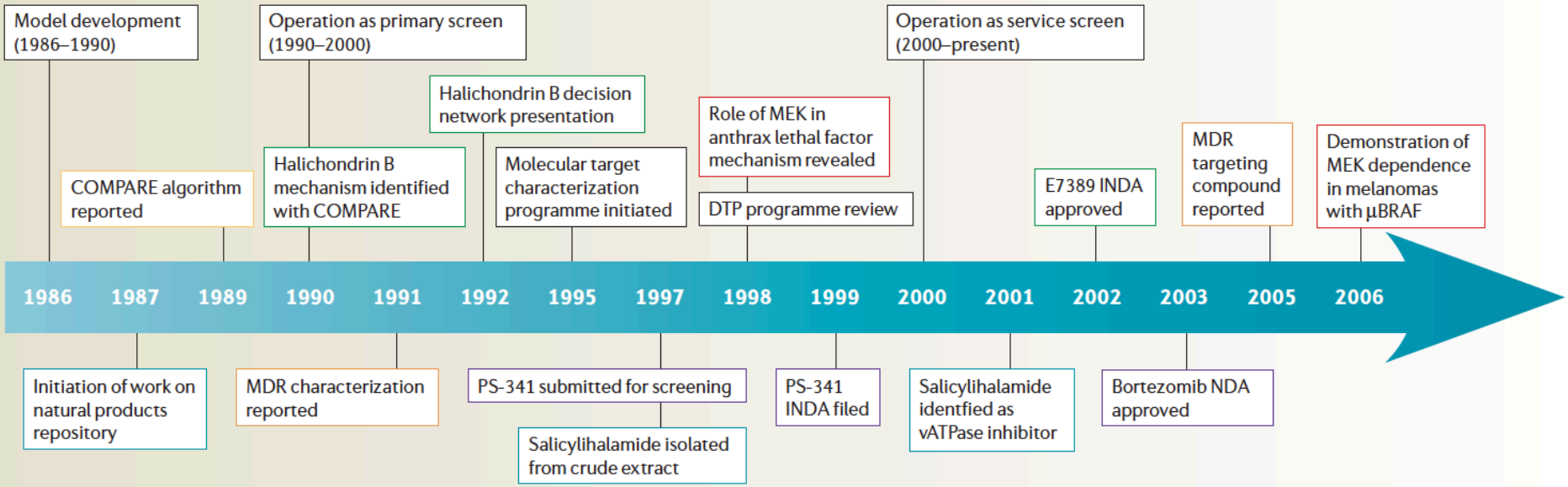

Related events are indicated by colour coding. DTP, Developmental Therapeutics Program; INDA, investigational new drug application; MDR, multidrug resistance; MEK, mitogen-activated ERK kinase; NDA, new drug application.

NCI-60

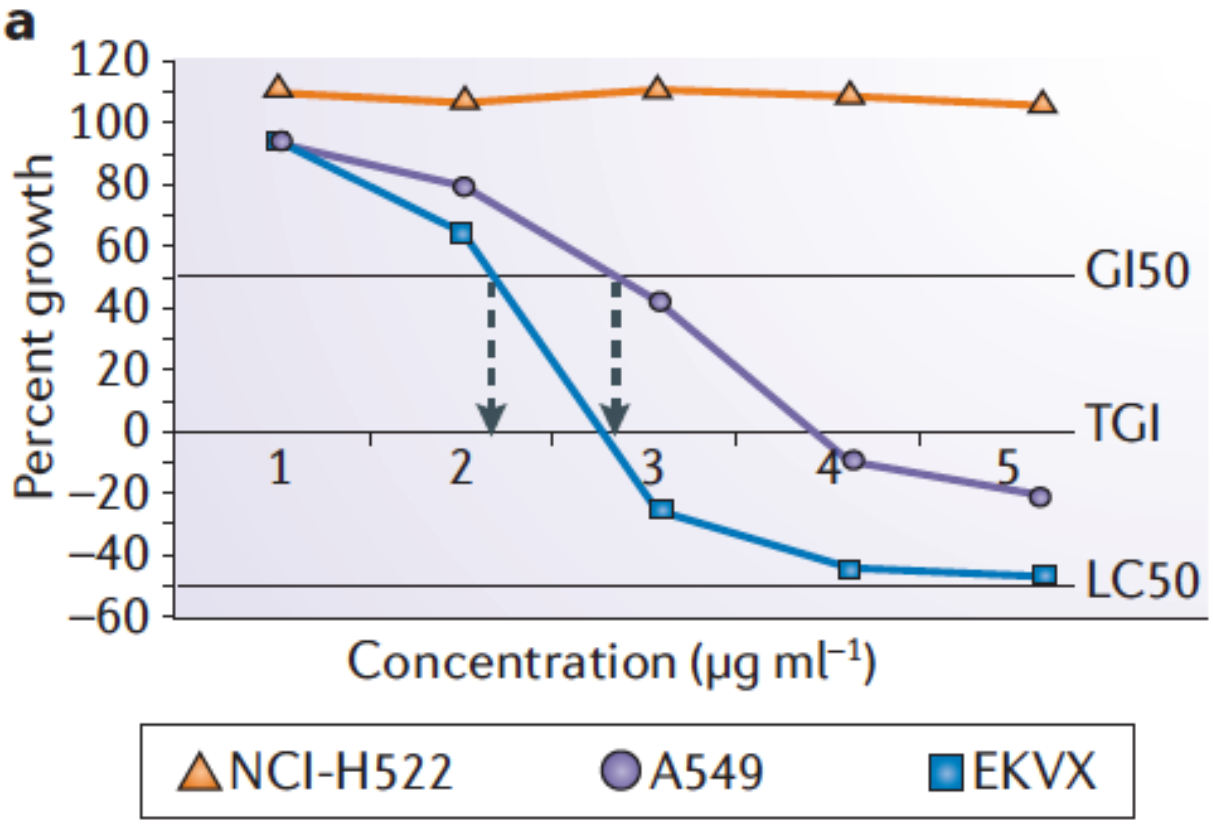

GI50 (50% growth inhibition)
LC50 (50% lethal concentration)
TGI (total growth inhibition)

NCI-60

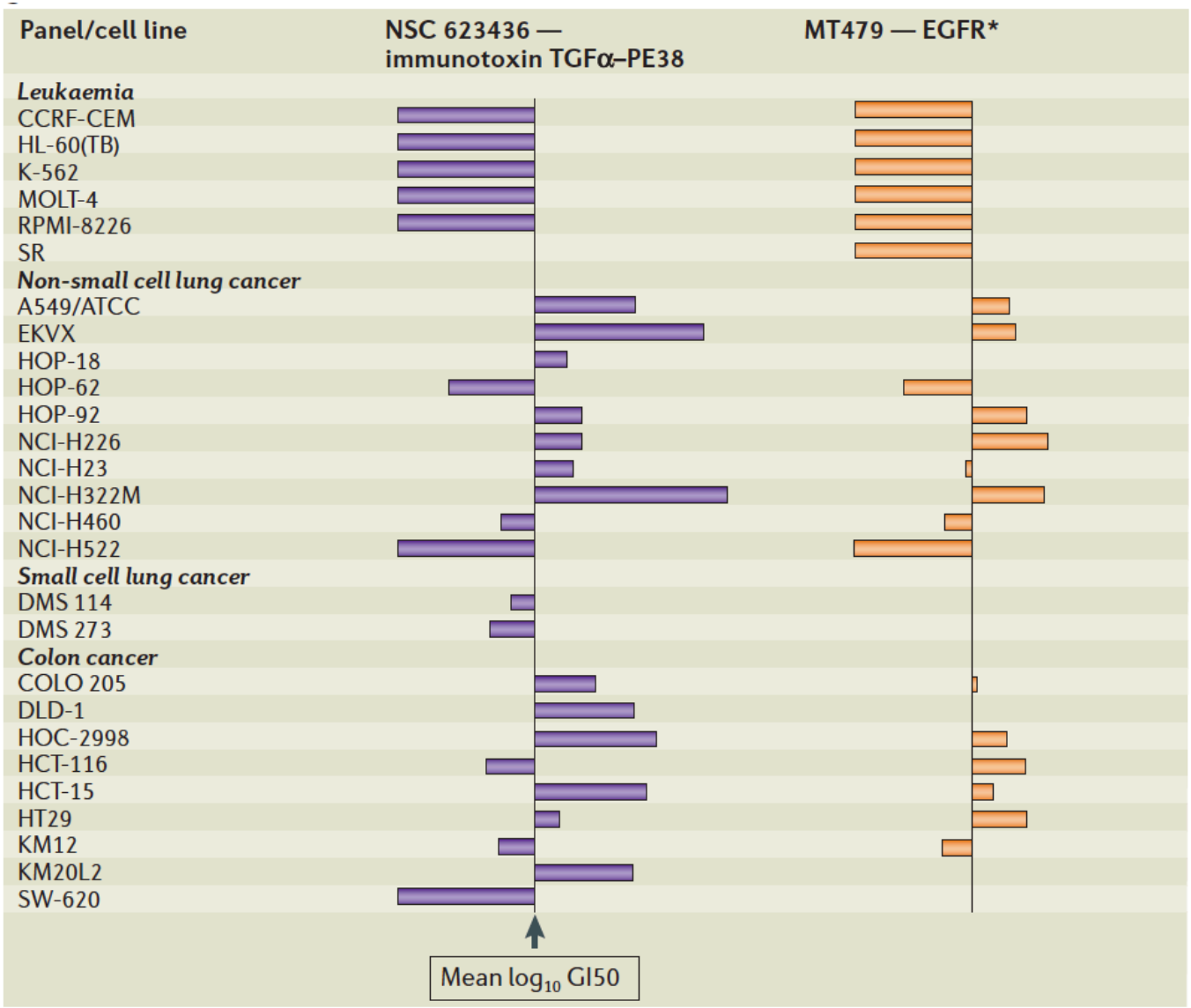

*The *EGFR* mRNA levels shown were generated using RNAse protection assays by Susan Bates, and are part of the publicly searchable database (designated MT479 in database).

NCI-60 DTP website

NCI-60 DTP website

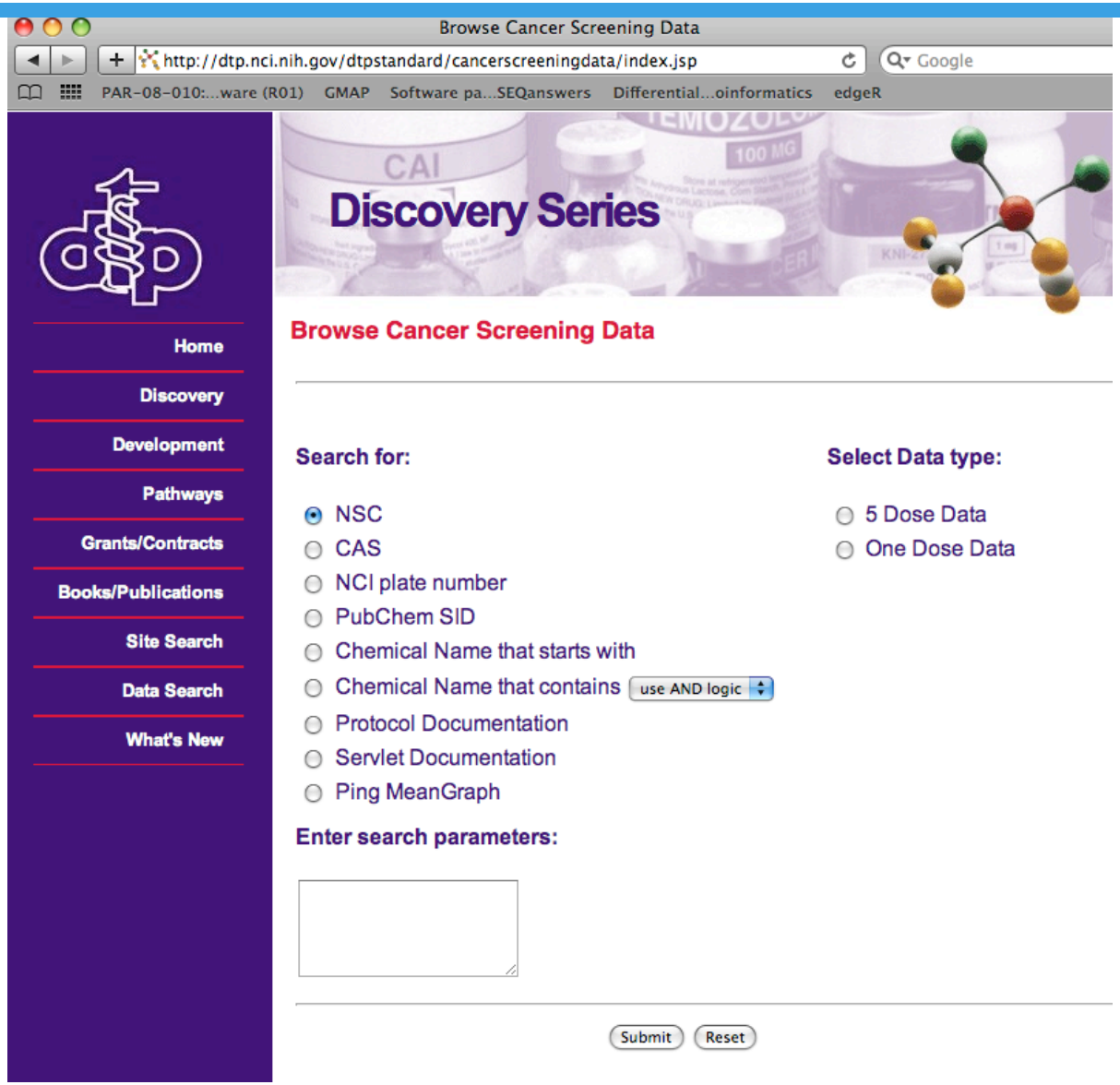

NCI-60 DTP website

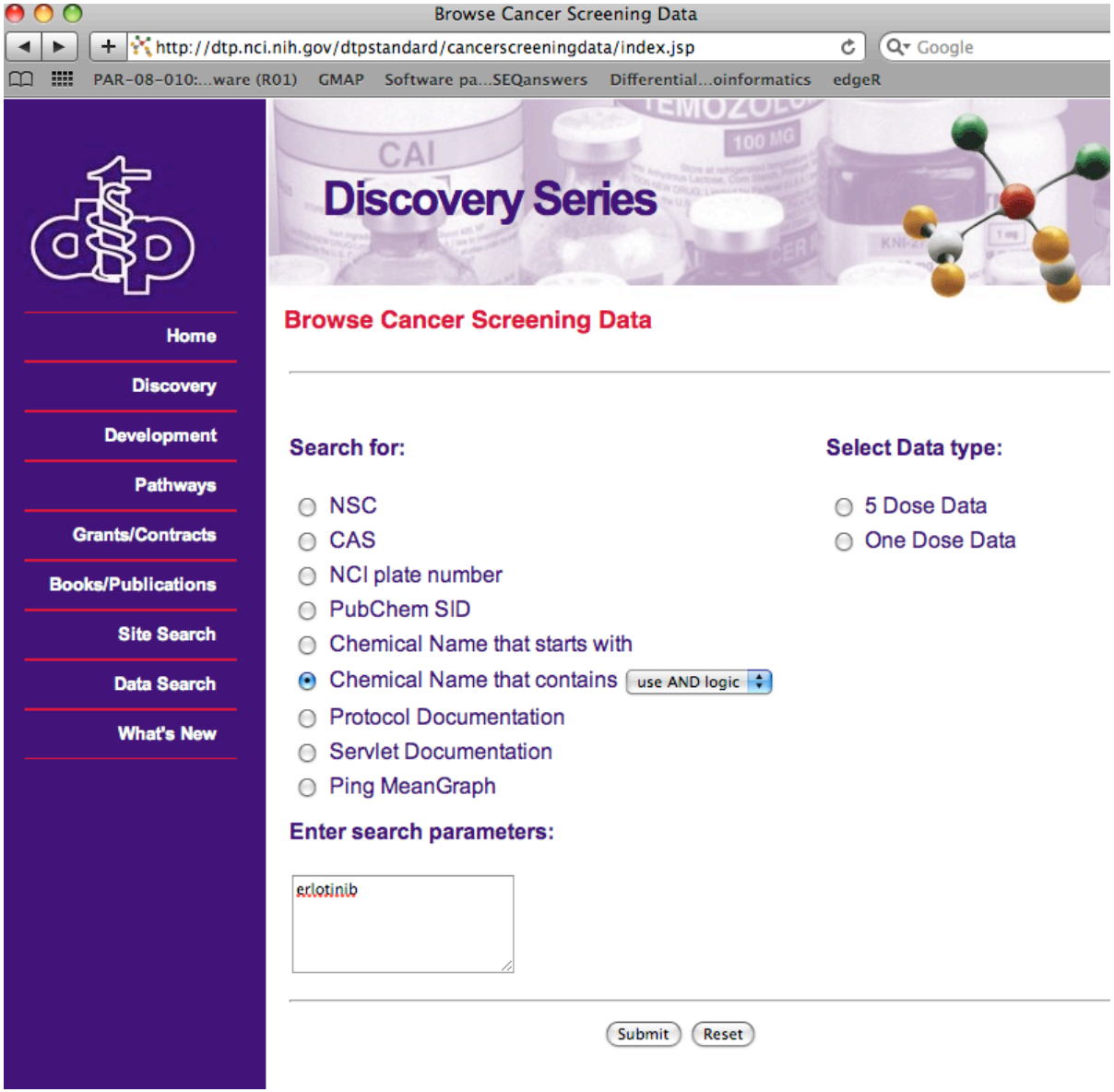

NCI-60 DTP website

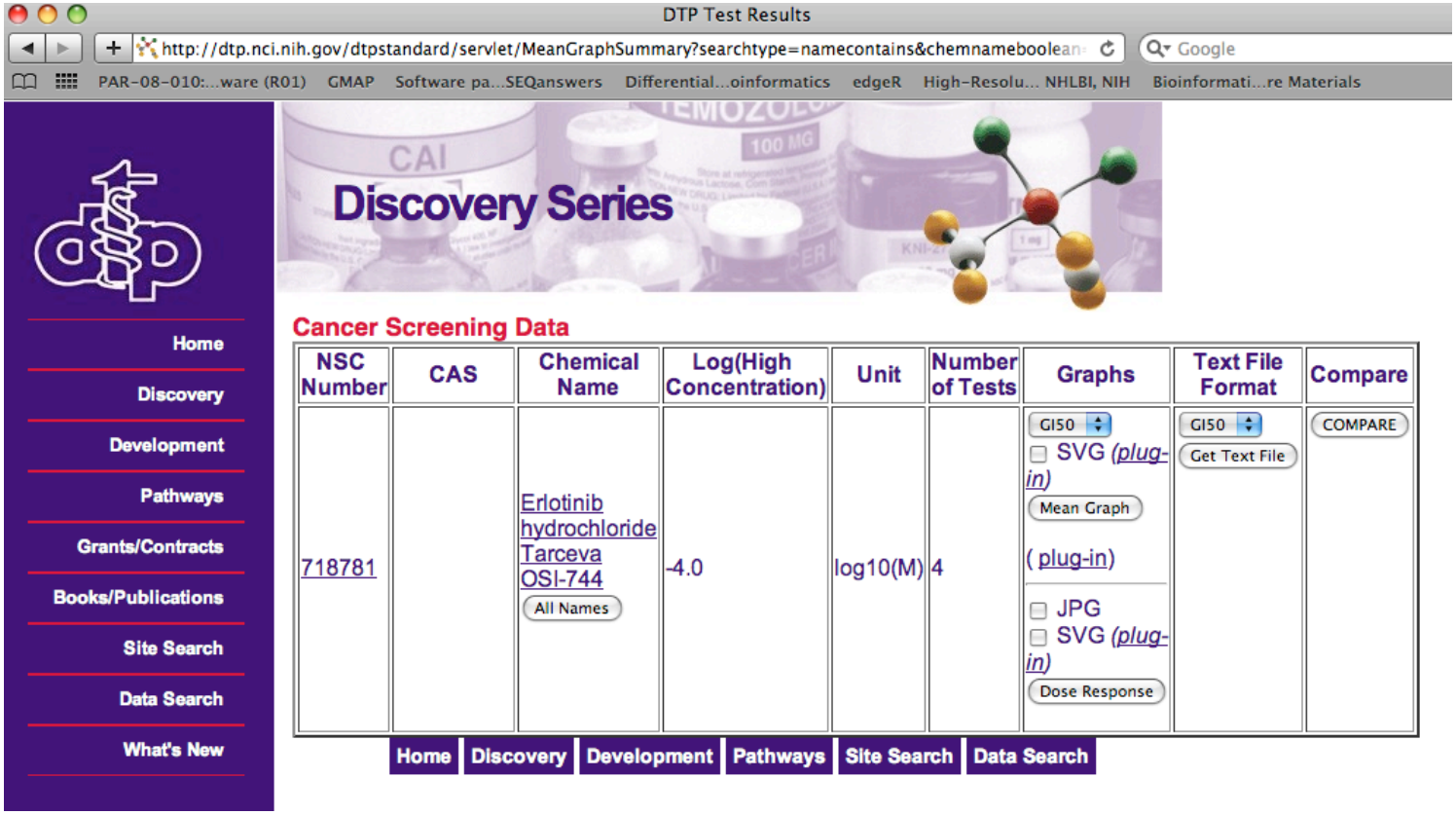

NCI-60 Mean GI50 Graph

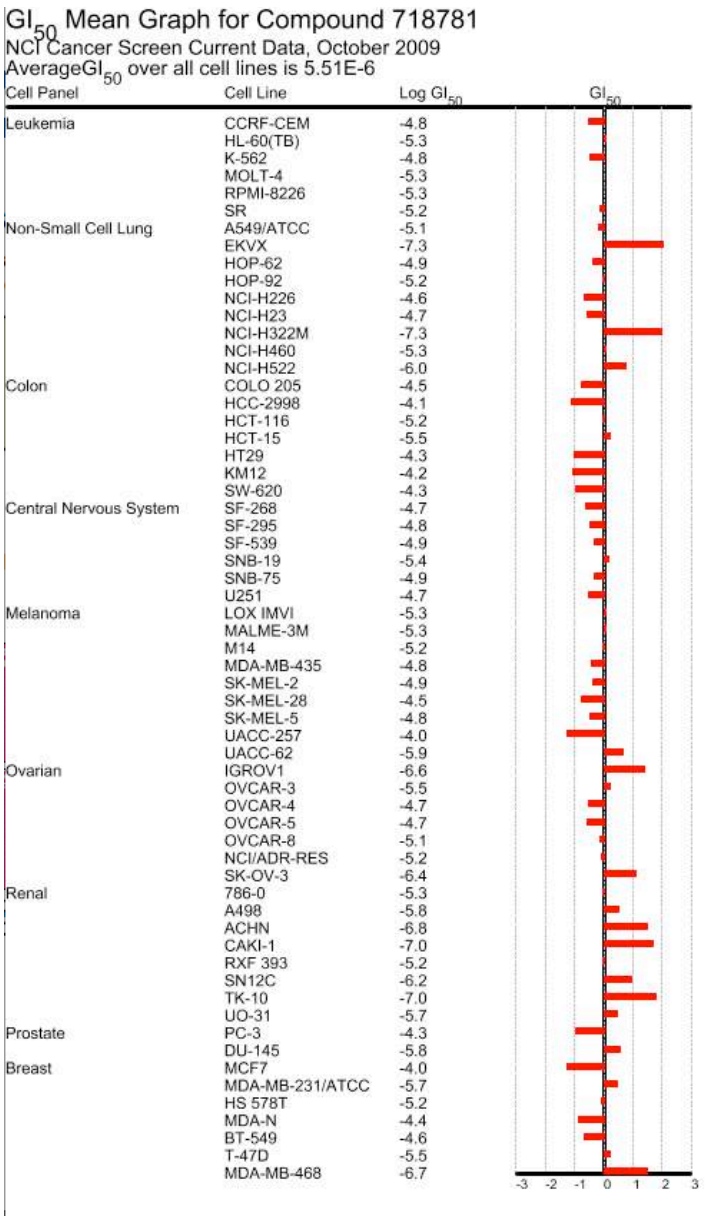

NCI-60 Dose-Response Curves

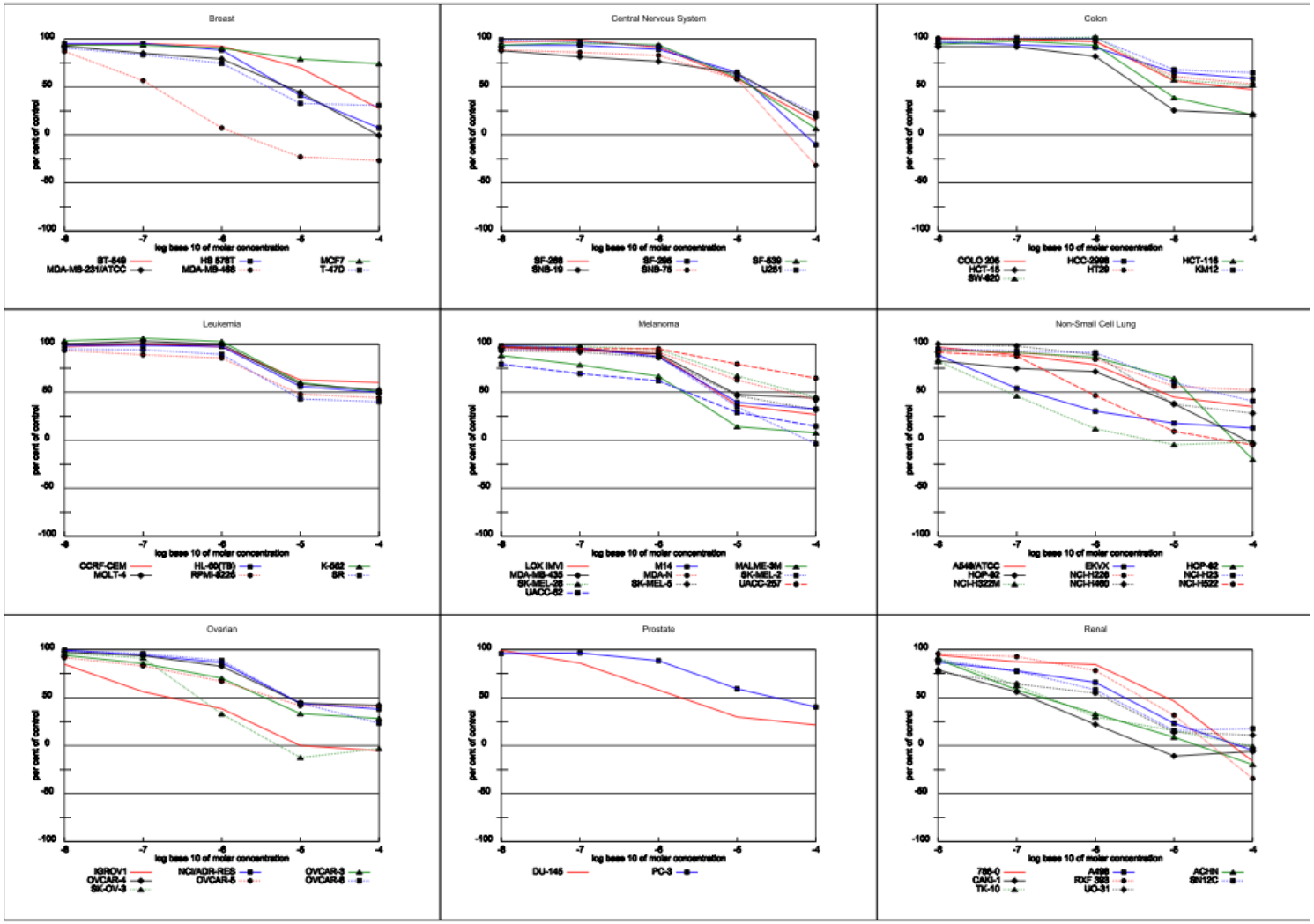

Download Data

Search The DTP Data

- Search for all data for compounds
- Instructions for Searching the DTP Open Compound Collection by Structure
- Basic Chemical Data
- Assays of Molecular Targets
- Browse Cancer Screening Data (September 2012 Release)
- Bulk Data Download
- Search In Vivo Screening Data
- Search Yeast Screening Data
- AIDS Screening Data (May 2004 Release)
- NCI Plate Map
- Search for Chemical Names
- Smiles Search

Search for Molecular Target Data

- Search by gene name, text string, or pattern ID
- Download Molecular Target Data

Search for Natural Product Data

- Browse by phylum and family

Molecular Target Data

https://wiki.nci.nih.gov/display/NCIDTPdata/Molecular+Target+Data

Molecular Target Data

20 Added by Daniel Zaharevitz, last edited by Daniel Zaharevitz on Sep 09, 2013 (view change)

Data from the DTP Molecular Target program.

Email questions concerning DTP's molecular targets program to: Molecular Target Team [moltarget@mail.nih.gov]

Primary molecular target data (excluding microarray data)

includes protein, mRNA, miRNA, DNA methylation, mutations, SNPs, enzyme activity, metabolites

WEB_DATA_ALL_MT.ZIP	A 3.4 Mb zip file - The uncompressed file is approximately 82.7 Mb.

When uncompressed the file is comma delimited in the following format:

File Format: MOLTID (NCI pattern #), GENE, TITLE, MOLTNBR (NCI exp. id #), PANELNBR, CELLNBR, pname, cellname, ENTITY_MEASURED, GeneID, UNITS, METHOD, VALUE

Protein Data Only

A subset of WEB_DATA_ALL_MT containing just the protein data

WEB_DATA_PROTEIN.ZIP	A 219 Kb zip file - The uncompressed file is approximately 3.2 Mb.

When uncompressed the file is comma delimited in the following format:

File Format: MOLTID (NCI pattern #), GENE, TITLE, MOLTNBR (NCI exp. id #), PANELNBR, CELLNBR, pname, cellname, ENTITY_MEASURED, GeneID, UNITS, METHOD, VALUE

DNA Data Only

A subset of WEB_DATA_ALL_MT containing just the DNA data

WEB_DATA_DNA.ZIP	A 26 kb zip file - The uncompressed file is approximately 580 Kb.

When uncompressed the file is comma delimited in the following format:

File Format: MOLTID (NCI pattern #), GENE, TITLE, MOLTNBR (NCI exp. id #), PANELNBR, CELLNBR, pname, cellname, ENTITY_MEASURED, GeneID, UNITS, METHOD, VALUE

DNA Methylation Data From Sequenom

A subset of WEB_DATA_ALL_MT containing just the DNA methylation data, Proc Natl Acad Sci USA 2008, Mar 25; 105(12): 4844-9.

WEB_DATA_SEQUENOM_METHYLATION.ZIP	A 5.2 Mb zip file - The uncompressed file is approximately 43.8 Mb.

When uncompressed the file is comma delimited in the following format:

File Format: MOLTID (NCI pattern #), GENE, TITLE, MOLTNBR (NCI exp. id #), PANELNBR, CELLNBR, pname, cellname, ENTITY_MEASURED, GeneID, VALUE

microRNA Data From the Israel Lab

A subset of WEB_DATA_ALL_MT containing just the microRNA data from the Israel lab. Cancer Res. 2007, Mar 15; 67(6): 2456-68.

WEB_DATA_ISRAEL_MIR.ZIP	A 98 Kb zip file - The uncompressed file is approximately 1.1 Mb.

When uncompressed the file is comma delimited in the following format:

File Format: MOLTID (NCI pattern #), TITLE, MOLTNBR (NCI exp. id #), PANELNBR, CELLNBR, pname, cellname, ENTITY_MEASURED, UNITS, METHOD, VALUE, TEXT

microRNA Data From the Weinstein and Croce Labs

A subset of WEB_DATA_ALL_MT containing just the microRNA data from the Weinstein and Croce labs. Mol Cancer Ther 2007, May; 6(5): 1483-91.

WEB_DATA_CROCE-WEINSTEIN_MIR.ZIP	A 601 Kb zip file - The uncompressed file is approximately 6.3 Mb.

When uncompressed the file is comma delimited in the following format:

File Format: MOLTID (NCI pattern #), TITLE, MOLTNBR (NCI exp. id #), PANELNBR, CELLNBR, pname, cellname, ENTITY_MEASURED, UNITS, METHOD, VALUE, TEXT

Metabolomic Data From Metabolon- data averaged from triplicate experiments

A subset of WEB_DATA_ALL_MT containing just the metabolomic data from Metabolon.

WEB_DATA_METABOLON.ZIP	A 171 Kb zip file - The uncompressed file is approximately 1.2 Mb.

When uncompressed the file is comma delimited in the following format:

File Format: MOLTID (NCI pattern #), TITLE, MOLTNBR (NCI exp. id #), PANELNBR, CELLNBR, pname, cellname, VALUE, STD DEV

Metabolomic Data From Metabolon - individual data from each of the triplicate experiments

WEB_DATA_METABOLON_ALL.ZIP	A 404 Kb zip file - The uncompressed file is approximately 3.2 Mb.

When uncompressed the file is comma delimited in the following format:

File Format: SAMPLENAME, TITLE, PANELNBR, CELLNBR, pname, cellname, VALUE

THE FOLLOWING DATASETS ARE DERIVED FROM LARGE-SCALE EXPERIMENTS

Estimated chromosomal band copy number, extracted from spectral karyotyping Cancer Res 63, 8634-47 (2003).

Data is provided as an Excel file listing copy number of each chromosomal band for each cell line. Download excel file

Affymetrix 125K SNP array data from the Sellers' lab Nature 436, 117-122 (2005).

Data is provided as 3 datasets: Copy number, allele calls and identifiers.

The Copy Number Data:

COPYNUM.ZIP	A 51.6 Mb zip file - The uncompressed file is approximately 307 Mb.

When uncompressed the file is comma delimited in the following format:

File Format: MARKER, CellID, COPYNBR, PANELNBR, CELLNBR, pname, cellname

The Allele Call Data:

ALLELECALL.ZIP	A 29.6 Mb zip file - The uncompressed file is approximately 290 Mb.

NCI ALMANAC

Therapeutics, Targets, and Chemical Biology

Cancer Research

The National Cancer Institute ALMANAC: A Comprehensive Screening Resource for the Detection of Anticancer Drug Pairs with Enhanced Therapeutic Activity

Susan L. Holbeck[1], Richard Camalier[1], James A. Crowell[1], Jeevan Prasaad Govindharajulu[2], Melinda Hollingshead[1], Lawrence W. Anderson[1], Eric Polley[1], Larry Rubinstein[1], Apurva Srivastava[2], Deborah Wilsker[2], Jerry M. Collins[1], and James H. Doroshow[1,3]

Abstract

To date, over 100 small-molecule oncology drugs have been approved by the FDA. Because of the inherent heterogeneity of tumors, these small molecules are often administered in combination to prevent emergence of resistant cell subpopulations. Therefore, new combination strategies to overcome drug resistance in patients with advanced cancer are needed. In this study, we performed a systematic evaluation of the therapeutic activity of over 5,000 pairs of FDA-approved cancer drugs against a panel of 60 well-characterized human tumor cell lines (NCI-60) to uncover combinations with greater than additive growth-inhibitory activity. Screening results were compiled into a database, termed the NCI-ALMANAC (A Large Matrix of Anti-Neoplastic Agent Combinations), publicly available at https://dtp.cancer.gov/ncialmanac. Subsequent *in vivo* experiments in mouse xenograft models of human cancer confirmed combinations with greater than single-agent efficacy. Concomitant detection of mechanistic biomarkers for these combinations *in vivo* supported the initiation of two phase I clinical trials at the NCI to evaluate clofarabine with bortezomib and nilotinib with paclitaxel in patients with advanced cancer. Consequently, the hypothesis-generating NCI-ALMANAC web-based resource has demonstrated value in identifying promising combinations of approved drugs with potent anticancer activity for further mechanistic study and translation to clinical trials. *Cancer Res; 77(13); 3564–76. ©2017 AACR.*

NCI ALMANAC

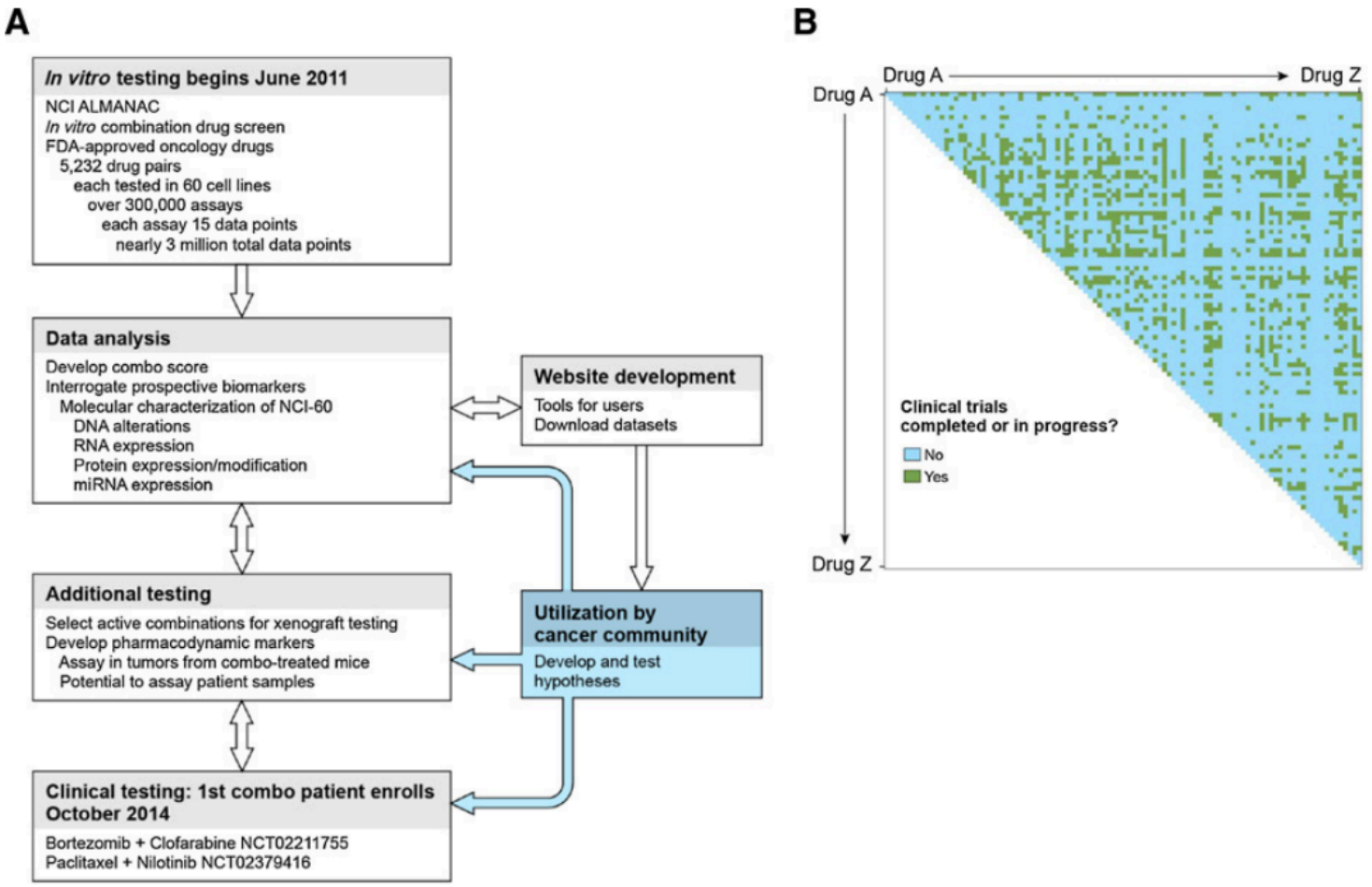

Figure 1.

NCI-ALMANAC screen strategy and summary results. **A,** Workflow diagram for the NCI-ALMANAC screen and follow-up preclinical and clinical studies. Double-headed arrows indicate the iterative flow of information between different stages of the project. **B,** NCI-ALMANAC reveals a large number of potentially active, clinically novel drug combinations (according to clinicaltrials.gov analysis). Data were downloaded from clinicaltrials.gov and processed to identify the cancer trials that had utilized the drug combinations examined in this study. Each drug is shown as both the abscissa and ordinate, alphabetically, with green indicating drug pairs that were identified as having been reported as tested in combination in a clinical trial and blue indicating pairs that have not.

NCI ALMANAC

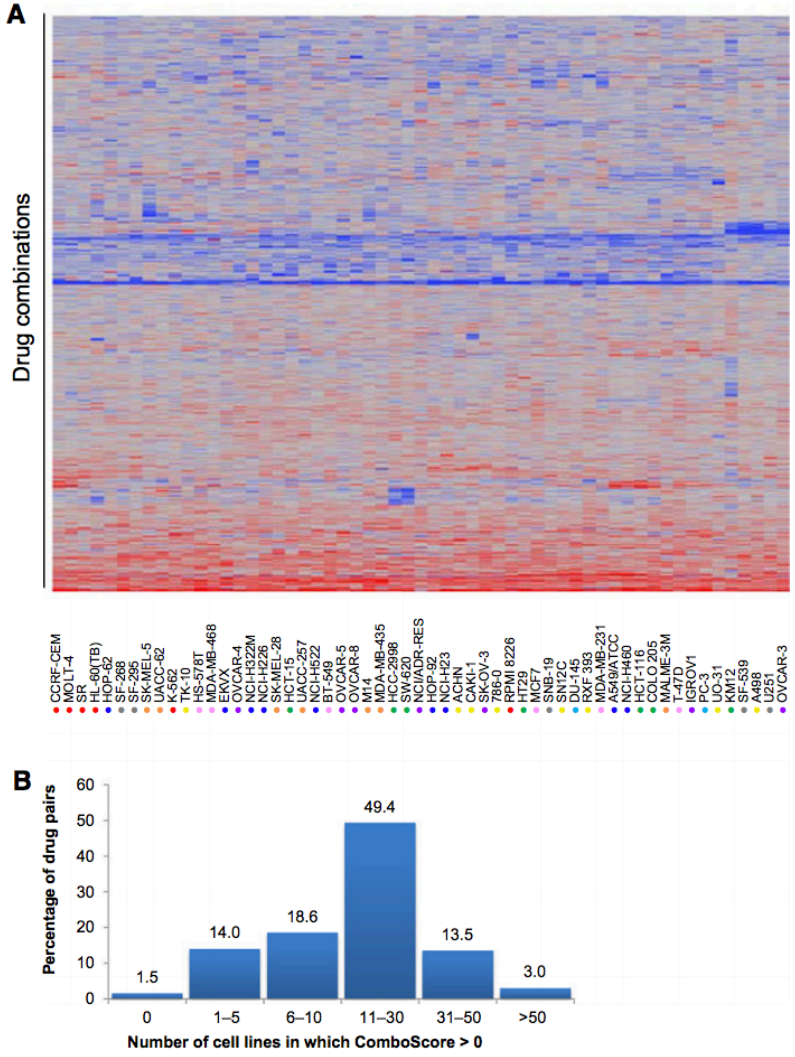

Figure 2.
In vitro activity of drug combinations in the NCI-60 panel. **A,** Two-way hierarchical clustering was used to cluster ComboScores for 57 cell lines (the SK-MEL-2, SNB-75, and LOX-IMVI lines had many missing values and were excluded) and 4,629 drug combinations. Red, positive ComboScores (i.e., better-than-additive effects; blue, negative values (i.e., less-than-additive effects). Tumor tissue derivations for the NCI-60 cell lines are indicated by colored circles: red, leukemia; green, colon; blue, non–small cell lung; gray, CNS; orange, melanoma; purple, ovarian; yellow, renal; turquoise, prostate; and pink, breast. **B,** The majority of drug pairs had *in vitro* activity in 11–30 cell lines of the NCI-60 panel, indicating that most drug pairs only have greater than additive activity in a subset of the NCI-60 cell lines.

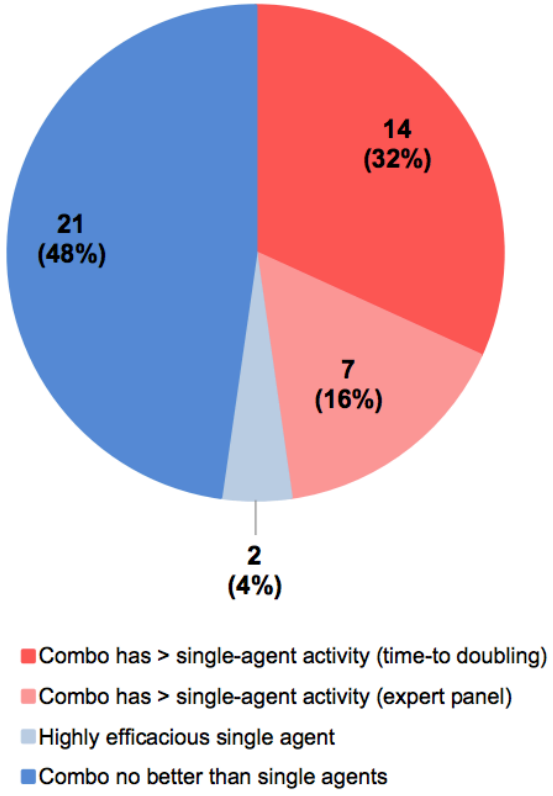

Figure 3.
Antitumor efficacy of NCI-ALMANAC–derived drug combinations in the tested NCI-60 xenograft models. A total of 44 unique xenograft efficacy experiments, involving 20 different drug combinations that had not previously undergone clinical testing (according to clinicaltrials.gov), were performed using sets of drug combinations and NCI-60–derived models that demonstrated positive *in vitro* ComboScores. Experiments in which combination treatment yielded improved antitumor efficacy compared with both single-agent treatments were identified by Kaplan–Meier and log-rank analysis of time-to-tumor-volume-doubling ($P < 0.05$; dark pink) or by a panel of xenograft experts (light pink). Experiments with no greater-than-single-agent activity are shown in dark blue, while those for which one single agent was highly efficacious are shown in light blue. See Supplementary Table S4 for a complete list of xenograft experiments and results.

NCI ALMANAC

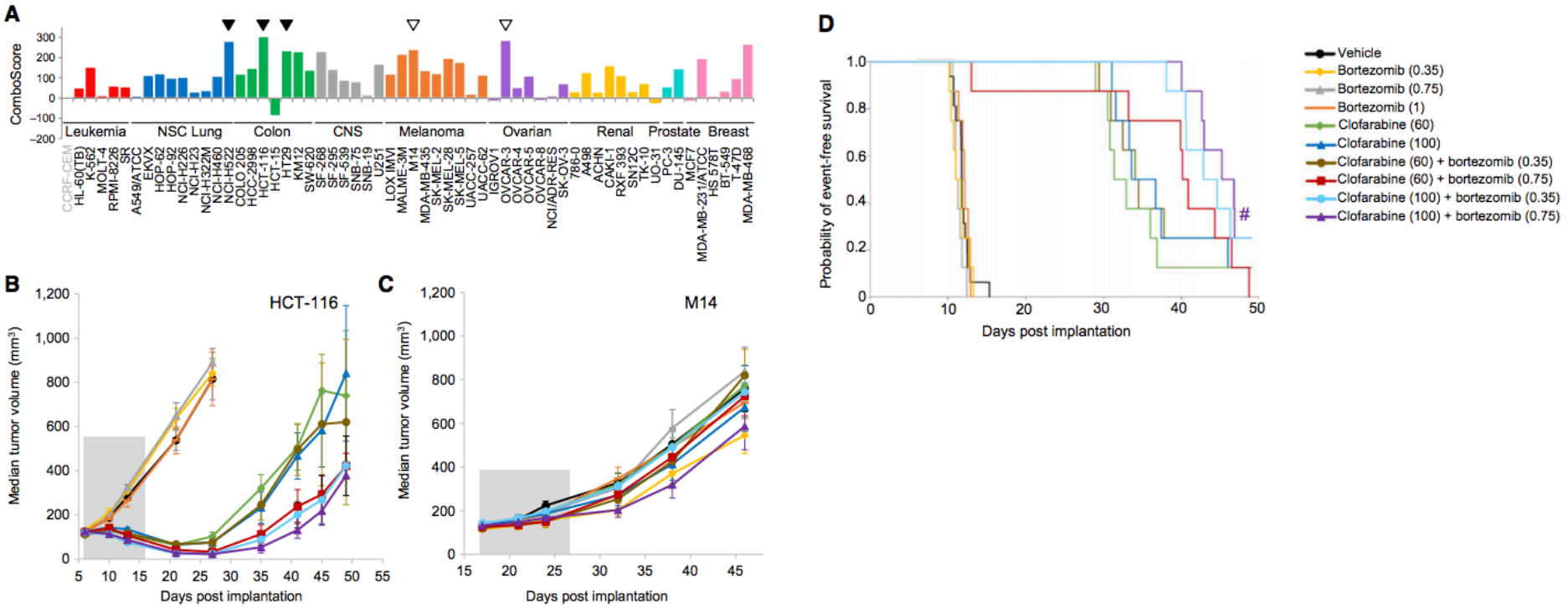

Figure 4.

Therapeutic activity of the NCI-ALMANAC–derived combination of bortezomib and clofarabine. **A,** The combination of bortezomib and clofarabine *in vitro* yielded positive ComboScores across several cell types. Tumor tissue derivations for the NCI-60 cell lines are indicated by bar color: red, leukemia; green, colon; blue, non-small cell lung; gray, CNS; orange, melanoma; purple, ovarian; yellow, renal; turquoise, prostate; and pink, breast. A leukemia cell line for which no ComboScore was available for this combination is indicated by gray text. Models for which xenograft experiments revealed the presence or absence of *in vivo* greater-than-single-agent activity are indicated by filled triangles or empty triangles, respectively. **B** and **C,** Clofarabine–bortezomib combination treatment exhibits enhanced efficacy relative to the respective single-agent treatments in the human colon cancer HCT-116 xenograft model (**B**) but not in the M14 melanoma xenograft model (**C**). Median tumor volumes are shown for mice treated with vehicle, single-agent bortezomib [5 × every two days (Q2D), intraperitoneal injection], single-agent clofarabine [5 × every two days (Q2D), oral administration], or the combination (schedule and administration for each agent as indicated for the respective single-agent treatments); treatment commenced on day 6 for the HCT-116 experiment (**B**) and on day 17 for the M14 experiment (**C**; dosing period indicated by gray-shaded area in both graphs). **D,** Kaplan–Meier curves for time-to-tumor doubling analysis of HCT-116 xenograft models treated with the clofarabine–bortezomib combination. The *y*-axis indicates probability of event-free survival, where an event is defined as one tumor doubling or drug-related death (the latter occurred for only one animal in the 60 mg/kg clofarabine + 0.75 mg/kg bortezomib-treated group). #, the combination-treated group exhibiting greater-than-single-agent time-to-tumor-doubling compared with both bortezomib-alone and clofarabine-alone groups at the corresponding doses ($P < 0.1$), as determined by log-rank tests. Doses (mg/kg) for each treatment group are indicated in the legend ($n = 16$ mice for the vehicle group; $n = 8$ mice for all other groups). Error bars, SE of the median.

NCI ALMANAC

Trial of the Combination of Bortezomib and Clofarabine in Adults With Relapsed Solid Tumors

This study is currently recruiting participants.

See Contacts and Locations

Verified October 13, 2017 by National Institutes of Health Clinical Center (CC) (National Cancer Institute (NCI))

Sponsor:
National Cancer Institute (NCI)

ClinicalTrials.gov Identifier:
NCT02211755

First Posted: August 7, 2014
Last Update Posted: October 27, 2017

Information provided by (Responsible Party):
National Institutes of Health Clinical Center (CC) (National Cancer Institute (NCI))

Purpose

Background:

- Researchers want to develop better ways to treat cancer. In this study, they will give people with cancer two drugs. These drugs have been used on their own to treat some blood cell cancers.

Objectives:

- To test the safety and efficacy of the drug combination of bortezomib and clofarabine.

Condition	Intervention	Phase
Neoplasms Myelodysplastic Syndromes	Drug: Bortezomib plus Clofarabine	Phase 1

Study Type: Interventional
Study Design: Intervention Model: Single Group Assignment
Masking: None (Open Label)
Primary Purpose: Treatment

Official Title: Phase I Trial of the Combination of Bortezomib and Clofarabine in Adults With Refractory Solid Tumors, Lymphomas, or Myelodysplastic Syndromes

NCI ALMANAC

https://dtp.cancer.gov/ncialmanac/

NCI ALMANAC

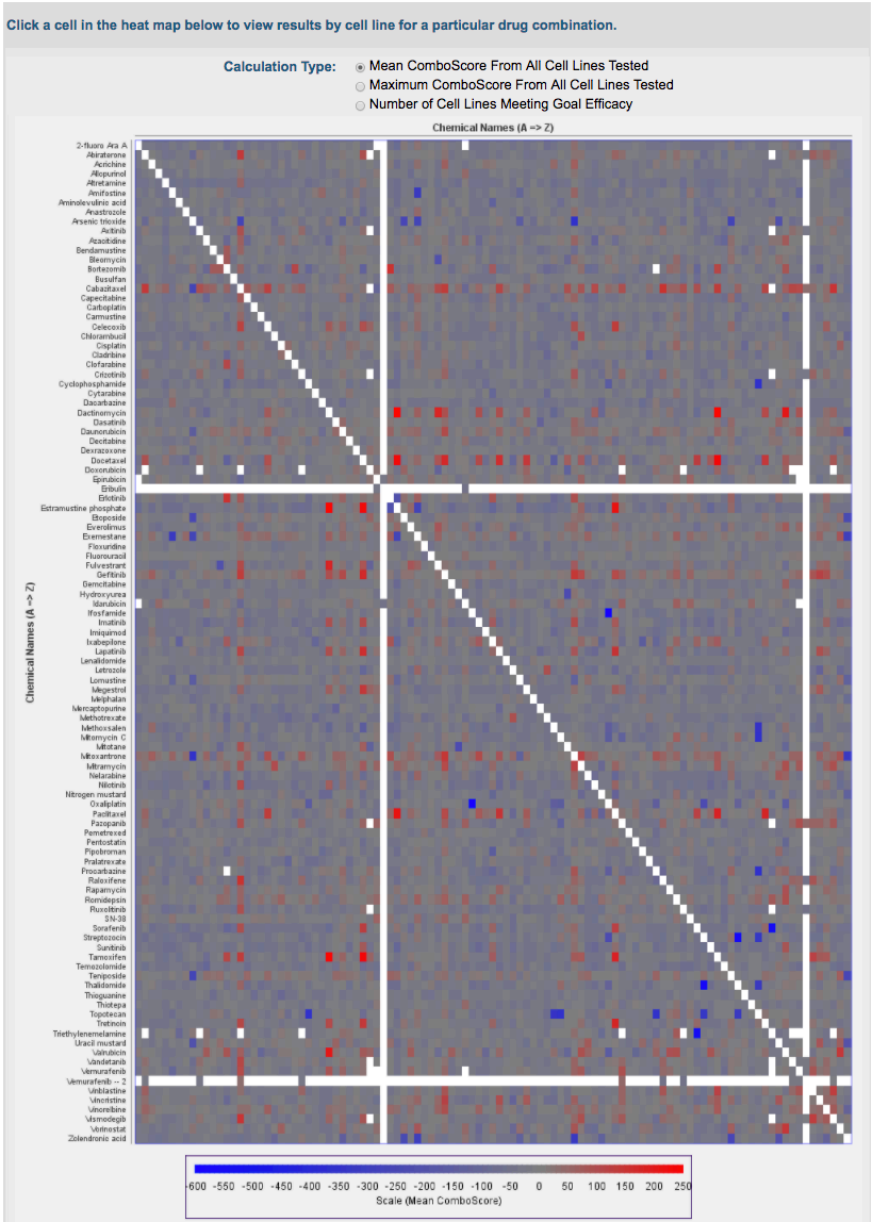
Click a cell in the heat map below to view results by cell line for a particular drug combination.
Calculation Type:
Mean ComboScore From All Cell Lines Tested
Maximum ComboScore From All Cell Lines Tested
Number of Cell Lines Meeting Goal Efficacy
Chemical Names (A => Z)
Chemical Names (A => Z)
-600 -550 -500 -450 -400 -350 -300 -250 -200 -150 -100 -50 0 50 100 150 200 250
Scale (Mean ComboScore)

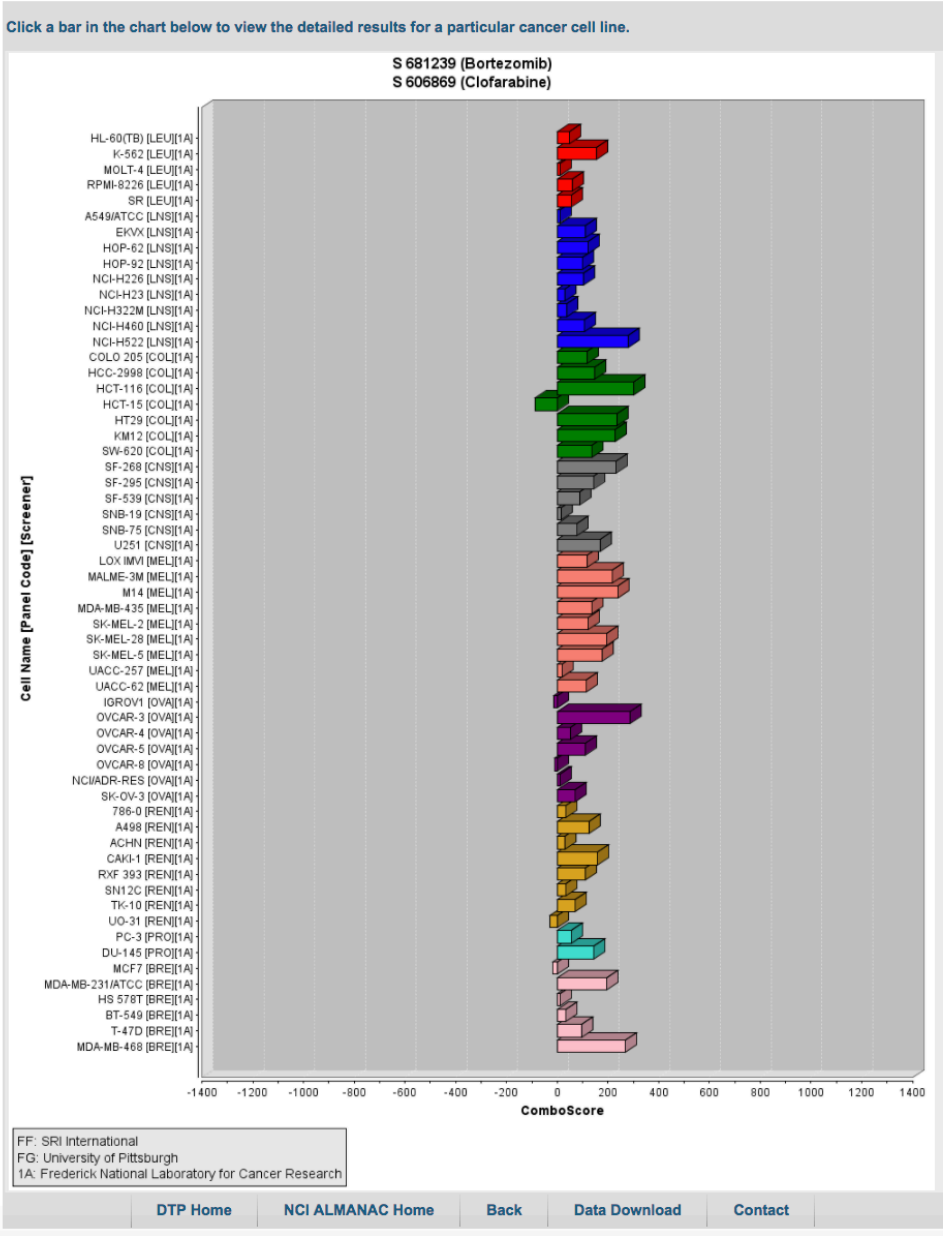
Click a bar in the chart below to view the detailed results for a particular cancer cell line.
S 681239 (Bortezomib)
S 606869 (Clofarabine)
Cell Name [Panel Code] [Screener]
HL-60(TB) [LEU][1A]
K-562 [LEU][1A]
MOLT-4 [LEU][1A]
RPMI-8226 [LEU][1A]
SR [LEU][1A]
A549/ATCC [LNS][1A]
EKVX [LNS][1A]
HOP-62 [LNS][1A]
HOP-92 [LNS][1A]
NCI-H226 [LNS][1A]
NCI-H23 [LNS][1A]
NCI-H322M [LNS][1A]
NCI-H460 [LNS][1A]
NCI-H522 [LNS][1A]
COLO 205 [COL][1A]
HCC-2998 [COL][1A]
HCT-116 [COL][1A]
HCT-15 [COL][1A]
HT29 [COL][1A]
KM12 [COL][1A]
SW-620 [COL][1A]
SF-268 [CNS][1A]
SF-295 [CNS][1A]
SF-539 [CNS][1A]
SNB-19 [CNS][1A]
SNB-75 [CNS][1A]
U251 [CNS][1A]
LOX IMVI [MEL][1A]
MALME-3M [MEL][1A]
M14 [MEL][1A]
MDA-MB-435 [MEL][1A]
SK-MEL-2 [MEL][1A]
SK-MEL-28 [MEL][1A]
SK-MEL-5 [MEL][1A]
UACC-257 [MEL][1A]
UACC-62 [MEL][1A]
IGROV1 [OVA][1A]
OVCAR-3 [OVA][1A]
OVCAR-4 [OVA][1A]
OVCAR-5 [OVA][1A]
OVCAR-8 [OVA][1A]
NCI/ADR-RES [OVA][1A]
SK-OV-3 [OVA][1A]
786-0 [REN][1A]
A498 [REN][1A]
ACHN [REN][1A]
CAKI-1 [REN][1A]
RXF 393 [REN][1A]
SN12C [REN][1A]
TK-10 [REN][1A]
UO-31 [REN][1A]
PC-3 [PRO][1A]
DU-145 [PRO][1A]
MCF7 [BRE][1A]
MDA-MB-231/ATCC [BRE][1A]
HS 578T [BRE][1A]
BT-549 [BRE][1A]
T-47D [BRE][1A]
MDA-MB-468 [BRE][1A]
-1400 -1200 -1000 -800 -600 -400 -200 0 200 400 600 800 1000 1200 1400
ComboScore
FF: SRI International
FG: University of Pittsburgh
1A: Frederick National Laboratory for Cancer Research
DTP Home
NCI ALMANAC Home
Back
Data Download
Contact

NCI ALMANAC

NCI ALMANAC Study Results

This page will generate a heat map containing a summary of the results for each mechanism of the selected agent. The heat map displays the various cell lines of cancer and the set of mechanisms with which the selected agent was tested. The scale illustrates how well the drug pair tested against each cell line of cancer, where the color red generally indicates more effective results. Scroll over a cell to see the calculated score value for a drug pair and cancer cell line.

Retrieve data for all mechanisms containing the selected agent:

Primary Drug: Erlotinib

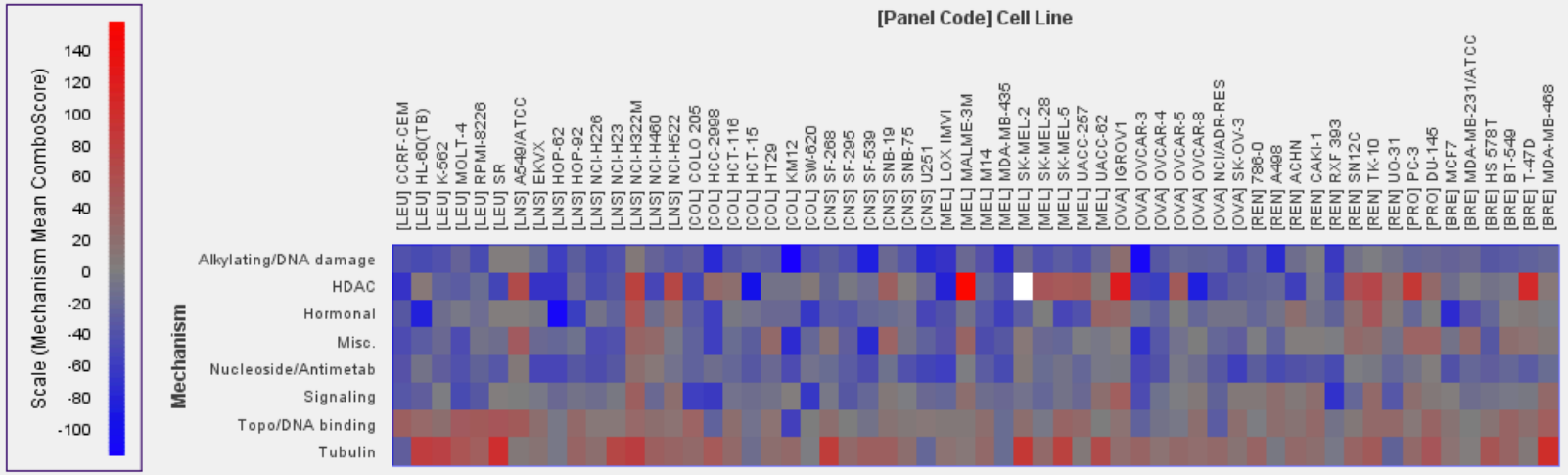

DTP Home | NCI ALMANAC Home | Data Download | Contact

Catalogue of Somatic Mutations in Cancer (COSMIC)

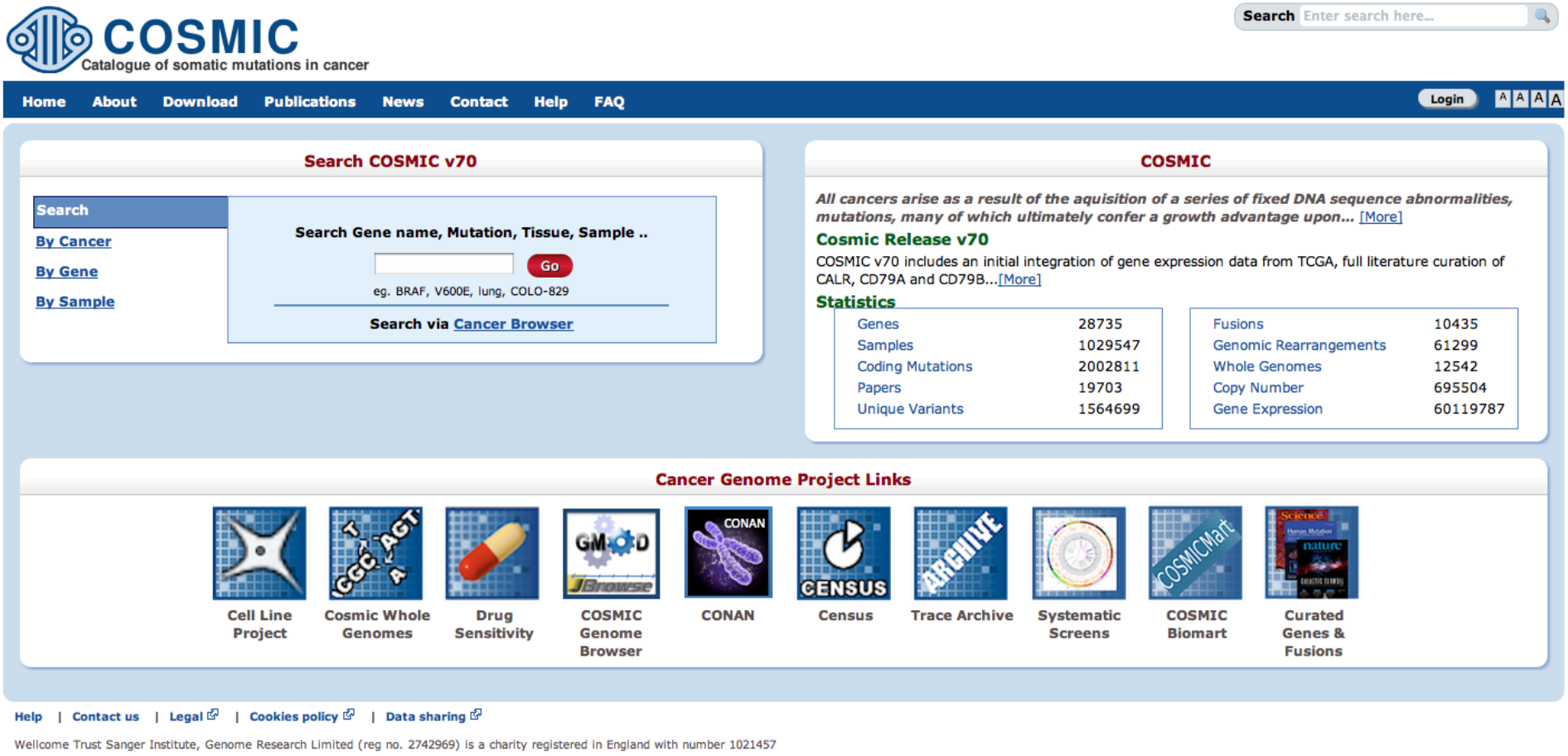

http://cancer.sanger.ac.uk/cancergenome/projects/cosmic/

Querying Gene Mutation in COSMIC

Cosmic » Gene » Overview » BRAF

Overview | Genome View | Sequence | Fusions | Studies | References

Gene name BRAF

Gene Id COSG2

Synonyms B-raf 1,B-raf1,BRAF1,MGC126806,MGC138284,RAFB1,CCDS5863.1,P15056,ENSG00000157764

Genomic Summary

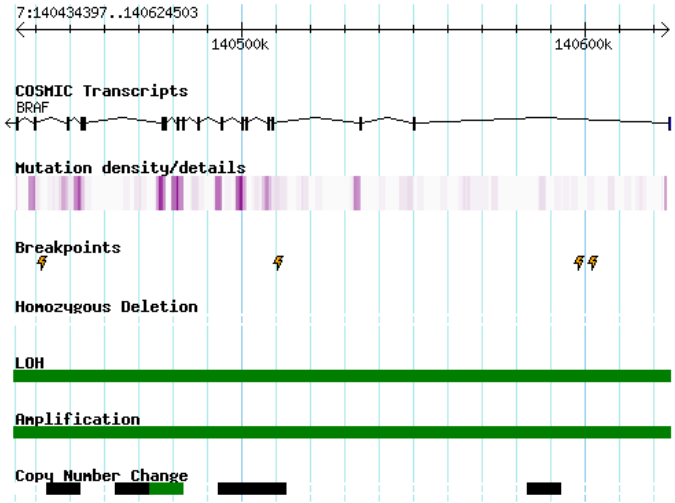

Drug Sensitivity Data: Click here for BRAF drug sensitivity data

Mutations in BRAF are associated with altered sensitivity to the following drug(s) :

Inceased sensitivity: PF-562271, CEP-701, FTI-277, 17-AAG, PD-0325901, SB590885, AZD6244, PD-173074, ZM-447439, BIBW2992, Temsirolimus, Metformin, AZD6482, Gefitinib, PLX4720, Nutlin-3a, AZ628, Bortezomib, Embelin, RDEA119, FH535, CI-1040, CHIR-99021, AP-24534, Obatoclax Mesylate

No.of Samples Total number of unique samples: 168311

Unique samples with mutations: 33263

Mutation Analysis

Histogram Distribution

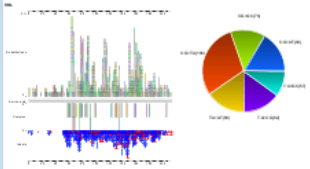

External Links

OMIM:	164757
Transcript:	NM_004333
Ensembl Contig View:	BRAF
UCSC Browser:	BRAF
Copy Number:	CONAN
CCDS:	CCDS5863.1
Pfam:	P15056
Atlas Genetic Oncology:	BRAFID828
HGNC:	1097

Querying Gene Mutation in COSMIC

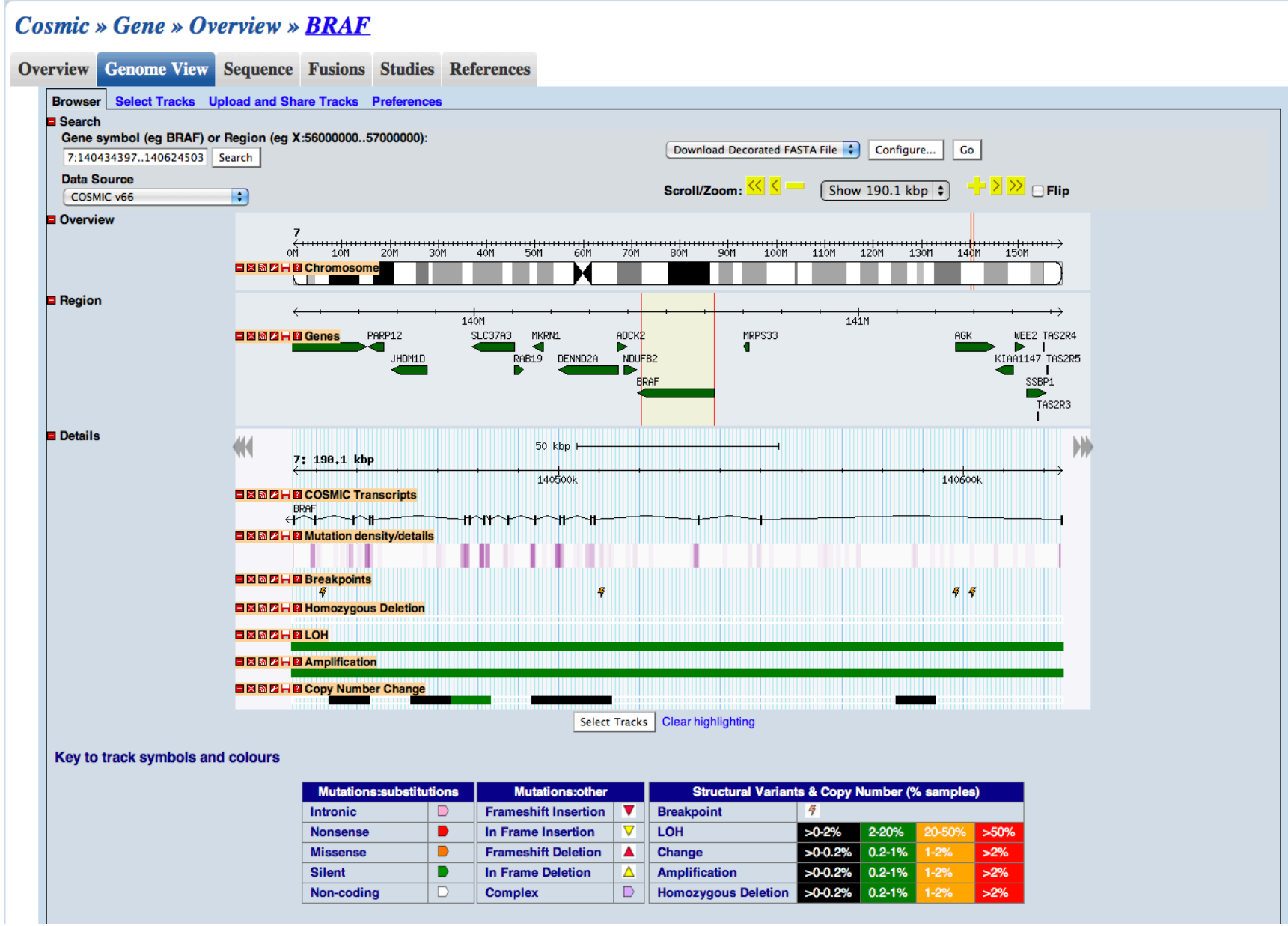

Querying Gene Mutation in COSMIC

Cosmic » Gene » Overview » BRAF

Overview | Genome View | **Sequence** | Fusions | Studies | References

cDNA Sequence	NM_004333
Protein Sequence	BRAF
Transcript and Protein Aligned	NM_004333+BRAF

Cosmic » Gene » Overview » BRAF

Overview | Genome View | Sequence | **Fusions** | Studies | References

BRAF is involved in fusions with :

AGTRAP (1 mutations in 1 samples)
FAM131B_ENST00000443739 (3 mutations in 9 samples)
SLC45A3 (1 mutations in 6 samples)
FCHSD1 (1 mutations in 2 samples)
KIAA1549 (462 mutations in 1091 samples)
AKAP9_ENST00000356239 (4 mutations in 292 samples)

Querying Gene Mutation in COSMIC

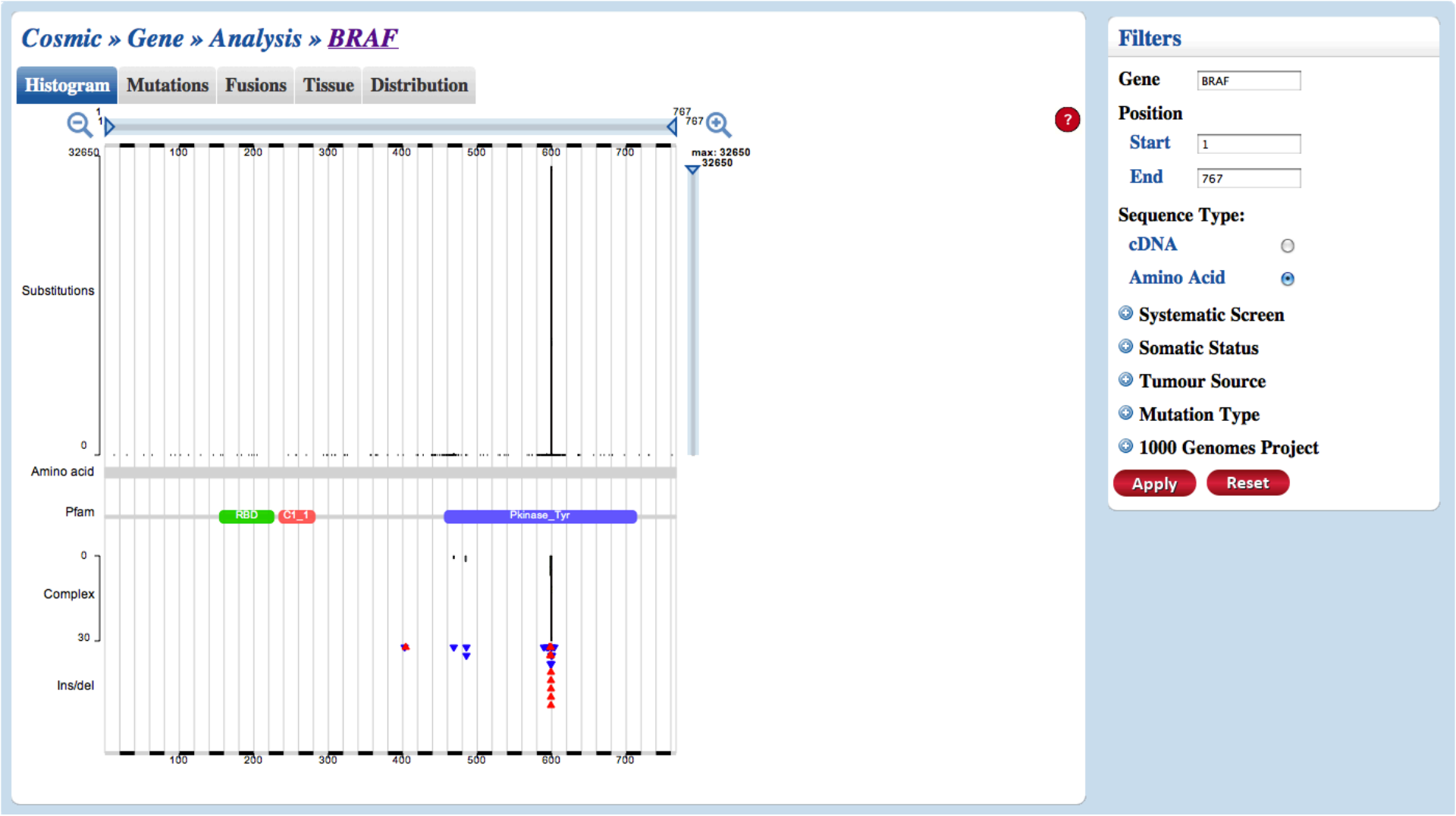

Querying Gene Mutation in COSMIC

Cosmic » Gene » Analysis » BRAF

Histogram | Mutations | Fusions | Tissue | Distribution

Export: CSV TSV

Show 10 entries

Search:

Position	Mutation (CDS)	Mutation (Amino Acid)	Mutation ID (COSM)	Count	Mutation Type
13	c.37G>T	p.E13*	COSM1622438	1	Substitution - Nonsense
30	c.89G>A	p.G30D	COSM303873	1	Substitution - Missense
53	c.158T>C	p.M53T	COSM1184861	2	Substitution - Missense
64	c.190C>A	p.L64I	COSM1086272	1	Substitution - Missense
89	c.267A>G	p.L89L	COSM745342	1	Substitution - coding silent
95	c.284G>C	p.R95T	COSM745343	1	Substitution - Missense
102	c.305C>T	p.S102F	COSM1167905	1	Substitution - Missense
113	c.338G>T	p.S113I	COSM599331	1	Substitution - Missense
129	c.386C>T	p.S129L	COSM1312758	1	Substitution - Missense
146	c.436C>T	p.R146W	COSM1548502	1	Substitution - Missense

Showing 1 to 10 of 374 entries

First Previous 1 2 3 4 5 Next Last

Querying Gene Mutation in COSMIC

* This link opens in a new window

Cosmic » Gene » Analysis » BRAF

Histogram | Mutations | Fusions | Tissue | Distribution

Mutation Distribution Pie Charts

Distribution Overview | Substitutions (coding strand) |

Substitutions (both strands) | Deletions | Insertions

Color	Mutation Type	Mutant samples	Percentage
	Substitution nonsense	23	0.07
	Substitution missense	32955	99.07
	Substitution synonymous	80	0.24
	Insertion inframe	25	0.08
	Insertion frameshift	1	0.00
	Deletion inframe	13	0.04
	Deletion frameshift	5	0.02
	Complex	39	0.12
	Other	172	0.52
	Total	33263	100

Querying Cancer Cell Line in COSMIC

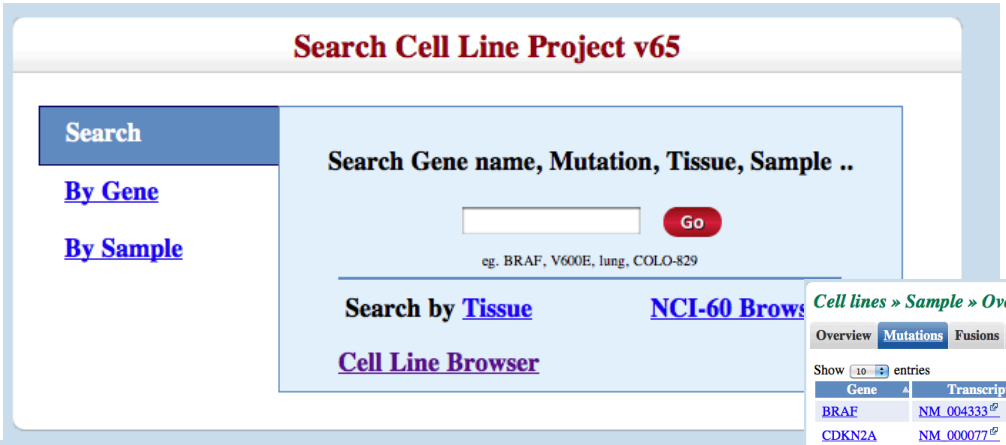

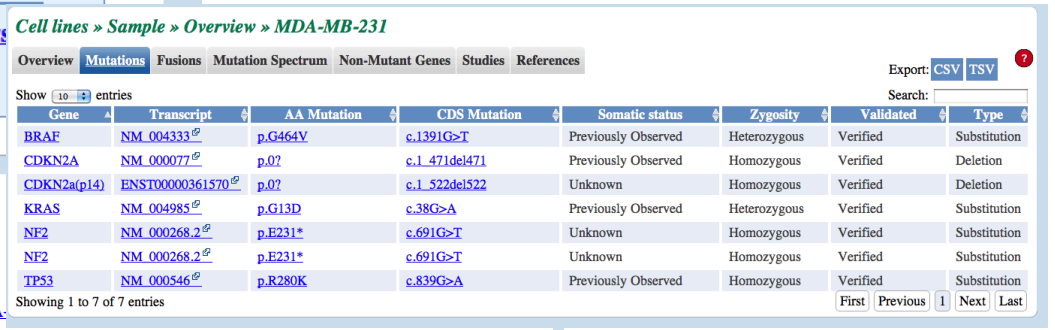

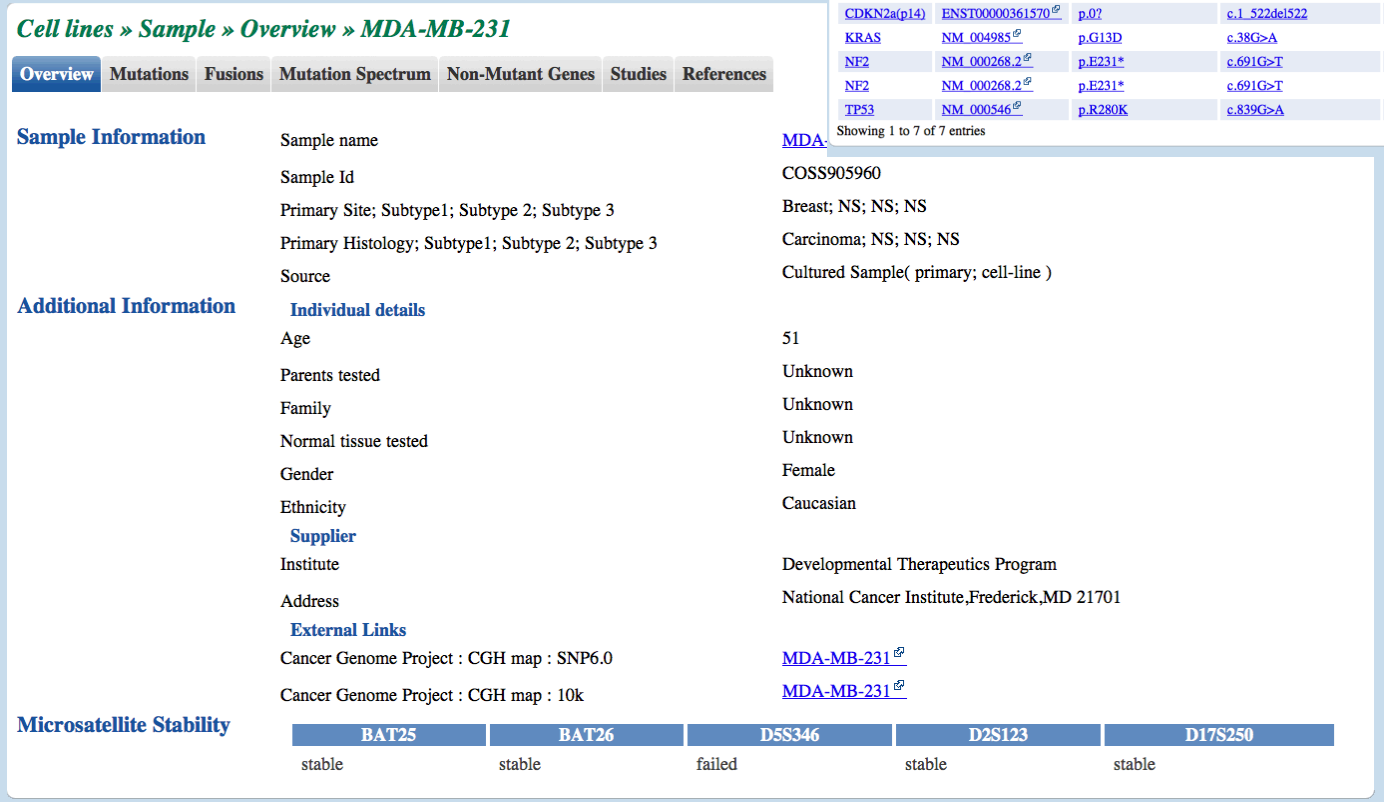

Genomics of Drug Sensitivity in Cancer (GDSC COSMIC)

Genomics of Drug Sensitivity in Cancer

Home | Compounds | Genes | Cell Lines | About | News | Downloads | Documentation

wellcome trust sanger institute

MASSACHUSETTS GENERAL HOSPITAL CANCER CENTER

The Genomics of Drug Sensitivity in Cancer project is an academic research program to identify molecular features of cancers that predict response to anti-cancer drugs.

Browse our data

Compounds

Cancer Genes

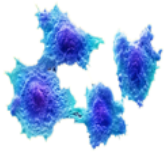

Cell Lines

Please be aware that our website and results are part of an ongoing project. These webpages are updated frequently and our results are not final or complete.

Search

Enter drug, gene or ce | Search

e.g. Docetaxel, RP-56976, BRAF, COLO-829

What's new!

Release 5 (June 2014)

Sensitivity data can now be browsed by cell line. The cell line page shows the sensitivity across all drugs for each cell line using a z-score value.

Mailing List

To receive news and data release alert, please sign up Translation-announce

wellcome trust

The Genomics of Drug Sensitivity in Cancer Project is a collaboration between the Cancer Genome Project at the Wellcome Trust Sanger Institute (UK) and the Center for Molecular Therapeutics, Massachusetts General Hospital Cancer Center (USA). This work is funded by the Wellcome Trust.

This site is hosted by the Wellcome Trust Sanger Institute.

Contact us | Cookies policy | Terms & Conditions.

http://www.cancerrxgene.org/

ARTICLE

doi:10.1038/nature11005

Systematic identification of genomic markers of drug sensitivity in cancer cells

Mathew J. Garnett[1]*, Elena J. Edelman[2]*, Sonja J. Heidorn[1]*, Chris D. Greenman[1]†, Anahita Dastur[2], King Wai Lau[1], Patricia Greninger[2], I. Richard Thompson[1], Xi Luo[2], Jorge Soares[1], Qingsong Liu[3,4], Francesco Iorio[1,5], Didier Surdez[6], Li Chen[2], Randy J. Milano[2], Graham R. Bignell[1], Ah T. Tam[2], Helen Davies[1], Jesse A. Stevenson[2], Syd Barthorpe[1], Stephen R. Lutz[2], Fiona Kogera[1], Karl Lawrence[1], Anne McLaren-Douglas[1], Xeni Mitropoulos[2], Tatiana Mironenko[1], Helen Thi[2], Laura Richardson[1], Wenjun Zhou[3,4], Frances Jewitt[1], Tinghu Zhang[3,4], Patrick O'Brien[1], Jessica L. Boisvert[2], Stacey Price[1], Wooyoung Hur[3,4], Wanjuan Yang[1], Xianming Deng[3,4], Adam Butler[1], Hwan Geun Choi[3,4], Jae Won Chang[3,4], Jose Baselga[2], Ivan Stamenkovic[7], Jeffrey A. Engelman[2], Sreenath V. Sharma[2]†, Olivier Delattre[6], Julio Saez-Rodriguez[5], Nathanael S. Gray[3,4], Jeffrey Settleman[2], P. Andrew Futreal[1], Daniel A. Haber[2,8], Michael R. Stratton[1], Sridhar Ramaswamy[2], Ultan McDermott[1] & Cyril H. Benes[2]

639 cell lines treated with 130 drugs

Clinical responses to anticancer therapies are often restricted to a subset of patients. In some cases, mutated cancer genes are potent biomarkers for responses to targeted agents. Here, to uncover new biomarkers of sensitivity and resistance to cancer therapeutics, we screened a panel of several hundred cancer cell lines—which represent much of the tissue-type and genetic diversity of human cancers—with 130 drugs under clinical and preclinical investigation. In aggregate, we found that mutated cancer genes were associated with cellular response to most currently available cancer drugs. Classic oncogene addiction paradigms were modified by additional tissue-specific or expression biomarkers, and some frequently mutated genes were associated with sensitivity to a broad range of therapeutic agents. Unexpected relationships were revealed, including the marked sensitivity of Ewing's sarcoma cells harbouring the *EWS* (also known as *EWSR1*)-*FLI1* gene translocation to poly(ADP-ribose) polymerase (PARP) inhibitors. By linking drug activity to the functional complexity of cancer genomes, systematic pharmacogenomic profiling in cancer cell lines provides a powerful biomarker discovery platform to guide rational cancer therapeutic strategies.

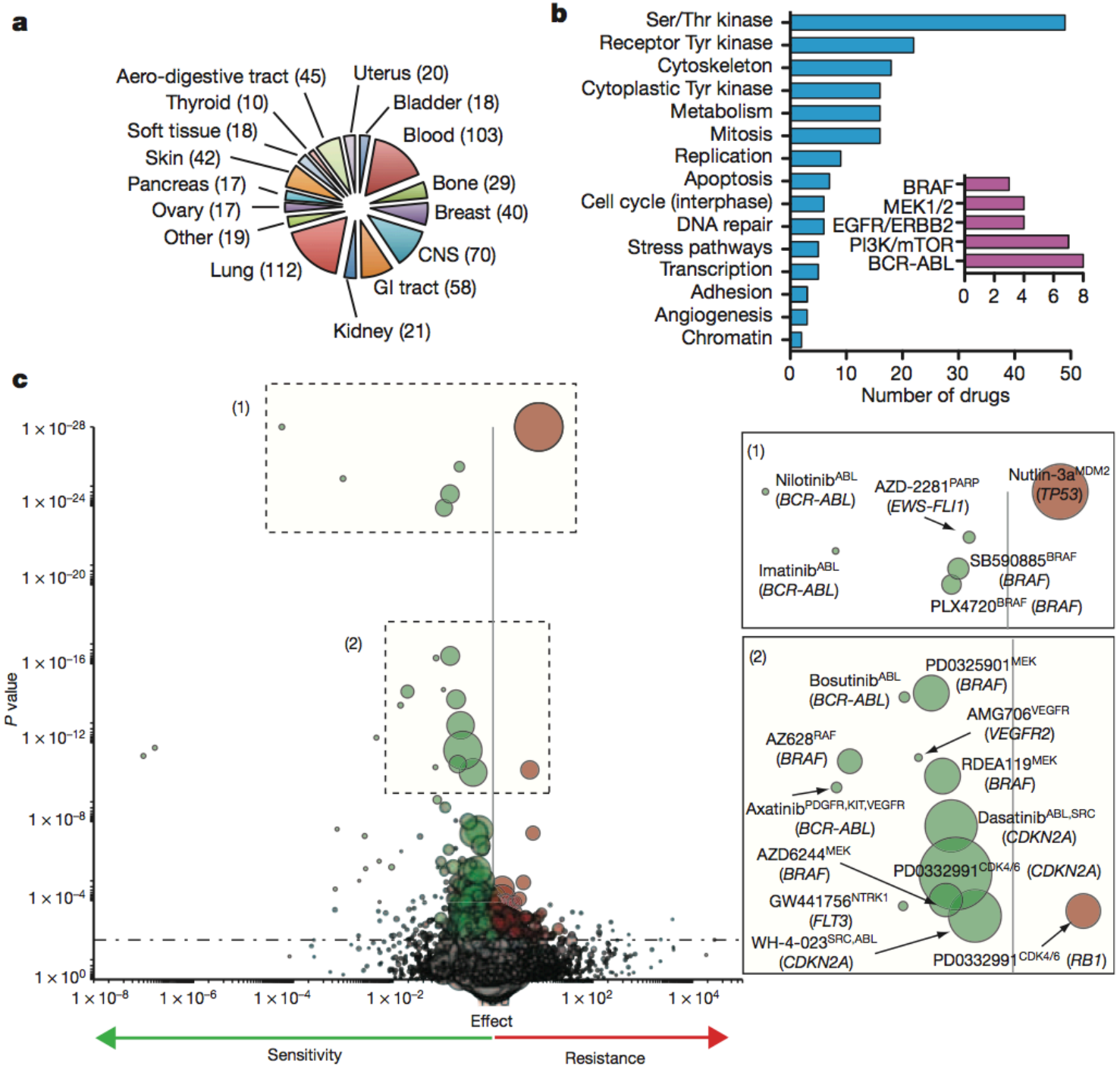
a
Aero-digestive tract (45)
Uterus (20)
Thyroid (10)
Bladder (18)
Soft tissue (18)
Blood (103)
Skin (42)
Pancreas (17)
Bone (29)
Ovary (17)
Breast (40)
Other (19)
CNS (70)
Lung (112)
GI tract (58)
Kidney (21)
b
Ser/Thr kinase
Receptor Tyr kinase
Cytoskeleton
Cytoplastic Tyr kinase
Metabolism
Mitosis
Replication
Apoptosis
Cell cycle (interphase)
DNA repair
Stress pathways
Transcription
Adhesion
Angiogenesis
Chromatin
0 10 20 30 40 50
Number of drugs
BRAF
MEK1/2
EGFR/ERBB2
PI3K/mTOR
BCR-ABL
0 2 4 6 8
c
(1)
(2)
P value
1 × 10−28
1 × 10−24
1 × 10−20
1 × 10−16
1 × 10−12
1 × 10−8
1 × 10−4
1 × 10^0
1 × 10−8 1 × 10−6 1 × 10−4 1 × 10−2 1 × 10^2 1 × 10^4
Effect
Sensitivity
Resistance
(1)
Nilotinib ABL (BCR-ABL)
AZD-2281 PARP (EWS-FLI1)
Nutlin-3a MDM2 (TP53)
Imatinib ABL (BCR-ABL)
SB590885 BRAF (BRAF)
PLX4720 BRAF (BRAF)
(2)
Bosutinib ABL (BCR-ABL)
PD0325901 MEK (BRAF)
AMG706 VEGFR (VEGFR2)
AZ628 RAF (BRAF)
RDEA119 MEK (BRAF)
Axatinib PDGFR,KIT,VEGFR (BCR-ABL)
Dasatinib ABL,SRC (CDKN2A)
AZD6244 MEK (BRAF)
PD0332991 CDK4/6 (CDKN2A)
GW441756 NTRK1 (FLT3)
WH-4-023 SRC,ABL (CDKN2A)
PD0332991 CDK4/6 (RB1)

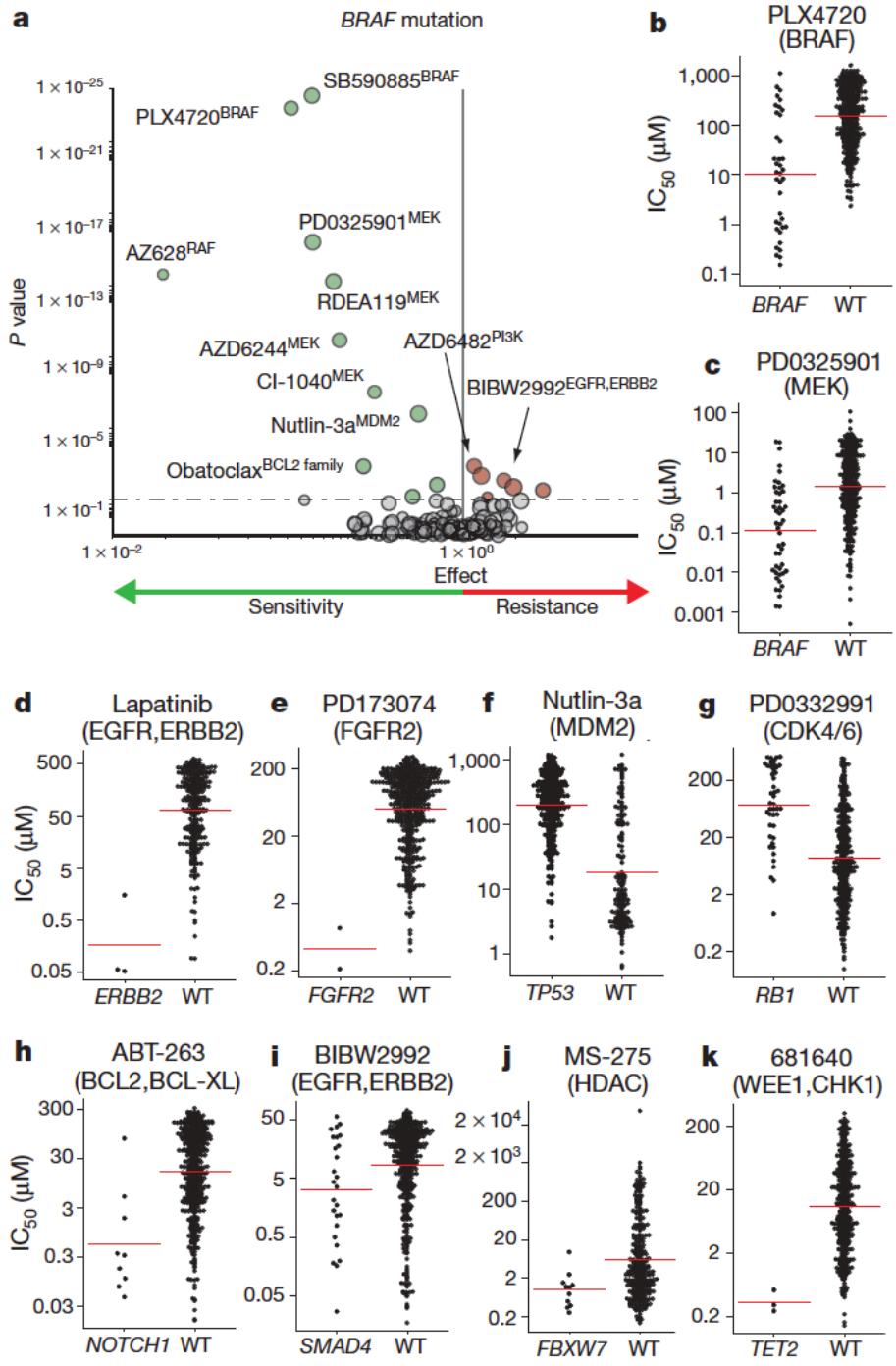
a
BRAF mutation
SB590885BRAF
PLX4720BRAF
PD0325901MEK
AZ628RAF
RDEA119MEK
AZD6244MEK
AZD6482PI3K
CI-1040MEK
BIBW2992EGFR,ERBB2
Nutlin-3aMDM2
ObatoclaxBCL2 family
P value
1 × 10−25
1 × 10−21
1 × 10−17
1 × 10−13
1 × 10−9
1 × 10−5
1 × 10−1
1 × 10−2
1 × 100
Effect
Sensitivity
Resistance
b
PLX4720 (BRAF)
IC50 (μM)
1,000
100
10
1
0.1
BRAF
WT
c
PD0325901 (MEK)
100
10
1
0.1
0.01
0.001
BRAF
WT
d
Lapatinib (EGFR,ERBB2)
500
50
5
0.5
0.05
ERBB2
WT
e
PD173074 (FGFR2)
200
20
2
0.2
FGFR2
WT
f
Nutlin-3a (MDM2)
1,000
100
10
1
TP53
WT
g
PD0332991 (CDK4/6)
200
20
2
0.2
RB1
WT
h
ABT-263 (BCL2,BCL-XL)
300
30
3
0.3
0.03
NOTCH1
WT
i
BIBW2992 (EGFR,ERBB2)
50
5
0.5
0.05
SMAD4
WT
j
MS-275 (HDAC)
2 × 104
2 × 103
200
20
2
0.2
FBXW7
WT
k
681640 (WEE1,CHK1)
200
20
2
0.2
TET2
WT

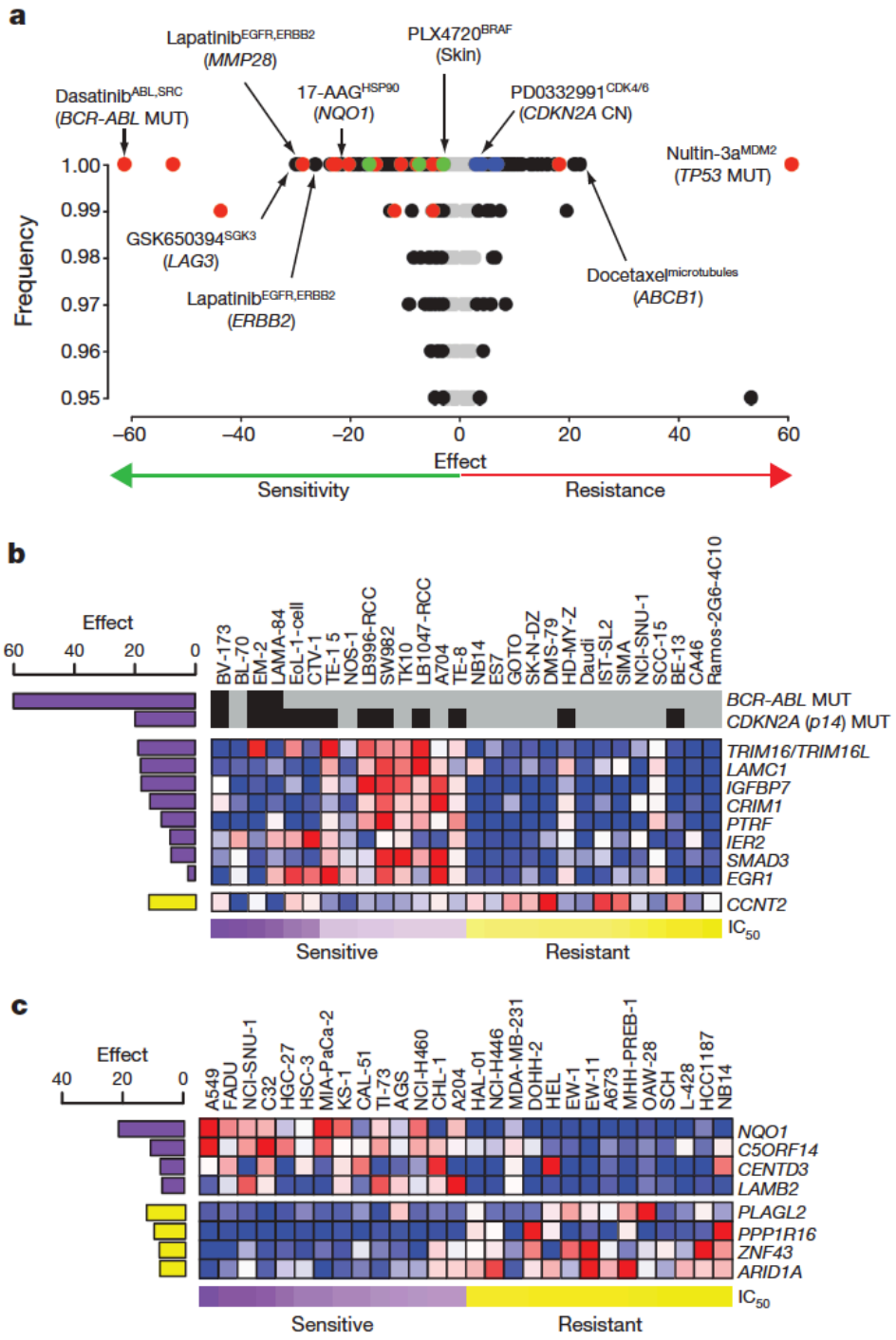
a
Lapatinib EGFR,ERBB2 (MMP28)
PLX4720 BRAF (Skin)
Dasatinib ABL,SRC (BCR-ABL MUT)
17-AAG HSP90 (NQO1)
PD0332991 CDK4/6 (CDKN2A CN)
Nultin-3a MDM2 (TP53 MUT)
GSK650394 SGK3 (LAG3)
Lapatinib EGFR,ERBB2 (ERBB2)
Docetaxel microtubules (ABCB1)
Frequency
1.00
0.99
0.98
0.97
0.96
0.95
−60
−40
−20
0
20
40
60
Effect
Sensitivity
Resistance
b
Effect
60
40
20
0
BV-173
BL-70
EM-2
LAMA-84
EoL-1-cell
CTV-1
TE-1 5
NOS-1
LB996-RCC
SW982
TK10
LB1047-RCC
A704
TE-8
NB14
ES7
GOTO
SK-N-DZ
DMS-79
HD-MY-Z
Daudi
IST-SL2
SIMA
NCI-SNU-1
SCC-15
BE-13
CA46
Ramos-2G6-4C10
BCR-ABL MUT
CDKN2A (p14) MUT
TRIM16/TRIM16L
LAMC1
IGFBP7
CRIM1
PTRF
IER2
SMAD3
EGR1
CCNT2
IC50
Sensitive
Resistant
c
Effect
40
20
0
A549
FADU
NCI-SNU-1
C32
HGC-27
HSC-3
MIA-PaCa-2
KS-1
CAL-51
TI-73
AGS
NCI-H460
CHL-1
A204
HAL-01
NCI-H446
MDA-MB-231
DOHH-2
HEL
EW-1
EW-11
A673
MHH-PREB-1
OAW-28
SCH
L-428
HCC1187
NB14
NQO1
C5ORF14
CENTD3
LAMB2
PLAGL2
PPP1R16
ZNF43
ARID1A
IC50
Sensitive
Resistant

Analytical Framework for Biomarkers Discovery in GDSC

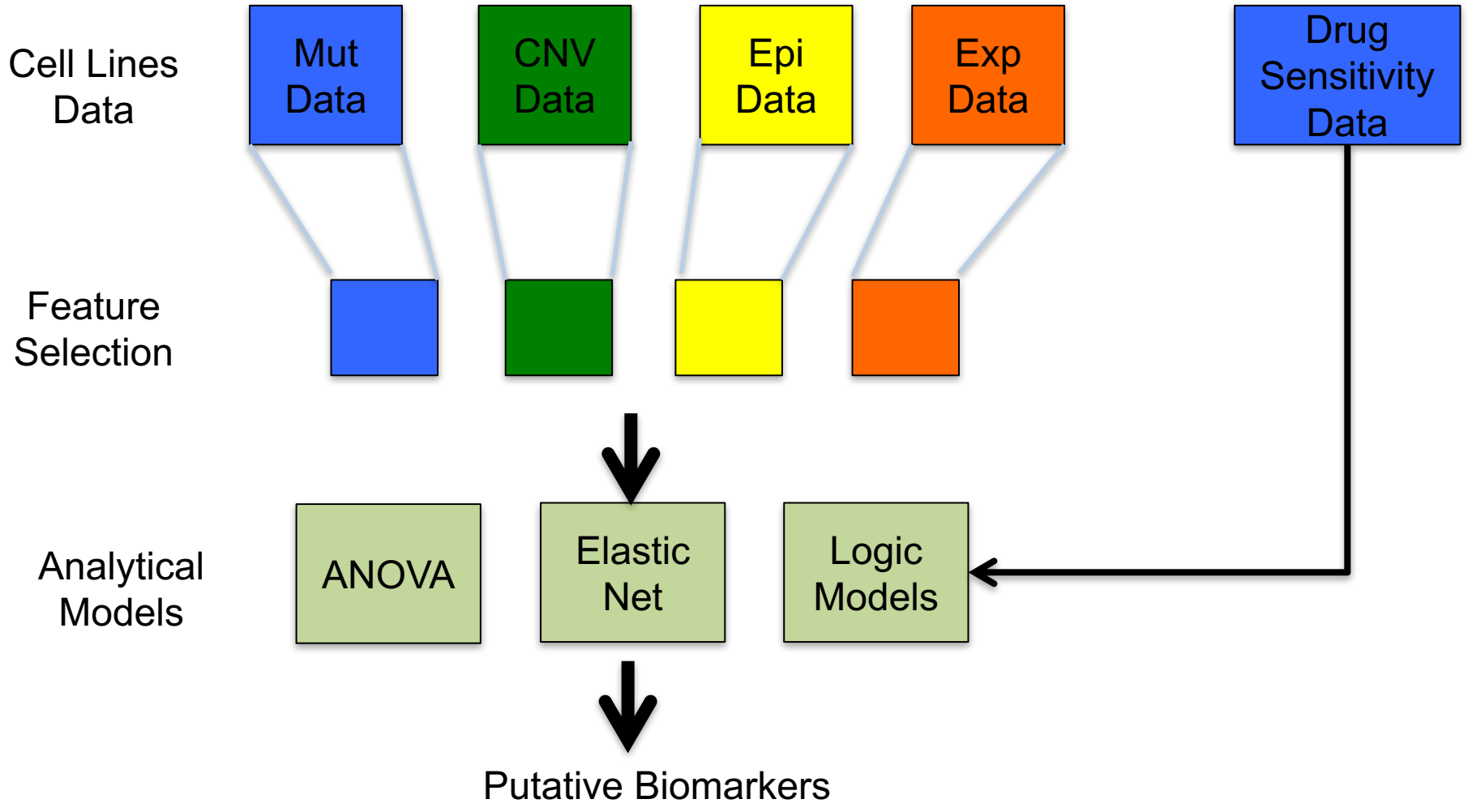

Querying Drug in GDSC

Drug : Erlotinib

Targets	EGFR
PubCHEM	176870
Legacy data	Legacy data for Erlotinib

Help

- Description of statistical approaches
- Interpreting Volcano plots
- Interpreting EN heatmaps
- Detail of download files

Analysis of drug sensitivity data

Overview | Volcano plot | Volcano Data | Elastic net | Scatter plots | Download data

IC50 | IC90 | IC75 | IC25 | AUC

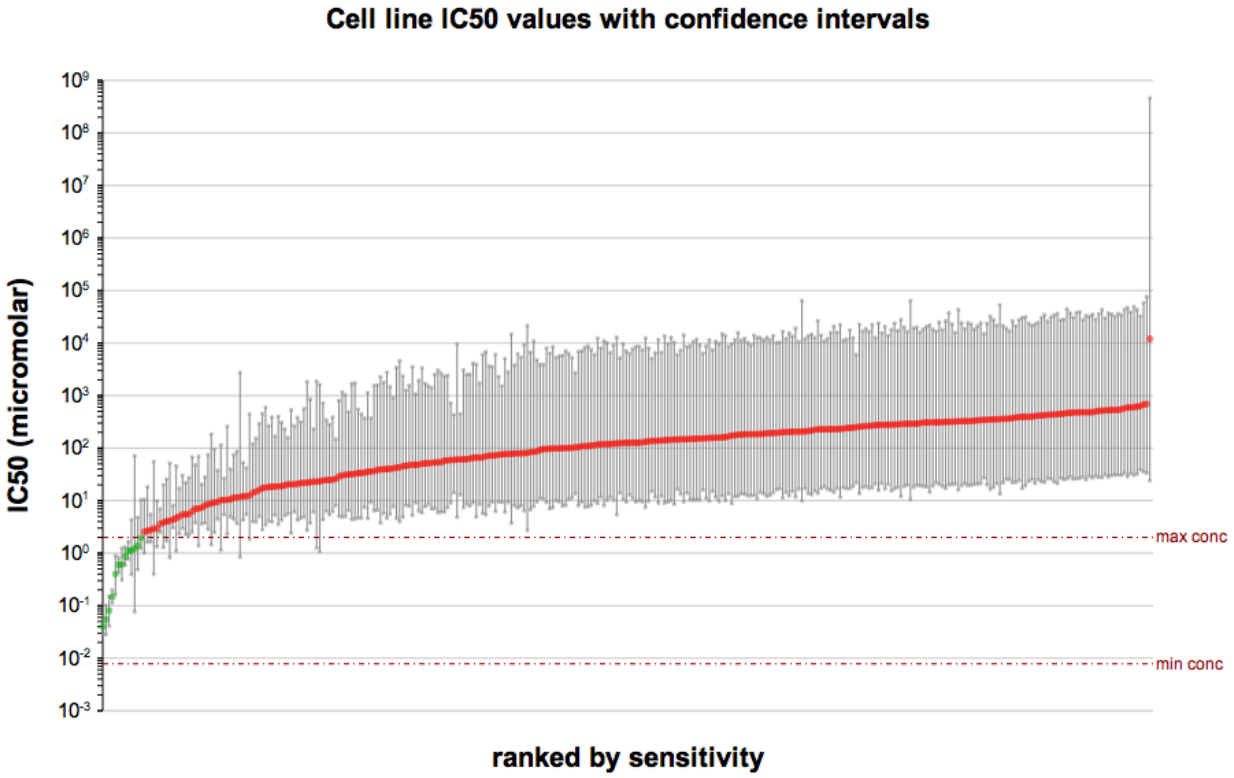

Number of cell lines screened	329
Maximum IC50	1.20e+4
Geometric mean	78.9
Minimum IC50	0.0400
Min screening concentration	0.00781
Max screening concentration	2.00

Download SVG | Download PNG

Volcano Plot

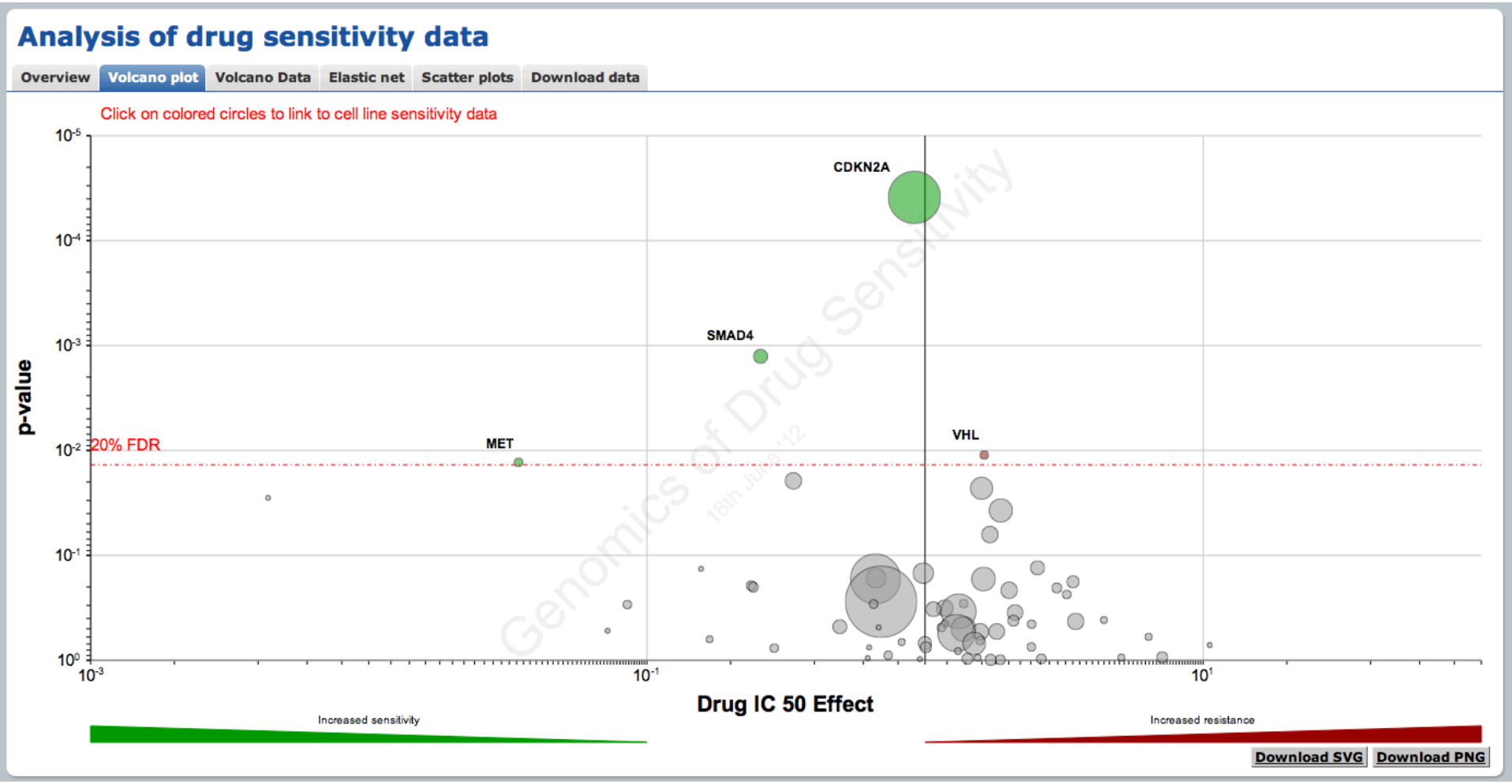

Querying Drug in GDSC

Analysis of drug sensitivity data

Overview | Volcano plot | Volcano Data | Elastic net | Scatter plots | Download data

Filter: 64 entries 1 2 3 25 per page CSV TAB XLS

Gene	Effect	P-value	No. of mutations
CDKN2A	0.916	0.0000387	112
SMAD4	0.256	0.00127	8
VHL	1.63	0.0110	3
MET	0.0345	0.0130	3
NF2	0.336	0.0195	11
NRAS	1.60	0.0229	20
WT1	0.00434	0.0283	1
KRAS	1.87	0.0373	22
CCND1	1.71	0.0633	11
MLH1	2.54	0.131	8
SETD2	0.157	0.134	1
KDM6A	0.985	0.148	17
PIK3CA	0.667	0.165	16
CDKN2a(p14)	0.663	0.168	102
BRAF	1.62	0.168	23
CDKN2C	3.41	0.178	6
BCR_ABL	0.237	0.195	4
MDM2	0.241	0.201	4
MSH2	2.98	0.204	4
MLLT3	2.01	0.215	11
FGFR2	3.23	0.236	3
TP53	0.695	0.276	209
SMARCA4	1.38	0.288	3
JAK2	0.653	0.291	3
BRCA2	0.0851	0.294	3

Analysis of drug sensitivity data

Overview | Volcano plot | Volcano Data | Elastic net | Scatter plots | Download data

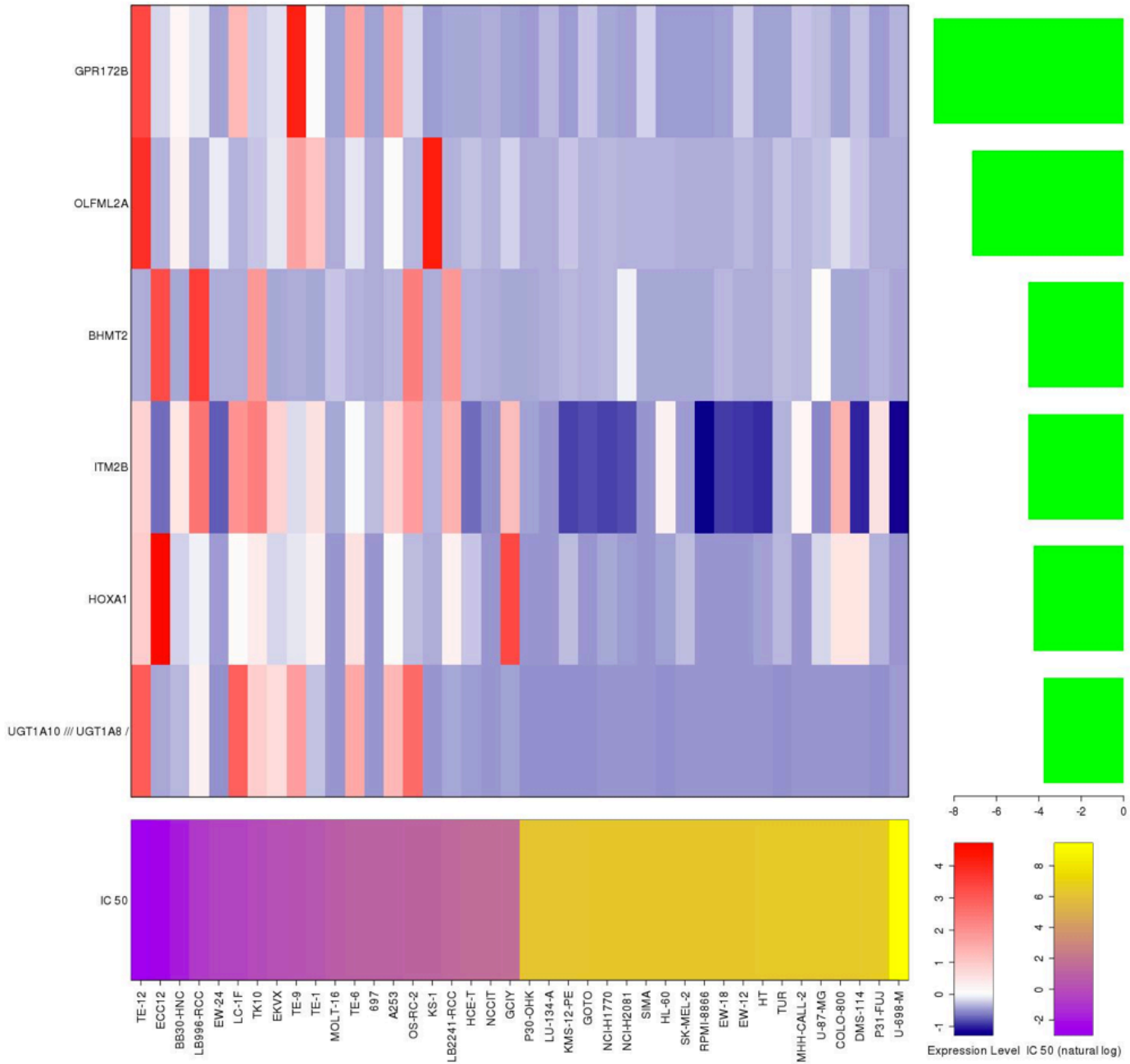

Correlating Mutation with Drug

Analysis of drug sensitivity data

Overview | Volcano plot | Volcano Data | Elastic net | Scatter plots | Download data

Select gene to plot

- CDKN2A
- SMAD4
- VHL
- MET

CDKN2A

By mutation type | By tissue type

Click on circles to link to cell line information

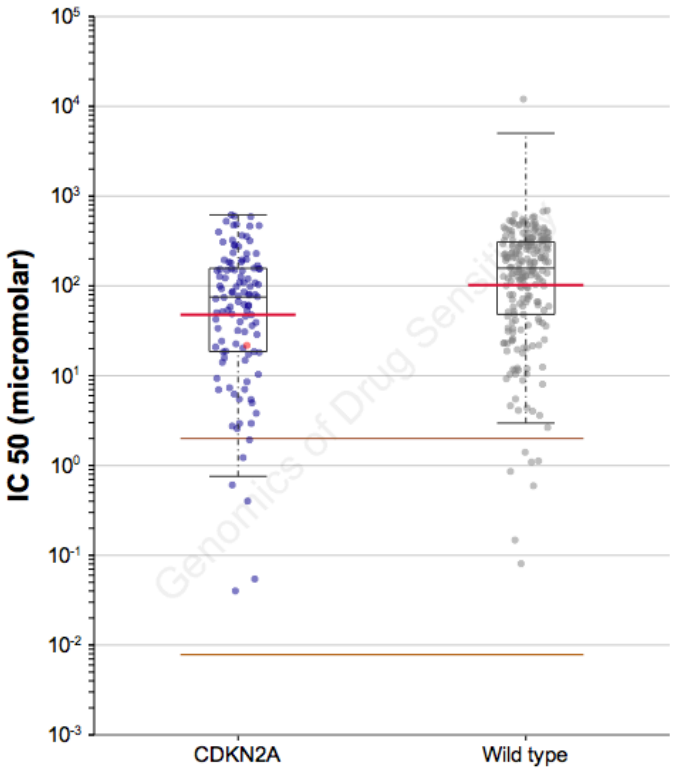

Download SVG | Download PNG

Screening concentration: 0.0078125 (lower brown line) - 2.0000 (upper brown line)

	CDKN2A	Wild type	Selected
Number of cell lines	112 of 112	217 of 217	
Upper quartile	156.99	308.74	
Median	75.207	157.81	
Geometric mean (red line)	47.741	102.18	
Lower quartile	18.582	48.156	
Mann-Whitney test p value	0.000019161		
Coding mutation	111	0	☑
Deletion	1	0	☑
Amplification	0	0	☑

Check all | Clear all

Correlating Mutation in Specific Tumor Type

Analysis of drug sensitivity data

Overview | Volcano plot | Volcano Data | Elastic net | Scatter plots | Download data

Select gene to plot

- CDKN2A
- SMAD4
- VHL
- MET

CDKN2A

By mutation type | By tissue type

Click on circles to link to cell line information

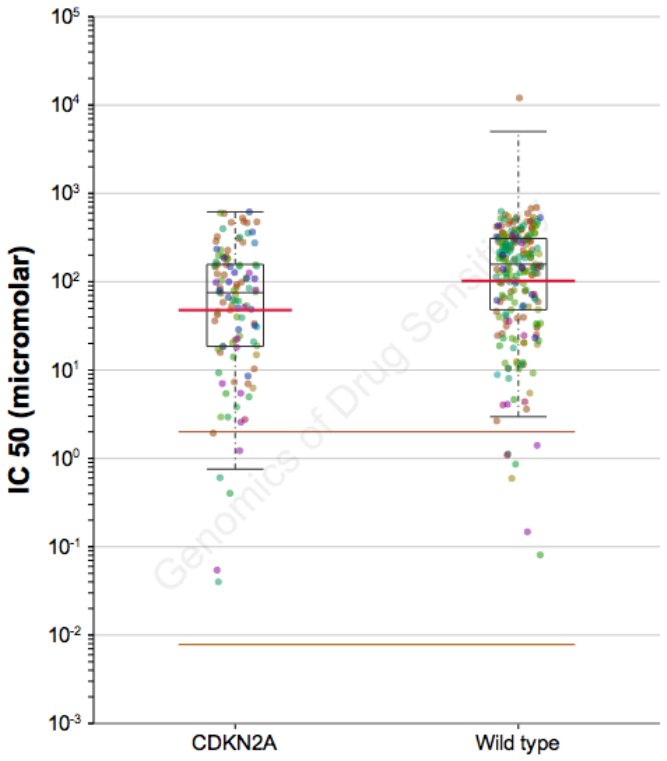

Download SVG | Download PNG

Screening concentration: 0.0078125 (lower brown line) - 2.0000 (upper brown line)

	CDKN2A	Wild type	Selected
Number of cell lines	112 of 112	217 of 217	
Upper quartile	156.99	308.74	
Median	75.207	157.81	
Geometric mean (red line)	47.741	102.18	
Lower quartile	18.582	48.156	
Mann-Whitney test p value	0.000019161		
Bladder	1	1	☑
Blood	33	66	☑
Bone	5	13	☑
Breast	0	12	☑
Central Nervous System	18	29	☑
Gastro-intestinal tract	4	21	☑
Kidney	7	2	☑
Lung	13	46	☑
Ovary	1	2	☑
Pancreas	2	0	☑
Skin	12	6	☑
Soft tissue	3	5	☑
Thyroid	2	0	☑
Upper aerodigestive	10	4	☑
Uterus	0	5	☑
Other tissue type	1	5	☑

Check all | Clear all

High Confidence Drivers

Comprehensive identification of mutational cancer driver genes across 12 tumor types

David Tamborero[1]*, Abel Gonzalez-Perez[1]*, Christian Perez-Llamas[1], Jordi Deu-Pons[1], Cyriac Kandoth[2], Jüri Reimand[3], Michael S. Lawrence[4], Gad Getz[4], Gary D. Bader[3], Li Ding[2,5,6,7] & Nuria Lopez-Bigas[1,8]

A Signals of positive selection used to identify driver genes

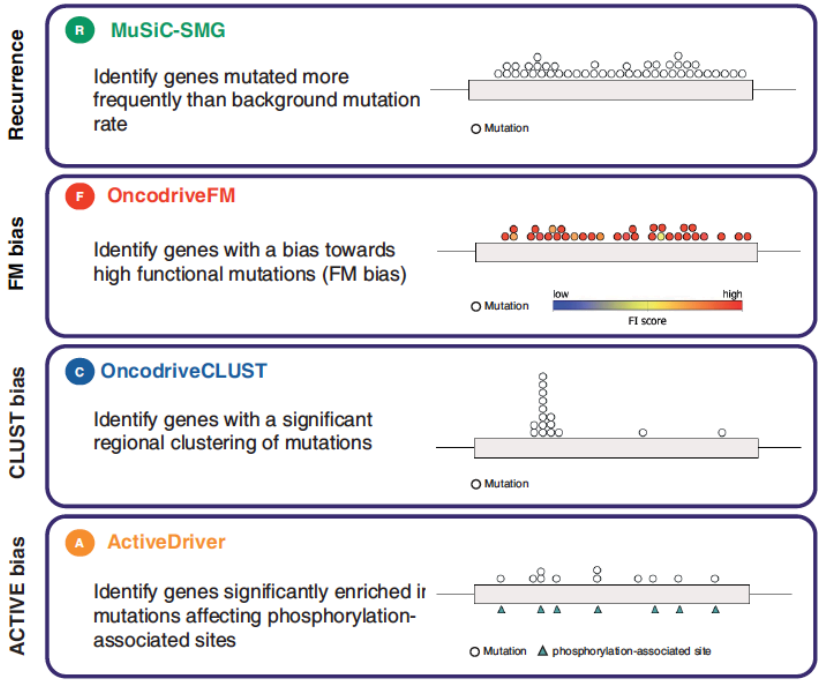

B High Confidence Drivers (HCDs) detected by each method

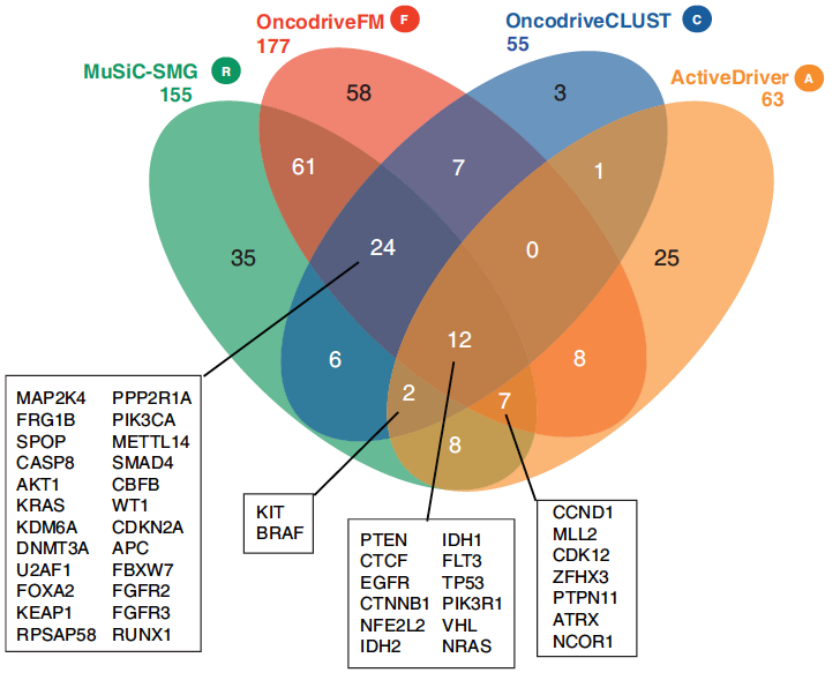

Stringent Filters using HCD

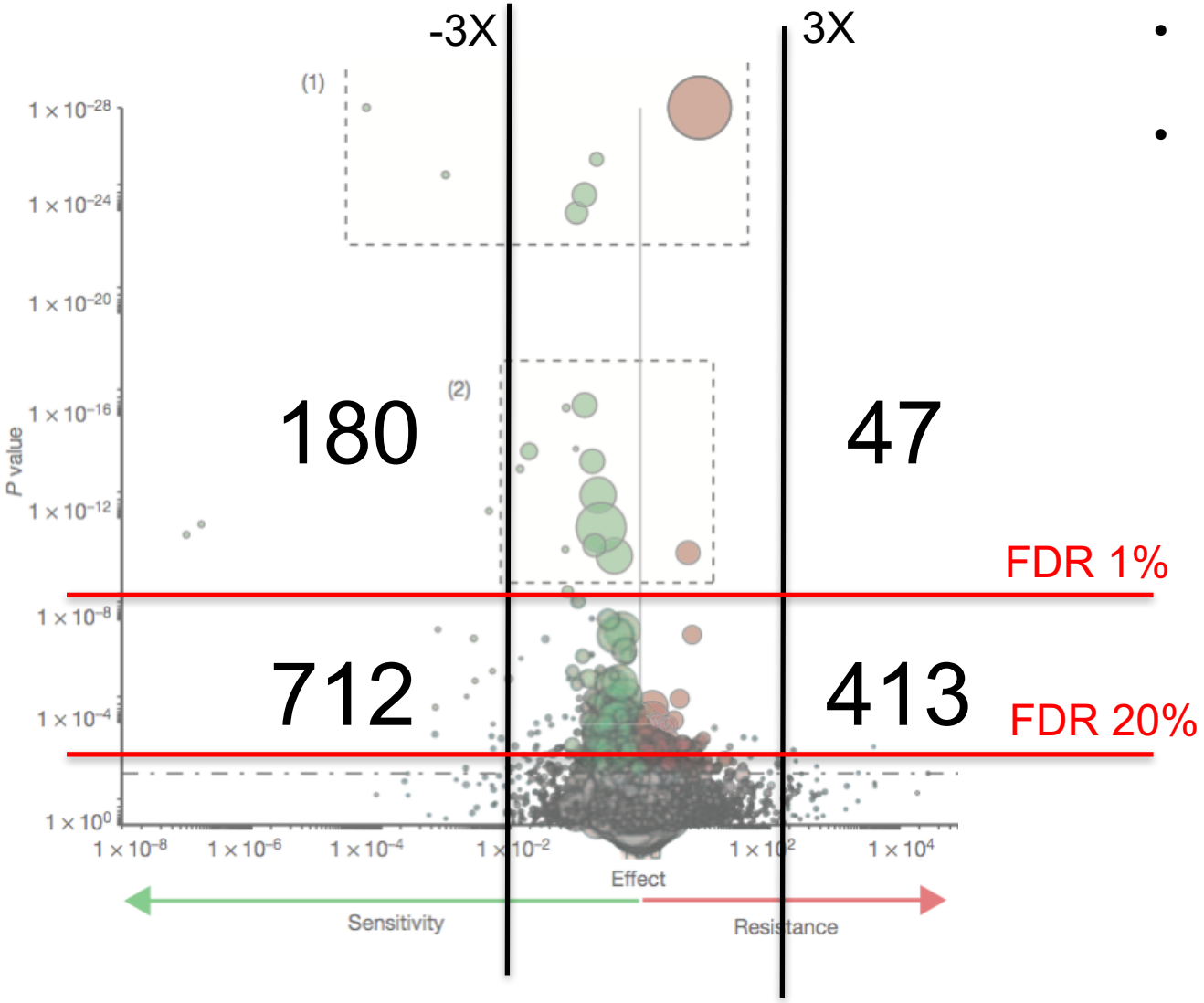

- 143,000 drug-gene interactions
- 2,286 significance associations ($p < 0.05$, FDR < 20%)

GDSC 2.0

A Landscape of Pharmacogenomic Interactions in Cancer

Francesco Iorio,[1,2,20] Theo A. Knijnenburg,[3,4,20] Daniel J. Vis,[4,20] Graham R. Bignell,[2,20] Michael P. Menden,[1,5,20] Michael Schubert,[1] Nanne Aben,[4,6] Emanuel Gonçalves,[1] Syd Barthorpe,[2] Howard Lightfoot,[2] Thomas Cokelaer,[1,2,17] Patricia Greninger,[7] Ewald van Dyk,[4] Han Chang,[8] Heshani de Silva,[8] Holger Heyn,[9] Xianming Deng,[10,11,18] Regina K. Egan,[7] Qingsong Liu,[10,11] Tatiana Mironenko,[2] Xeni Mitropoulos,[7] Laura Richardson,[2] Jinhua Wang,[10,11] Tinghu Zhang,[10,11] Sebastian Moran,[9] Sergi Sayols,[9,19] Maryam Soleimani,[2] David Tamborero,[12] Nuria Lopez-Bigas,[12,13] Petra Ross-Macdonald,[8] Manel Esteller,[9,13,14] Nathanael S. Gray,[10,11] Daniel A. Haber,[7,15] Michael R. Stratton,[2] Cyril H. Benes,[7] Lodewyk F.A. Wessels,[4,6,16,21] Julio Saez-Rodriguez,[1,5,21] Ultan McDermott,[2,21,*] and Mathew J. Garnett[2,21,*]

Highlights

- We integrate heterogeneous molecular data of 11,289 tumors and 1,001 cell lines
- We measure the response of 1,001 cancer cell lines to 265 anti-cancer drugs
- We uncover numerous oncogenic aberrations that sensitize to an anti-cancer drug
- Our study forms a resource to identify therapeutic options for cancer sub-populations

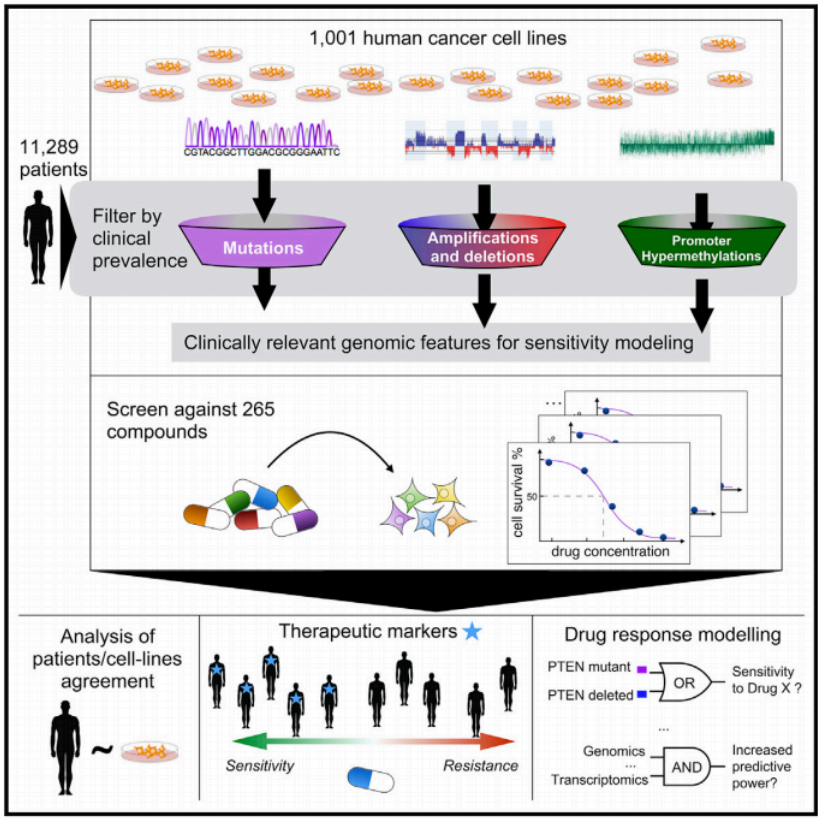

GDSC Download

Resources

This page allows access to all of our drug sensitivity data and the genomic datasets used in our analyses.

Data File Download Tool

> **Download dataset of your choice using** Data Download Tool .

Data Files

Data Class	Data Type	Objects	Brief description (with links)	Details	Last updated
Annotated	Reference	Cell lines	Annotated list of Cell lines	List of Cell lines included in the study with molecular and drug-response data availability, microsatellite instability status, growth properties and media, TCGA and COSMIC tissue classification	July 4th 2016
Annotated	Reference	Drugs	Screened compounds	List of screened drugs including targets, targeted process/pathways, clinical stage	July 4th 2016
Annotated	Reference	Cell lines	Shared cell lines and drugs (GDSC, CCLE & CTRP)	To aid comparison we list the cell lines and drugs within the GDSC study that are also in the CCLE (Barretina et al, Nature 2012) and/or CTRP (Seashore-Ludlow et al, Cancer Discovery 2015) studies	July 4th 2016
Copy number	Raw	Cell lines	Copy number data for Cell lines	Affymetrix SNP6 cel files at EGA (EGAS00001000978)	July 4th 2016
Copy number	Preprocessed	Cell lines	Gene level copy number data	Copy number data for all genes across all samples derived from PICNIC analysis of Affymetrix SNP6 segmentation data (available via COSMIC Cell Lines Project)	July 4th 2016
Copy number	Preprocessed	Cell lines	RACS in cell lines	Recurrently altered chromosomal segments in cell lines identified from the analysis of patient tumours. As described in Iorio F, et al. Cell. 2016	July 4th 2016
Copy number	Preprocessed	Cell lines	RACSs CNV BEMs for cell lines	Binary event matrix with status in cell lines of recurrently altered chromosomal segments (RACS) identified from the analysis of patient tumours. As described in Iorio F, et al. Cell. 2016.	July 4th 2016
Drug	Raw	Cell lines Drugs	compound sensitivity data for Cell lines	GDSC drug screening data	July 4th 2016
Drug	Preprocessed	Cell lines/Drugs	log(IC50) and AUC values	Natural log half maximal inhibitory concentration (IC50) and Area under the dose-response curve (AUCs) values for all screened cell line/drug combinations	July 4th 2016
Drug	Preprocessed	Cell lines/Drugs	ANOVA results	Results from Pan-Cancer and cancer specific ANOVA	July 4th 2016
Expression	Raw	Cell lines	Expression array data for Cell lines	Affymetrix Human Genome U219 array data at ArrayExpress (E-MTAB-3610)	July 4th 2016
Expression	Preprocessed	Cell lines	RMA normalised expression data for Cell lines	RMA normalised basal expression profiles for all the Cell lines	July 4th 2016
Methylation	Raw	Cell lines	DNA methylation data for Cell lines	IlluminaHumanMethylation450 BeadChip data at GEO (GSE68379)	July 4th 2016
Sequencing	Raw	Cell lines	WES data for Cell lines	Illumina HiSeq 2000 Whole exome sequence BAM files at EGA (EGAS00001000978)	July 4th 2016
Sequencing	Preprocessed	Cell lines	Cell-line sequence variants	List of genomic variants found in Cell lines by whole exome sequencing	July 4th 2016
Sequencing	Preprocessed	Cell lines	Sequencing BEMs for Cell lines	Binary event matrix with status in cell lines of selected cancer genes identified from the analysis of patient tumours. As described in Iorio F, et al. Cell. 2016.	July 4th 2016

Results of data analysis (from 'A landscape of pharmacogenomic interactions in cancer', Iorio F et al. Cell. 2016)

Click here to navigate linked webpages to access data and results associated with our publication "A landscape of Pharmacogenomic Interations in Cancer". We provide these as a resource but for our most current please access data through the GDSC website.

Archive

Click here to download all releases.

LETTER

doi:10.1038/nature11003

The Cancer Cell Line Encyclopedia enables predictive modelling of anticancer drug sensitivity

Jordi Barretina[1,2,3]†*, Giordano Caponigro[4]*, Nicolas Stransky[1]*, Kavitha Venkatesan[4]*, Adam A. Margolin[1]†*, Sungjoon Kim[5], Christopher J. Wilson[4], Joseph Lehár[4], Gregory V. Kryukov[1], Dmitriy Sonkin[4], Anupama Reddy[4], Manway Liu[4], Lauren Murray[1], Michael F. Berger[1]†, John E. Monahan[4], Paula Morais[1], Jodi Meltzer[4], Adam Korejwa[1], Judit Jané-Valbuena[1,2], Felipa A. Mapa[4], Joseph Thibault[5], Eva Bric-Furlong[4], Pichai Raman[4], Aaron Shipway[5], Ingo H. Engels[5], Jill Cheng[6], Guoying K. Yu[6], Jianjun Yu[6], Peter Aspesi Jr[4], Melanie de Silva[4], Kalpana Jagtap[4], Michael D. Jones[4], Li Wang[4], Charles Hatton[3], Emanuele Palescandolo[3], Supriya Gupta[1], Scott Mahan[1], Carrie Sougnez[1], Robert C. Onofrio[1], Ted Liefeld[1], Laura MacConaill[3], Wendy Winckler[1], Michael Reich[1], Nanxin Li[5], Jill P. Mesirov[1], Stacey B. Gabriel[1], Gad Getz[1], Kristin Ardlie[1], Vivien Chan[6], Vic E. Myer[4], Barbara L. Weber[4], Jeff Porter[4], Markus Warmuth[4], Peter Finan[4], Jennifer L. Harris[5], Matthew Meyerson[1,2,3], Todd R. Golub[1,3,7,8], Michael P. Morrissey[4]*, William R. Sellers[4]*, Robert Schlegel[4]* & Levi A. Garraway[1,2,3]*

978 cell lines treated with 24 drugs

compound name	other name
PHA-665752	
AZD6244	Selumetinib
Tozasertib	VX680
Nutlin-3	
Sorafenib	Nexavar
PF-2341066	Crizotinib
Staurosporine	
Docetaxel	Taxotere
Paclitaxel	Taxol
L-685458	
Irinotecan	Camptosar
Topotecan	Hycamtin
Cisplastin	
AEW541	
TAE684	
Panobinostat	Faridak
Erlotinib	Tarceva
PD-0332991	
Lapatinib	Tykerb
LBW242	
RAF265	
TKI258	Dovitinib
Vandetanib	Zactima
17-AAG	Tanespimycin
PD-0325901	
AZD0530	Saracatinib

Cancer Cell Lines Encyclopedia (CCLE) (Broad and Novartis)

CCLE Cancer Cell Line Encyclopedia

BROAD INSTITUTE

Username sign in
Password Forgot Password?
Register Why Register?

HOME | BROWSE▲ | ANALYSIS TOOLS | HELP▲ | ABOUT

Broad-Novartis Cancer Cell Line Encyclopedia (CCLE)

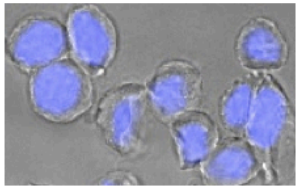

The Cancer Cell Line Encyclopedia (CCLE) project is a collaboration between the Broad Institute, and the Novartis Institutes for Biomedical Research and its Genomics Institute of the Novartis Research Foundation to conduct a detailed genetic and pharmacologic characterization of a large panel of human cancer models, to develop integrated computational analyses that link distinct pharmacologic vulnerabilities to genomic patterns and to translate cell line integrative genomics into cancer patient stratification. The CCLE provides public access to genomic data, analysis and visualization for about 1000 cell lines.

The CCLE is an ongoing project and some data are not complete yet. The CCLE website is subject to periodic changes and improvements. Please visit regularly!

This project is funded by Novartis.

What you can do on this portal

Search *Cell line, Annotation, Gene*

Search CCLE

Search for information

Enter a keyword to search for genes, news items and publications. Search results for a gene include links to annotations and analyses.

Data Sets

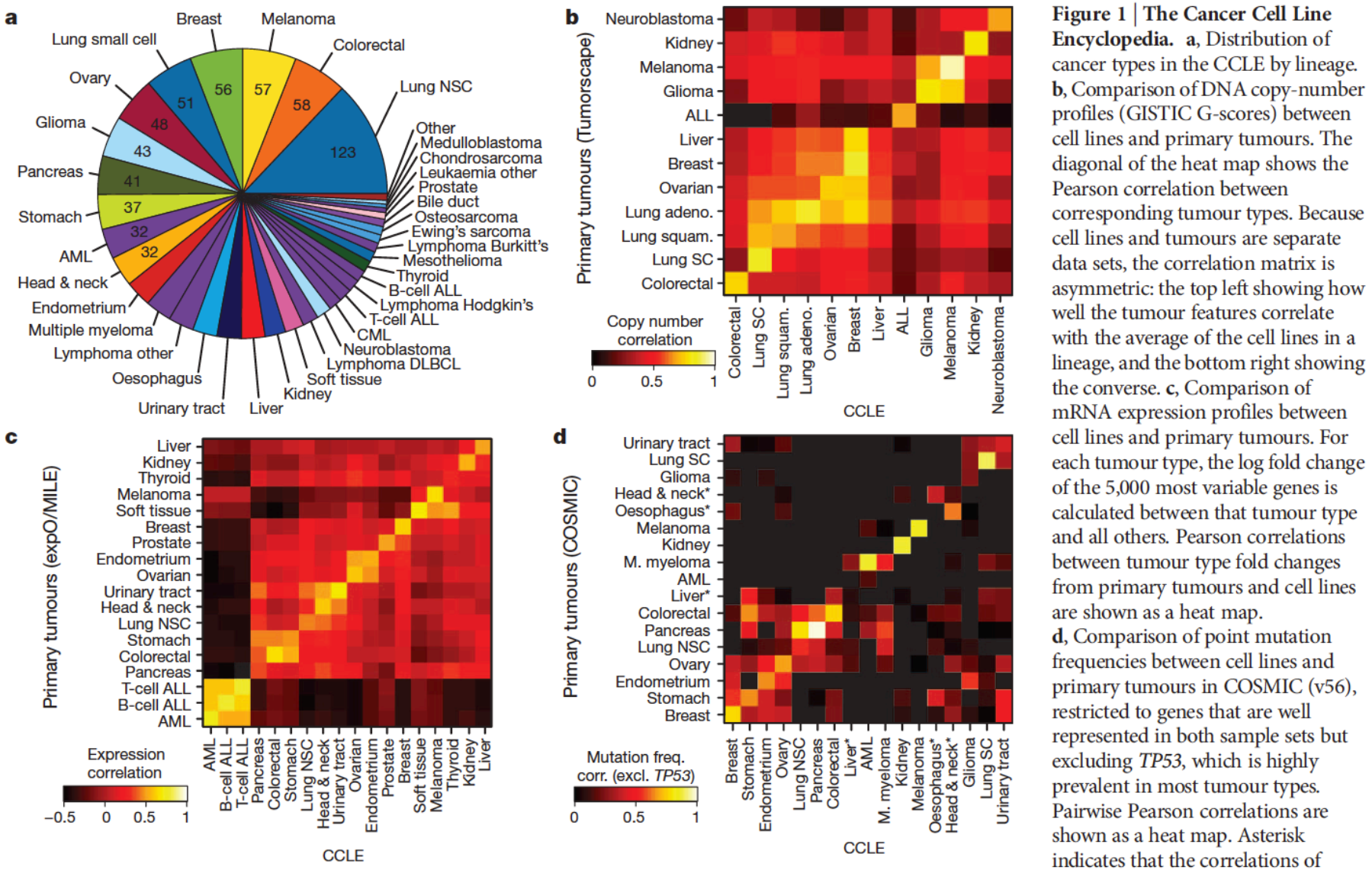

Figure 1 | The Cancer Cell Line Encyclopedia. **a**, Distribution of cancer types in the CCLE by lineage. **b**, Comparison of DNA copy-number profiles (GISTIC G-scores) between cell lines and primary tumours. The diagonal of the heat map shows the Pearson correlation between corresponding tumour types. Because cell lines and tumours are separate data sets, the correlation matrix is asymmetric: the top left showing how well the tumour features correlate with the average of the cell lines in a lineage, and the bottom right showing the converse. **c**, Comparison of mRNA expression profiles between cell lines and primary tumours. For each tumour type, the log fold change of the 5,000 most variable genes is calculated between that tumour type and all others. Pearson correlations between tumour type fold changes from primary tumours and cell lines are shown as a heat map. **d**, Comparison of point mutation frequencies between cell lines and primary tumours in COSMIC (v56), restricted to genes that are well represented in both sample sets but excluding *TP53*, which is highly prevalent in most tumour types. Pairwise Pearson correlations are shown as a heat map. Asterisk indicates that the correlations of oesophageal, liver, and head and neck cancer mutation frequencies are restored when including *TP53*.

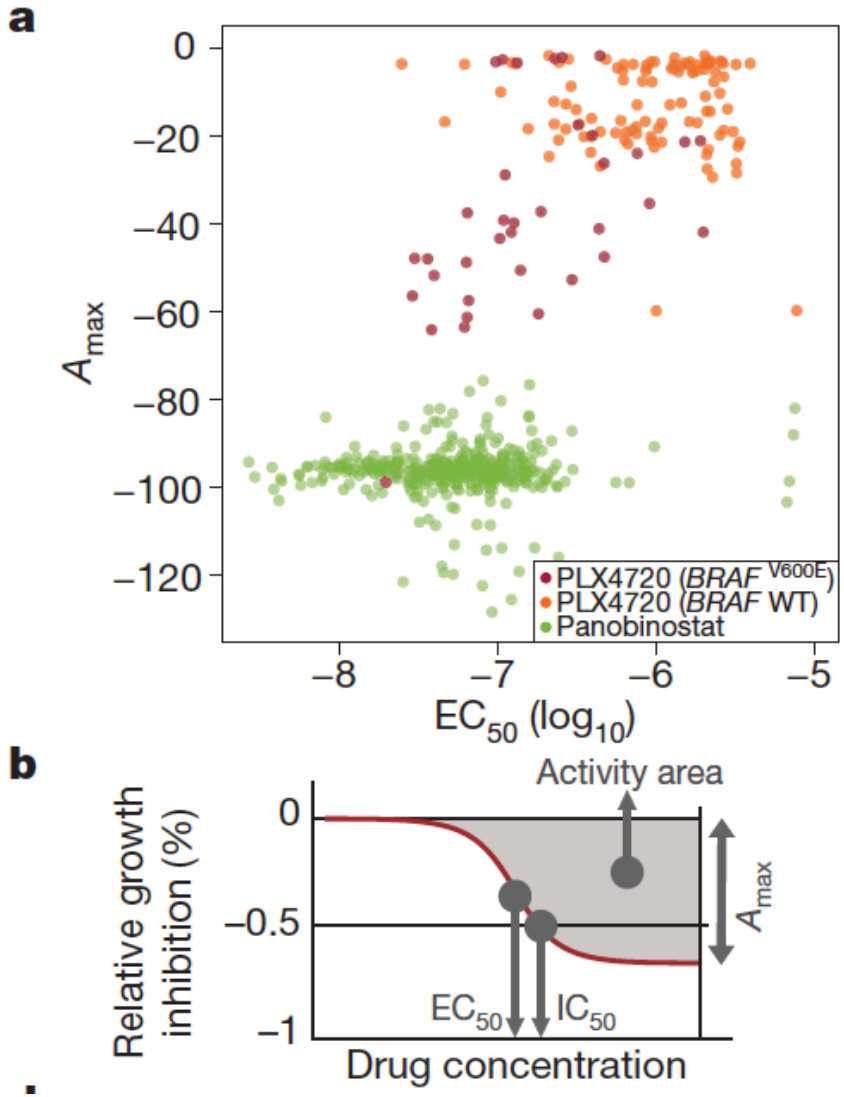
a
0
−20
−40
−60
−80
−100
−120
A_{max}
−8
−7
−6
−5
EC_{50} (log_{10})
PLX4720 (*BRAF* ^{V600E})
PLX4720 (*BRAF* WT)
Panobinostat
b
Activity area
Relative growth inhibition (%)
0
−0.5
−1
EC_{50}
IC_{50}
A_{max}
Drug concentration

Browse Data

PAGE INFO▲

Data Type

☑ Affy SNP ☑ Drug data ☑ Gene expression ☑ Mutation ☑ Sample annotation

check all uncheck all

Cancer Cell Line Encyclopedia (55.7GB)

Include previously released (deprecated) files

DNA Copy Number (41.3GB) Affy SNP (Published)

Affymetrix SNP6.0 arrays.
Raw Affymetrix CEL files were converted to a single value for each probe set representing a SNP allele or a copy number probe. Copy numbers were then inferred based upon estimating probe set specific linear calibration curves, followed by normalization by the most similar HapMap normal samples. Segmentation of normalized log2 ratios (specifically, log2(CN/2)) was performed using the circular binary segmentation (CBS) algorithm.

▶ Show Available Data

mRNA expression (8.0GB) Gene expression (Published)

Affymetrix U133+2 arrays.
Raw Affymetrix CEL files were converted to a single value for each probe set using Robust Multi-array Average (RMA) and normalized using quantile normalization. Either the original Affymetrix U133+2 CDF file or a redefined custom CDF file (ENTREZG - v15) was used for the summarization.

▶ Show Available Data

Cell Line Annotations (196.1KB) Sample annotation (Published)

▶ Show Available Data

Oncomap mutations (464.8KB) Mutation (Published)

Oncomap mutation data.
The mutations were assessed in 33 genes (381 specific mutations) using Oncomap 3.0 core. See the associated publication.

▶ Show Available Data

Hybrid capture sequencing (6.4GB) Mutation (In process)

List of mutations and indels in 1651 genes, determined by targeted massively parallel sequencing. Note: the hybrid capture process might yield sequences in genes outside of the target list; those were kept in the analysis and mutations in these genes are present in the files below.

▶ Show Available Data

Pharmacological profiling (8.0MB) Drug data (Published)

Pharmacologic profiles for 24 anticancer drugs across 504 cell lines.

▶ Show Available Data

mRNA expression (8.0GB) Gene expression (Published)

Affymetrix U133+2 arrays.
Raw Affymetrix CEL files were converted to a single value for each probe set using Robust Multi-array Average (RMA) and normalized using quantile normalization. Either the original Affymetrix U133+2 CDF file or a redefined custom CDF file (ENTREZG - v15) was used for the summarization.

▼ Show Available Data

CCLE_Expression_2012-09-29.res	589.6MB	17-Oct-2012	RMA-normalized mRNA expression data. (Affymetrix annotations)
CCLE_Expression_Entrez_2012-09-29.gct	167.2MB	17-Oct-2012	Gene-centric RMA-normalized mRNA expression data. (ENTREZG v15 CDF file, see the Brainarray website for more details about the probe set annotations; gct file format.
CCLE_Expression.Arrays.sif_2012-10-18.txt	124.6KB	18-Oct-2012	Expression arrays samples info file.
CCLE_Expression_Entrez_2012-10-18.res	204.6MB	18-Oct-2012	Gene-centric RMA-normalized mRNA expression data. (ENTREZG v15 CDF file, see the Brainarray website for more details about the probe set annotations; res file format)
CCLE_Expression_Entrez_IGV_2012-09-29.tdf	2.0GB	19-Oct-2012	Gene-centric RMA-normalized mRNA expression data (ENTREZG v15 CDF). This format is only meant to be used with the Integrative Genomics Viewer (IGV, available in the "Analysis tools" section) and the value for each probe set is median-centered and divided by the MAD (robust z-score).
CCLE_Expression.Arrays_2013-03-18.tar.gz	5.0GB	19-Mar-2013	Raw CEL files in a compressed archive.
CCLE_expression_CN_muts_GENEE_2010-04-16.gctx	63.4MB	18-Sep-2013	The gctx file contains the Affymetrix mRNA expression levels, DNA copy number, mutations and indels in 1651 genes by targeted massively parallel sequencing, pharmacologic profiles for 24 anticancer drugs, and cell line annotations.

Analysis

Pharmacological profiling (8.0MB) Drug data (Published)

Pharmacologic profiles for 24 anticancer drugs across 504 cell lines.

▼ Show Available Data

CCLE_NP24.2009_Drug_data_2012.02.20.csv	2.3MB	20-Jun-2012	Pharmacologic profiles for 24 anticancer drugs across 504 CCLE lines.
CCLE_NP24.2009_profiling_2012.02.20.csv	2.4KB	17-Apr-2012	List of the 24 drugs profiled across 504 CCLE lines.
CCLE_GNF_data_090613.xls	5.7MB	06-Sep-2013	

Analysis

Analysis Tools in CCLE

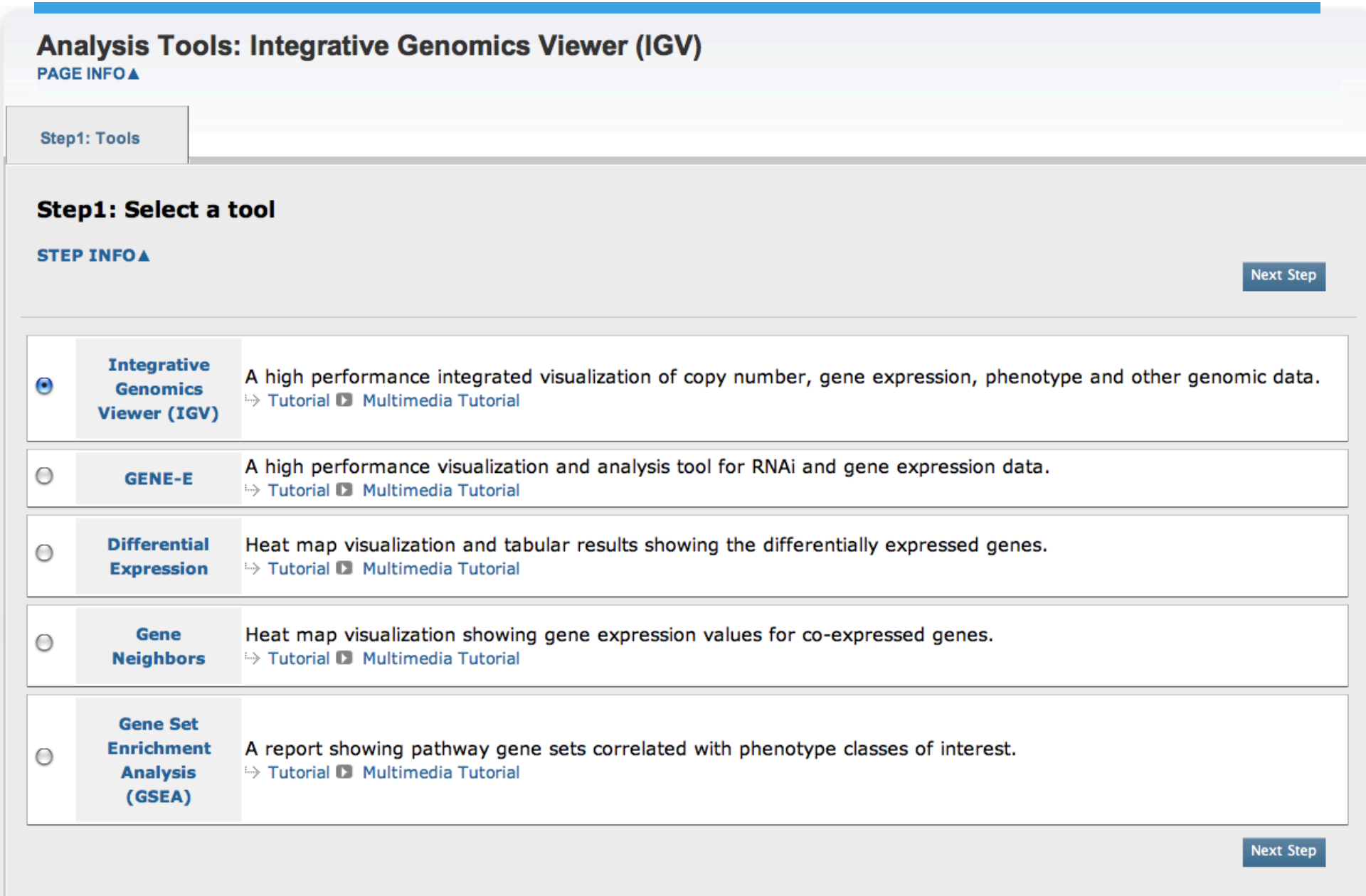

Reproducibility between CCLE & GDSC?

ANALYSIS

doi:10.1038/nature12831

Inconsistency in large pharmacogenomic studies

Benjamin Haibe-Kains[1,2], Nehme El-Hachem[1], Nicolai Juul Birkbak[3], Andrew C. Jin[4], Andrew H. Beck[4]*, Hugo J. W. L. Aerts[5,6,7]* & John Quackenbush[5,8]*

Two large-scale pharmacogenomic studies were published recently in this journal. Genomic data are well correlated between studies; however, the measured drug response data are highly discordant. Although the source of inconsistencies remains uncertain, it has potential implications for using these outcome measures to assess gene–drug associations or select potential anticancer drugs on the basis of their reported results.

Reproducibility between CCLE & GDSC?

ANALYSIS

doi:10.1038/nature12831

Inconsistency in large pharmacogenomic studies

Benjamin Haibe-Kains[1,2], Nehme El-Hachem[1], Nicolai Juul Birkbak[3], Andrew C. Jin[4], Andrew H. Beck[4]*, Hugo J. W. L. Aerts[5,6,7]* & John Quackenbush[5,8]*

Two large-scale pharmacogenomic studies were published recently in this journal. Genomic data are well correlated between studies; however, the measured drug response data are highly discordant. Although the source of inconsistencies remains uncertain, it has potential implications for using these outcome measures to assess gene–drug associations or select potential anticancer drugs on the basis of their reported results.

ANALYSIS

doi:10.1038/nature15736

Pharmacogenomic agreement between two cancer cell line data sets

The Cancer Cell Line Encyclopedia and Genomics of Drug Sensitivity in Cancer Investigators*

Large cancer cell line collections broadly capture the genomic diversity of human cancers and provide valuable insight into anti-cancer drug response. Here we show substantial agreement and biological consilience between drug sensitivity measurements and their associated genomic predictors from two publicly available large-scale pharmacogenomics resources: The Cancer Cell Line Encyclopedia and the Genomics of Drug Sensitivity in Cancer databases.

Genentech Cancer Cell Line Screening Initiative (gCSI)

RESOURCE

nature biotechnology

A comprehensive transcriptional portrait of human cancer cell lines

Christiaan Klijn[1], Steffen Durinck[1,2], Eric W Stawiski[1,2], Peter M Haverty[1], Zhaoshi Jiang[1], Hanbin Liu[1], Jeremiah Degenhardt[1], Oleg Mayba[1], Florian Gnad[1], Jinfeng Liu[1], Gregoire Pau[1], Jens Reeder[1], Yi Cao[1,3], Kiran Mukhyala[1], Suresh K Selvaraj[3], Mamie Yu[3], Gregory J Zynda[1], Matthew J Brauer[1], Thomas D Wu[1], Robert C Gentleman[1], Gerard Manning[1], Robert L Yauch[3], Richard Bourgon[1], David Stokoe[3], Zora Modrusan[2], Richard M Neve[3], Frederic J de Sauvage[2], Jeffrey Settleman[3], Somasekar Seshagiri[2] & Zemin Zhang[1]

Tumor-derived cell lines have served as vital models to advance our understanding of oncogene function and therapeutic responses. Although substantial effort has been made to define the genomic constitution of cancer cell line panels, the transcriptome remains understudied. Here we describe RNA sequencing and single-nucleotide polymorphism (SNP) array analysis of 675 human cancer cell lines. We report comprehensive analyses of transcriptome features including gene expression, mutations, gene fusions and expression of non-human sequences. Of the 2,200 gene fusions catalogued, 1,435 consist of genes not previously found in fusions, providing many leads for further investigation. We combine multiple genome and transcriptome features in a pathway-based approach to enhance prediction of response to targeted therapeutics. Our results provide a valuable resource for studies that use cancer cell lines.

Genentech Cancer Cell Line Screening Initiative (gCSI)

ANALYSIS

doi:10.1038/nature17987

Reproducible pharmacogenomic profiling of cancer cell line panels

Peter M. Haverty[1]*, Eva Lin[2]*, Jenille Tan[2], Yihong Yu[2], Billy Lam[2], Steve Lianoglou[1], Richard M. Neve[2], Scott Martin[2], Jeff Settleman[2], Robert L. Yauch[2] & Richard Bourgon[1]

The use of large-scale genomic and drug response screening of cancer cell lines depends crucially on the reproducibility of results. Here we consider two previously published screens, plus a later critique of these studies. Using independent data, we show that consistency is achievable, and provide a systematic description of the best laboratory and analysis practices for future studies.

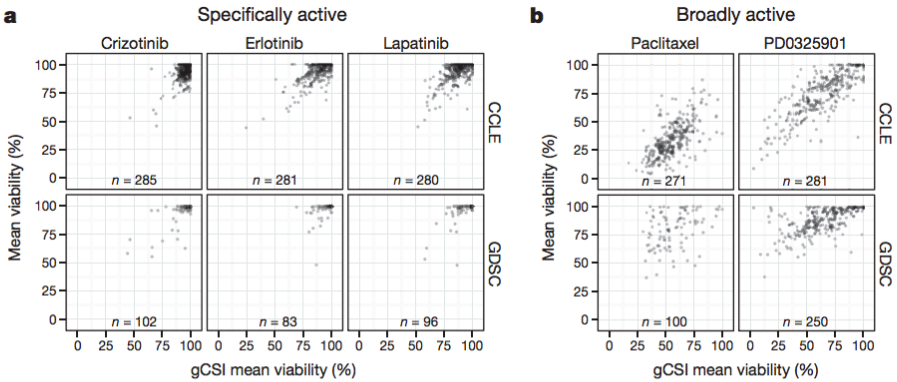

Figure 1 | gCSI, CCLE and GDSC drug response statistics reveal different patterns of response for specifically versus broadly active drugs. We include all lines in the two-way gCSI/CCLE overlap in the top rows, and all lines in the two-way gCSI/GDSC overlap in the bottom rows (see Extended Fig. Data 3 for restriction to only those lines included in the three-way overlap). In each panel, *n* refers to the number of lines in common and plotted for each pairwise comparison. Mean viability (equivalent to area under the log-dose/response curve) across tested drug concentrations for cell lines as assayed by each pair of projects is plotted for specifically active drugs (**a**) and broadly active drugs (**b**). 0% corresponds to complete growth inhibition at all doses; 100% corresponds to viability equal, on average, to untreated control wells. Values are capped at a maximum value of 100% for consistency with GDSC published data. gCSI values are derived from three biological replicates (Methods).

Cancer Therapeutics Response Portal

Identifying and targeting cancer dependencies with small molecules

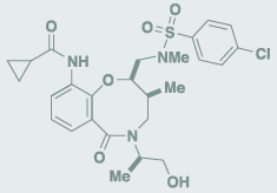

inhibitor of SHH pathway
J Am Chem Soc (2013)

The Cancer Therapeutics Response Portal (CTRP) links genetic, lineage, and other cellular features of cancer cell lines to small-molecule sensitivity with the goal of accelerating discovery of patient-matched cancer therapeutics.

We generated an 'Informer Set' of 481 small-molecule probes and drugs that selectively target distinct nodes in cell circuitry and that collectively modulate a broad array of cell processes. We quantitatively measured the sensitivity of 860 deeply characterized cancer-cell lines to Informer Set compounds, and have undertaken analyses connecting sensitivity to cancer features, including mutations, gene expression, copy-number variation, and lineage. These analyses, and links to the underlying data, are provided openly on the CTRP.

The CTRP is a living resource for the biomedical research community that can be mined to develop insights into small-molecule mechanisms of action and novel therapeutic hypotheses, and to support future discovery of drugs matched to patients based on predictive biomarkers.

Publications

Please cite our cancer cell-line profiling Resource by referencing: "Correlating chemical sensitivity and basal gene expression reveals mechanism of action" Rees *et al.*, *Nat Chem Biol*, **12**, 109-116 (2016), and "Harnessing Connectivity in a Large-Scale Small-Molecule Sensitivity Dataset" Seashore-Ludlow *et al.*, *Cancer Discovery*, **5**, 1210-1223 (2015), and "An Interactive Resource to Identify Cancer Genetic and Lineage Dependencies Targeted by Small Molecules" Basu, Bodycombe, Cheah, *et al.*, *Cell*, **154**, 1151-1161 (2013).

Acknowledgements

The Cancer Therapeutics Response Portal was developed by researchers at the Center for the Science of Therapeutics at the Broad Institute and is sponsored in part by the NCI's Cancer Target Discovery and Development Network.

Complementary Resources

The National Cancer Institute's CTD2 Network maintains an Open-Access Data Portal that makes available raw data downloads from member Centers, including all raw sensitivity and enrichment data and other supporting information from the Broad related to this portal.

The Cancer Cell Line Encyclopedia provides public access to genomic data, analysis and visualization for about 1000 cell lines.

The Genomics of Drug Sensitivity in Cancer provides public access to data on the sensitivity of genomically characterized cancer cell lines to select compounds.

Project Achilles is a systematic effort aimed at identifying and cataloging genetic vulnerabilities across hundreds of genomically characterized cancer cell lines.

CTRP v2

- 481 compounds X 860 CCLs
- annotations for small molecules by protein target
- annotations for CCLs by mutation and lineage
- interactive interface to explore clustering by small molecule and CCL
- cluster enrichments for small molecule and CCL annotations
- correlations to copy-number and gene-expression data
- correlation analysis on-the-fly
- box-whisker visualization
- drill-down to scatter plots and concentration-response curves
- filter by lineage/subtype, growth mode

<< You are here

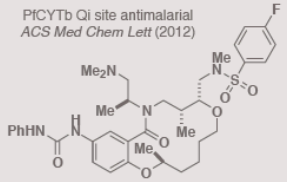

PfCYTb Qi site antimalarial
ACS Med Chem Lett (2012)

CTRP v1

- 185 compounds X 242 CCLs
- pre-computed enrichment analysis and visualizations
- filter by lineage. CCLE mutation source, confounding factors
- 76,703 significant connections (q<0.01)

Visit CTRPv1 >>

Project Achilles - CCLE

Project Achilles | BROAD INSTITUTE

Login

Data | Resources | About | Contact

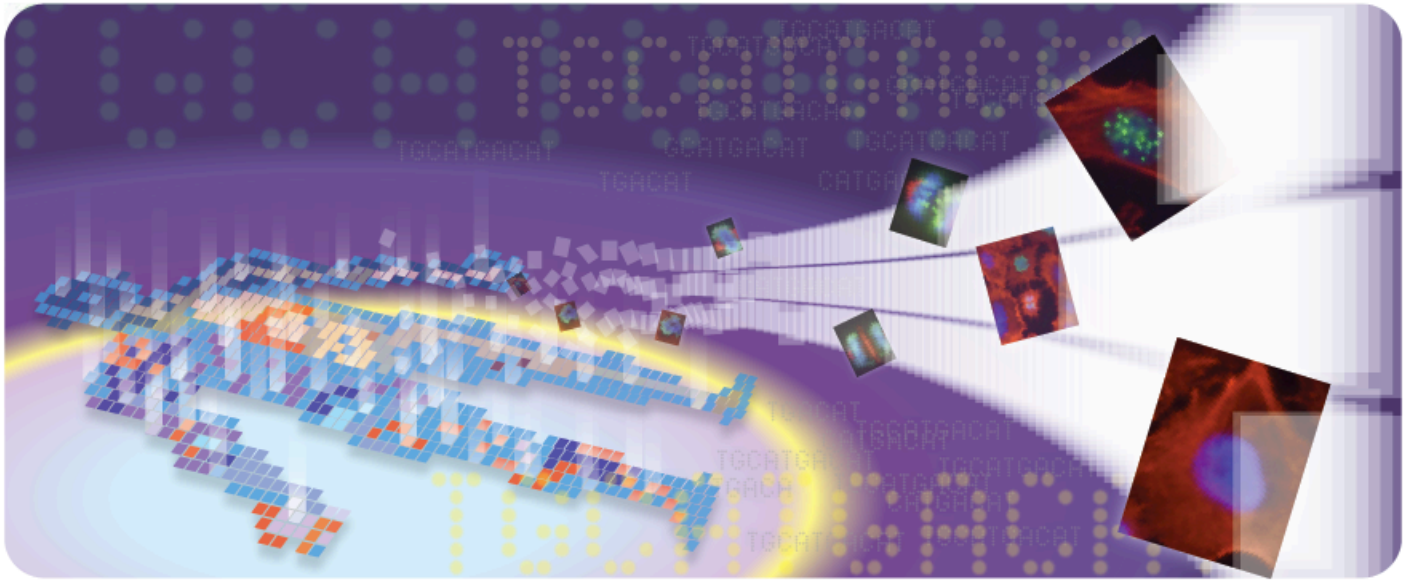

Project Achilles is a systematic effort aimed at identifying and cataloging genetic vulnerabilities across hundreds of genomically characterized cancer cell lines. The project uses genome-scale RNAi and CRISPR-Cas9 genetic perturbation reagents to silence or knockout individual genes and identify those genes that affect cell survival. By linking these genetic vulnerabilities to the genetic or molecular features of the tumors, this project is providing the foundation for a "Cancer Dependency Map".

Search Genes | Search

Citing Achilles

Cowley, Weir & Vazquez, et al. Parallel genome-scale loss of function screens in 216 cancer cell lines for the identification of context-specific genetic dependencies. *Nature Scientific Data* **1**, Article number: 140035. September 30, 2014.

A Word of Caution

FEATURES

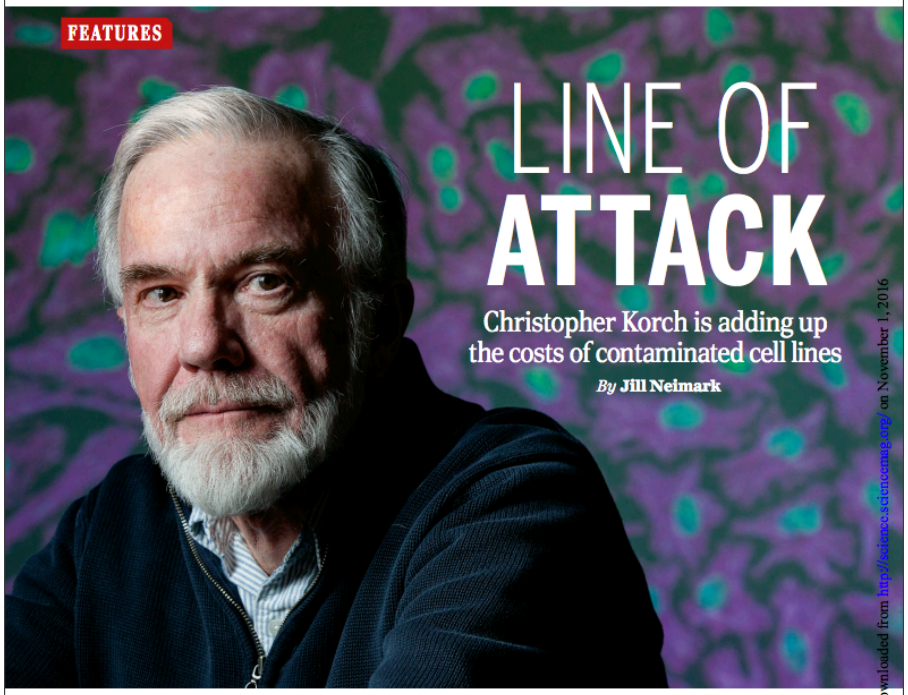

LINE OF ATTACK

Christopher Korch is adding up the costs of contaminated cell lines

By **Jill Neimark**

"I call myself a corrector," says University of Colorado geneticist Christopher Korch. What Korch passionately wants to correct is the contamination of laboratory cell cultures, a problem that has bedeviled biomedical research for more than half a century. Over the past 15 years, he has published on 78 widely used cell lines that turned out to be overgrown with other cells. Thyroid lines were actually composed of melanoma cells, prostate tissue was displaced by bladder cancer, and normal uterine cultures turned out to be nothing but breast cancer, casting doubt on countless studies of basic biology and disease.

And yet until recently he has felt more like a voice in the wilderness than a catalyst for change. "All too often, scientists have ignored my findings," Korch says. "Not one of my published papers has led to a retraction by a journal or scientist. Less than 10 corrections have been issued, when each false line I discovered affects the conclusions of hundreds or thousands of papers."

Now Korch has a band of allies and, he hopes, a novel way to persuade recalcitrant biologists: Zoom out from individual cases of contamination to show the big picture. After a year of intensive data gathering and analysis, he believes he has for the first time begun to quantify the damage done to the scientific enterprise by contaminated cell lines. "We're looking at tens of thousands of publications, millions of journal citations, and potentially hundreds of millions of research dollars," he says.

Many widely studied cell lines continue to be overrun by HeLa cancer cells (displayed behind Korch).

A few scientists who have seen a preliminary draft of Korch's white paper, which is now under review at a journal, have been moved to set changes in motion. "What impresses me about Dr. Korch's analysis is that the problem is more pervasive than I might have predicted," says Ferric Fang, a University of Washington, Seattle, microbiologist who recently co-authored a study estimating the amount of National Institutes of Health (NIH) funding wasted on a decade's worth of papers that had been retracted.

Fang, who edits the journal *Infection and Immunity*, says he will present Korch's findings to the leadership of the American

PHOTO: © JOANNA B PINNEO

A tale of two impostors

Christopher Korch estimated the impact of research on two cell lines, HEp-2 and INT 407. Due to contamination long ago, both are now widely acknowledged to be composed of cancer cells called HeLa.

5789
ARTICLES
in **1182** journals may have used HEp-2 inappropriately, producing an estimated **174,000** citations

1336
ARTICLES
in **271** journals may have used INT 407 inappropriately, producing an estimated **40,000** citations

$713
MILLION
Estimated amount spent on the original articles published on **INT 407** and **HEp-2**

$3.5
BILLION
Estimated amount spent on subsequent work based on those papers

Moving Forward

CCR Translations
Commentary on Julien et al., p. 5314

Clinical Cancer Research

The Promise of Patient-Derived Xenografts: The Best Laid Plans of Mice and Men

Scott Kopetz, Robert Lemos, and Garth Powis

Compared with xenografts from previously established cell lines, patient-derived xenogr
faithfully recapitulate the molecular diversity, cellular heterogeneity, and histology seen in p
although other limitations of murine models remain. The ability of these models to i
development and answer mechanistic questions will determine their ultimate use. *Clin Canc*
5160–2. ©2012 AACR.

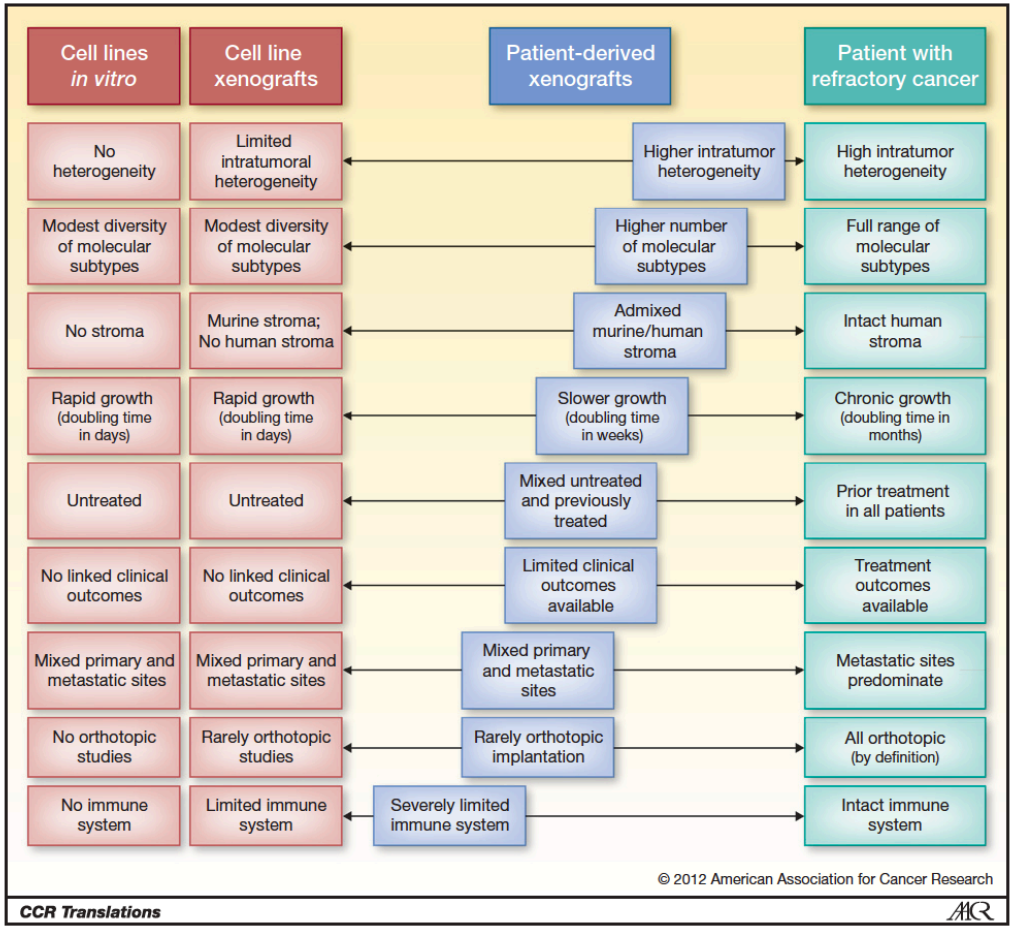

Figure 1. Cell line–based models have been criticized for their poor ability to predict outcomes for advanced patients with cancer (3). Patient-derived xenografts have several characteristics that better recapitulate the clinical reality for patients. This tumor model "abacus" highlights areas of strength and weakness of patient-derived xenografts as compared with the cell line and human models. Blue squares further to the right represent positive characteristics of the patient-derived xenografts that are closer to the tumor biology of the patient.

Patient-Derived Tumor Xenografts (PDX)

Patient-derived tumour xenografts as models for oncology drug development

John J. Tentler, Aik Choon Tan, Colin D. Weekes, Antonio Jimeno, Stephen Leong, Todd M. Pitts, John J. Arcaroli, Wells A. Messersmith and S. Gail Eckhardt

Abstract | Progress in oncology drug development has been hampered by a lack of preclinical models that reliably predict clinical activity of novel compounds in cancer patients. In an effort to address these shortcomings, there has been a recent increase in the use of patient-derived tumour xenografts (PDTX) engrafted into immune-compromised rodents such as athymic nude or NOD/SCID mice for preclinical modelling. Numerous tumour-specific PDTX models have been established and, importantly, they are biologically stable when passaged in mice in terms of global gene-expression patterns, mutational status, metastatic potential, drug responsiveness and tumour architecture. These characteristics might provide significant improvements over standard cell-line xenograft models. This Review will discuss specific PDTX disease examples illustrating an overview of the opportunities and limitations of these models in cancer drug development, and describe concepts regarding predictive biomarker development and future applications.

Tentler, J. J. *et al. Nat. Rev. Clin. Oncol.* **9**, 338–350 (2012); publishe

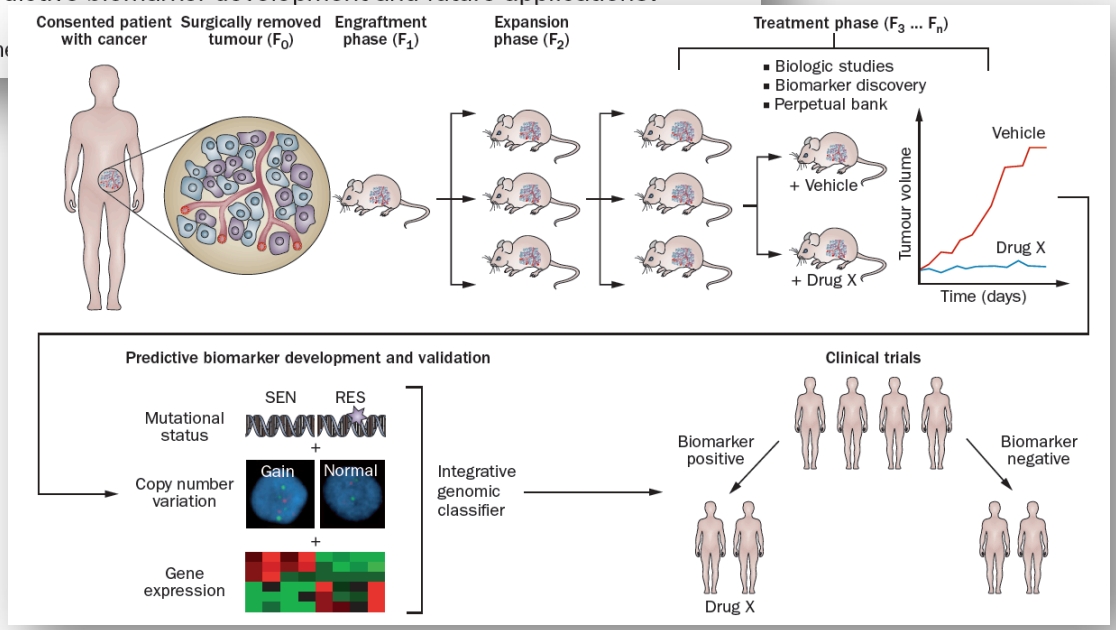

Patient-Derived Tumor Xenografts (PDX)

Endocrine-Therapy-Resistant *ESR1* Variants Revealed by Genomic Characterization of Breast-Cancer-Derived Xenografts

Shunqiang Li,[1,2,13] Dong Shen,[3,13] Jieya Shao,[1] Robert Crowder,[1] Wenbin Liu,[4] Aleix Prat,[5,6] Xiaping He,[6] Shuying Liu,[4] Jeremy Hoog,[1] Charles Lu,[3] Li Ding,[2,3,9] Obi L. Griffith,[3] Christopher Miller,[3] Dave Larson,[3] Robert S. Fulton,[3] Michelle Harrison,[3] Tom Mooney,[3] Joshua F. McMichael,[3] Jingqin Luo,[2,7] Yu Tao,[7] Rodrigo Goncalves,[1] Christopher Schlosberg,[8] Jeffrey F. Hiken,[8] Laila Saied,[9] Cesar Sanchez,[10] Therese Giuntoli,[1] Caroline Bumb,[1] Crystal Cooper,[1] Robert T. Kitchens,[1] Austin Lin,[1] Chanpheng Phommaly,[1] Sherri R. Davies,[1] Jin Zhang,[3] Megha Shyam Kavuri,[1] Donna McEachern,[11] Yi Yu Dong,[1] Cynthia Ma,[1,2] Timothy Pluard,[1,2] Michael Naughton,[1,2] Ron Bose,[1,2] Rama Suresh,[1] Reida McDowell,[1] Loren Michel,[1,2] Rebecca Aft,[12] William Gillanders,[12] Katherine DeSchryver,[1] Richard K. Wilson,[2,3] Shaomeng Wang,[11] Gordon B. Mills,[4] Ana Gonzalez-Angulo,[4] John R. Edwards,[8] Christopher Maher,[1,2,3] Charles M. Perou,[6] Elaine R. Mardis,[2,3] and Matthew J. Ellis[1,2,*]

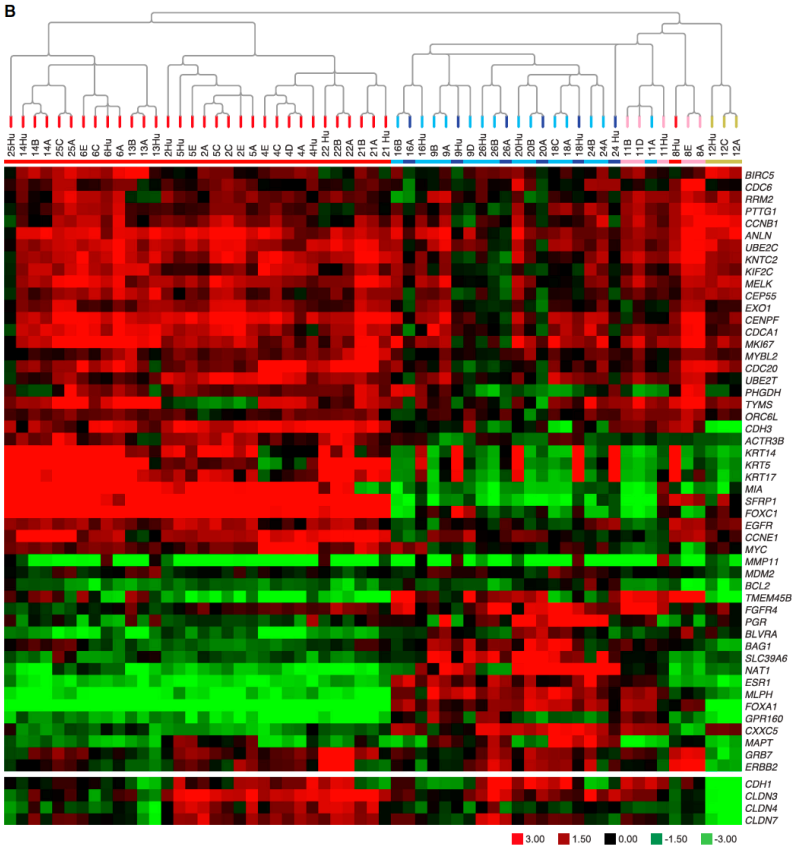

Patient-Derived Tumor Xenografts (PDX)

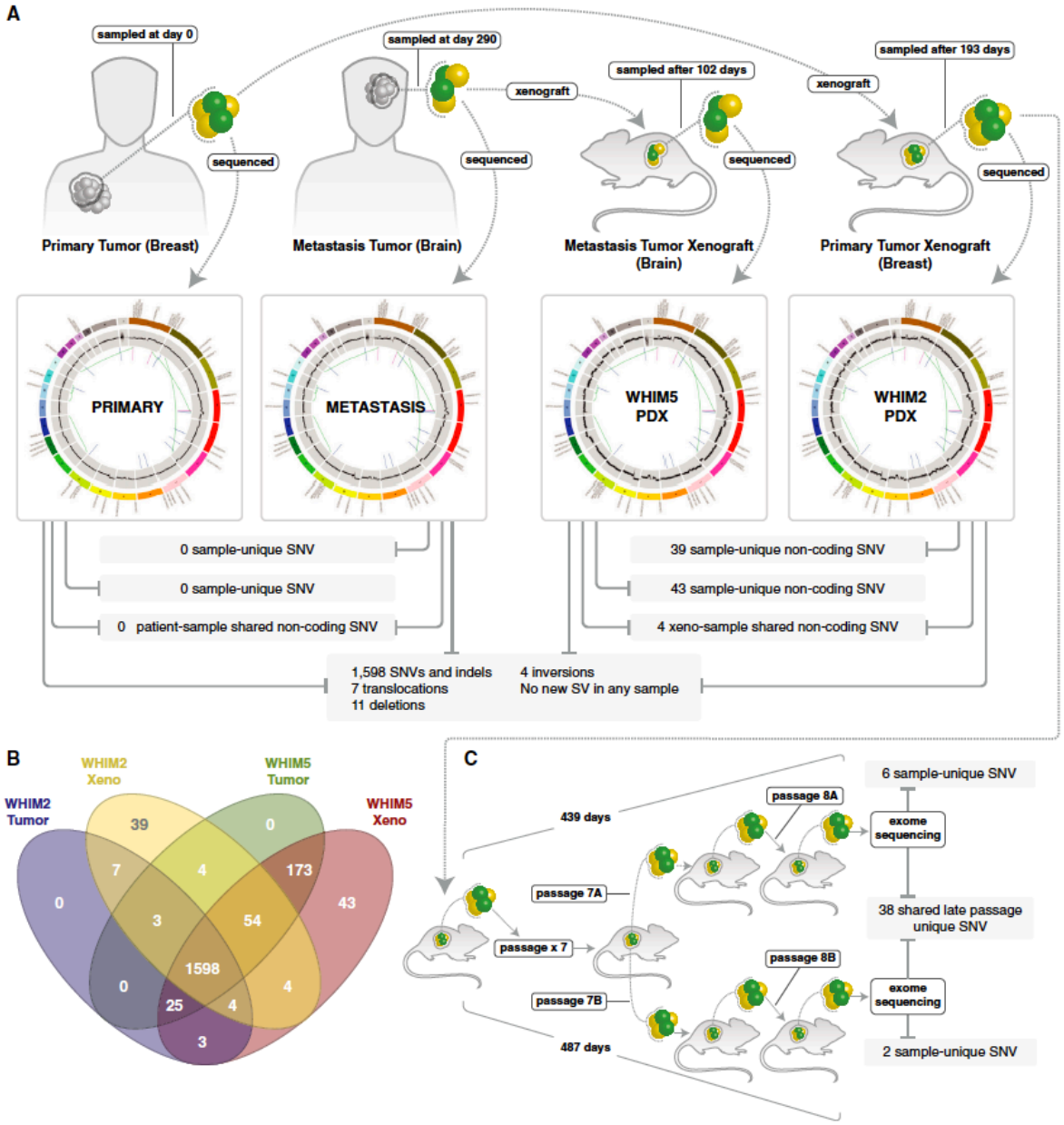

Patient-Derived Tumor Xenografts (PDX)

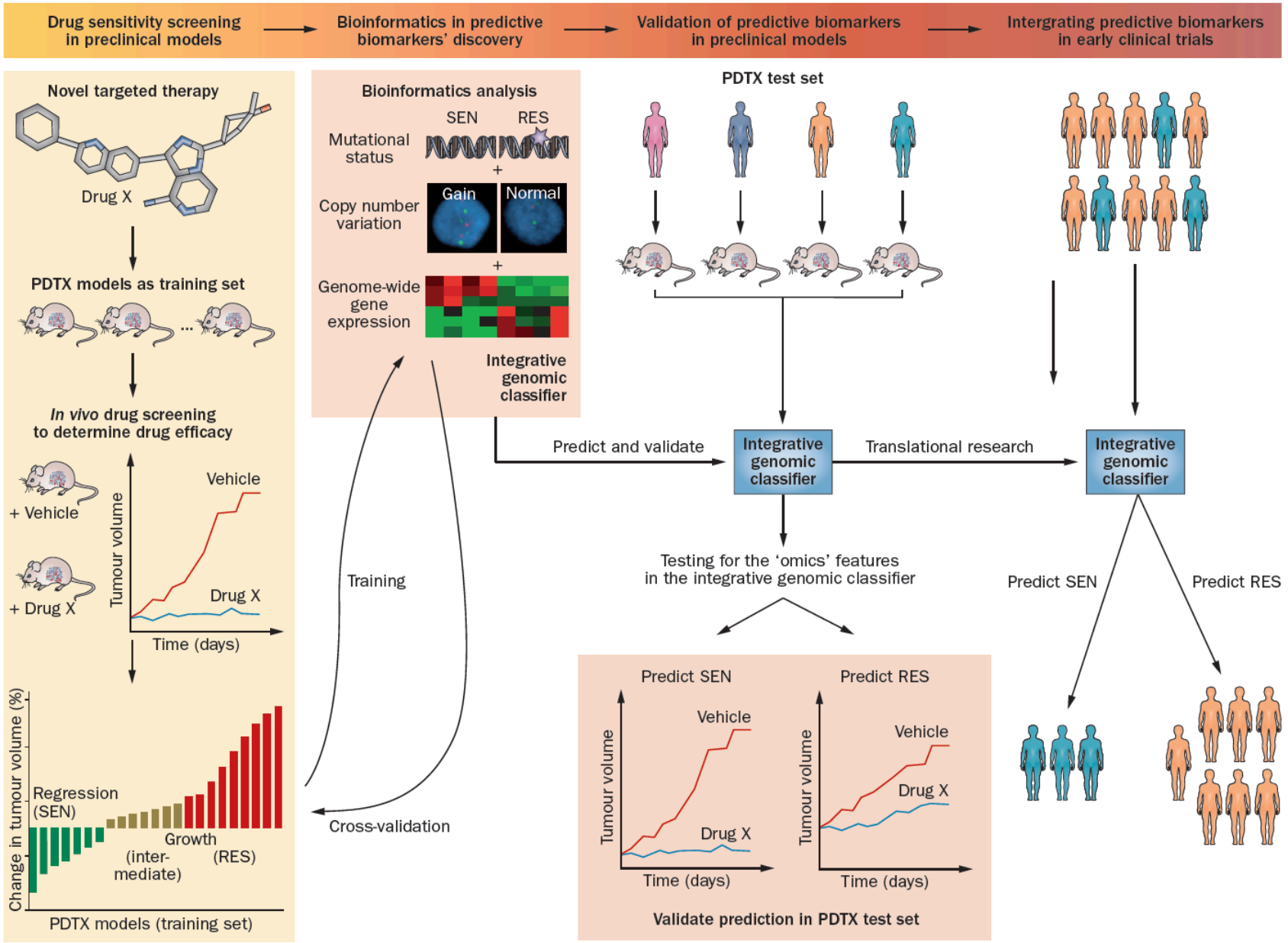

Patient-Derived Xenografts Encyclopedia (PDXE) (~1000 PDX models)

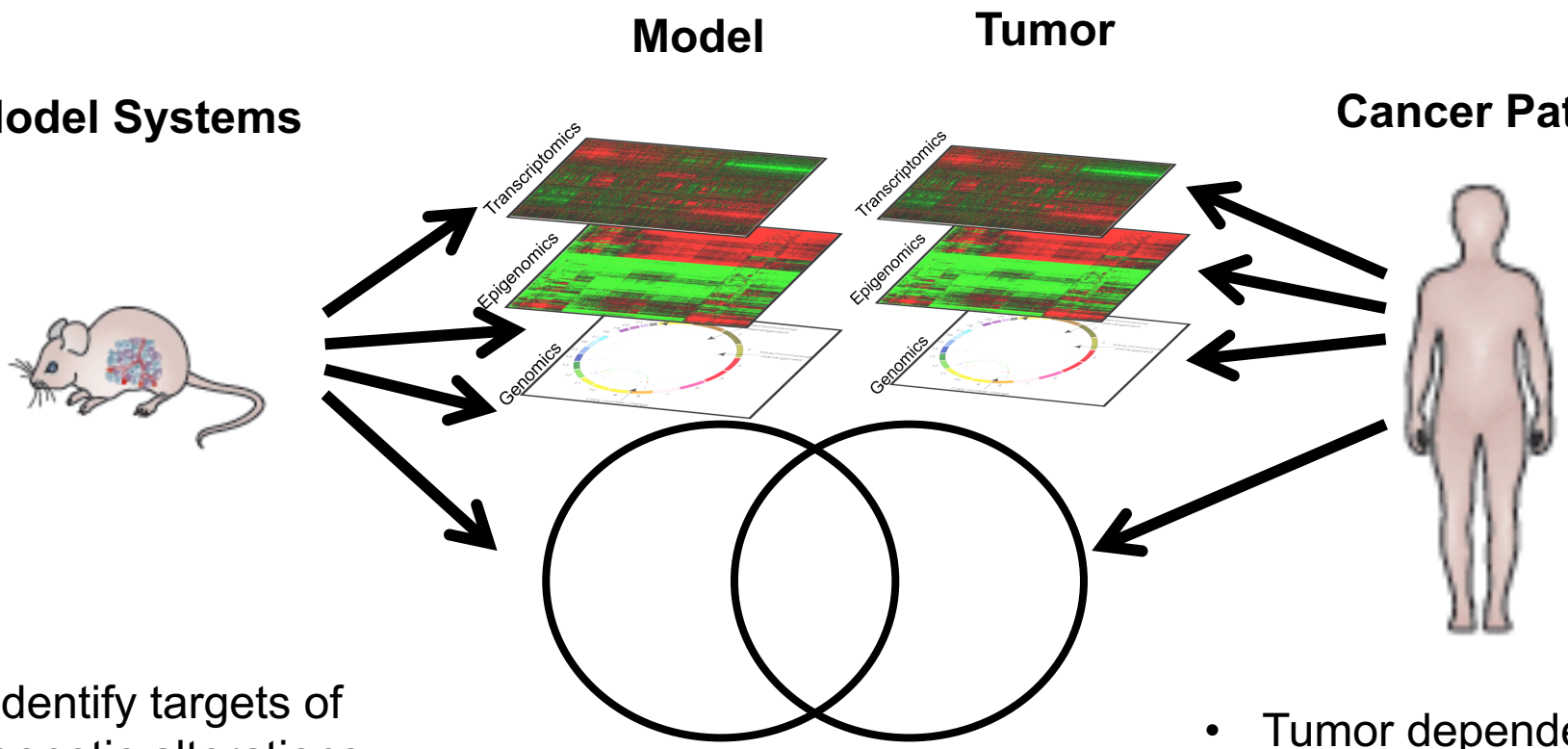

- Identify targets of genetic alterations
- Mechanistic studies
- Perturbagen data

Genetic/Molecular Information

- Tumor dependency
- Response to treatments
- Resistance mechanisms

nature medicine

NIBR PDXE

High-throughput screening using patient-derived tumor xenografts to predict clinical trial drug response

Hui Gao[1,7], Joshua M Korn[1,7], Stéphane Ferretti[2,7], John E Monahan[3], Youzhen Wang[4], Mallika Singh[5,6], Chao Zhang[4,6], Christian Schnell[2], Guizhi Yang[1], Yun Zhang[4], O Alejandro Balbin[1], Stéphanie Barbe[2], Hongbo Cai[1], Fergal Casey[5], Susmita Chatterjee[5], Derek Y Chiang[1], Shannon Chuai[4], Shawn M Cogan[1], Scott D Collins[1], Ernesta Dammassa[2], Nicolas Ebel[2], Millicent Embry[5], John Green[1], Audrey Kauffmann[2], Colleen Kowal[1], Rebecca J Leary[1], Joseph Lehar[3], Ying Liang[4], Alice Loo[1], Edward Lorenzana[5], E Robert McDonald III[1], Margaret E McLaughlin[3], Jason Merkin[1], Ronald Meyer[3], Tara L Naylor[3], Montesa Patawaran[5], Anupama Reddy[3,6], Claudia Röelli[2], David A Ruddy[3], Fernando Salangsang[5], Francesca Santacroce[2], Angad P Singh[1], Yan Tang[5], Walter Tinetto[2], Sonja Tobler[2], Roberto Velazquez[1], Kavitha Venkatesan[1], Fabian Von Arx[2], Hui Qin Wang[3], Zongyao Wang[4], Marion Wiesmann[2], Daniel Wyss[2], Fiona Xu[4], Hans Bitter[1], Peter Atadja[4], Emma Lees[5], Francesco Hofmann[2], En Li[4], Nicholas Keen[1], Robert Cozens[2], Michael Rugaard Jensen[2], Nancy K Pryer[5,6], Juliet A Williams[1,8] & William R Sellers[1,8]

Profiling candidate therapeutics with limited cancer models during preclinical development hinders predictions of clinical efficacy and identifying factors that underlie heterogeneous patient responses for patient-selection strategies. We established ~1,000 patient-derived tumor xenograft models (PDXs) with a diverse set of driver mutations. With these PDXs, we performed *in vivo* compound screens using a 1 × 1 × 1 experimental design (PDX clinical trial or PCT) to assess the population responses to 62 treatments across six indications. We demonstrate both the reproducibility and the clinical translatability of this approach by identifying associations between a genotype and drug response, and established mechanisms of resistance. In addition, our results suggest that PCTs may represent a more accurate approach than cell line models for assessing the clinical potential of some therapeutic modalities. We therefore propose that this experimental paradigm could potentially improve preclinical evaluation of treatment modalities and enhance our ability to predict clinical trial responses.

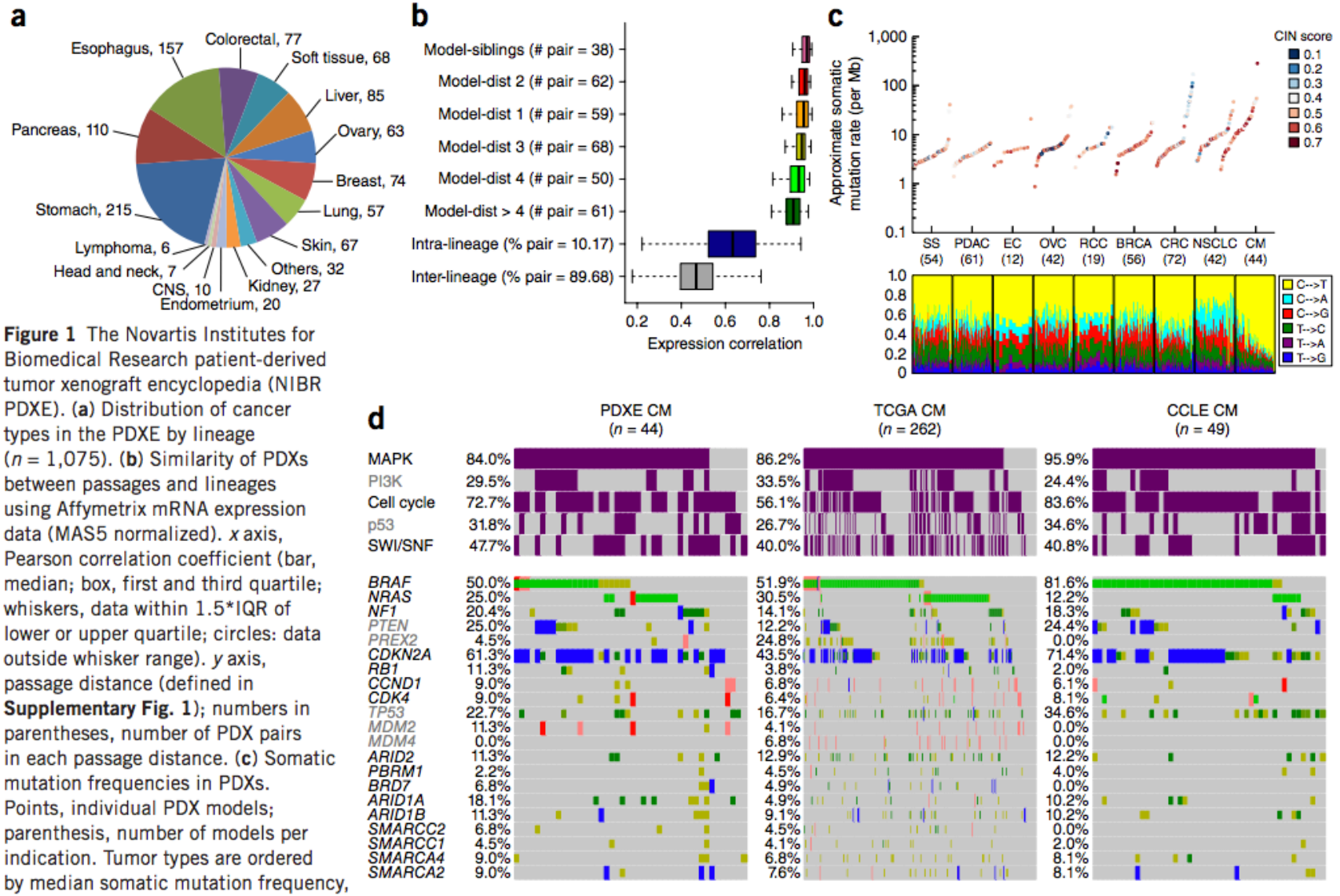

Figure 1 The Novartis Institutes for Biomedical Research patient-derived tumor xenograft encyclopedia (NIBR PDXE). (**a**) Distribution of cancer types in the PDXE by lineage (n = 1,075). (**b**) Similarity of PDXs between passages and lineages using Affymetrix mRNA expression data (MAS5 normalized). x axis, Pearson correlation coefficient (bar, median; box, first and third quartile; whiskers, data within 1.5*IQR of lower or upper quartile; circles: data outside whisker range). y axis, passage distance (defined in **Supplementary Fig. 1**); numbers in parentheses, number of PDX pairs in each passage distance. (**c**) Somatic mutation frequencies in PDXs. Points, individual PDX models; parenthesis, number of models per indication. Tumor types are ordered by median somatic mutation frequency, and colored by chromosomal instability (CIN) score. Lower panel, relative proportions of the six different possible base-pair substitutions. SS, soft tissue sarcoma; PDAC, pancreatic ductal carcinoma; EC, esophageal cancer; OVC, ovarian carcinoma; RCC, renal cell carcinoma; BRCA, breast carcinoma; CRC, colorectal cancer; NSCLC, non-small cell lung carcinoma; CM, cutaneous melanoma. (**d**) Genomic landscape analysis of melanoma across PDXE, TCGA and CCLE data sets. Parenthesis, number of models per indication; blue, homozygous deletions; salmon, amplification >5 copies; red, amplification > 8 copies; light green, known COSMIC (Catalog of Somatic Mutations in Cancer) gain-of-function mutations; dark green, truncating mutations/frameshift or known COSMIC loss-of-function; mustard, novel mutation; purple, pathway altered in at least one gene; gene names colored black or gray to indicate inclusion in same-colored pathway listed above; percentages indicate percentage of samples altered for the given gene or pathway.

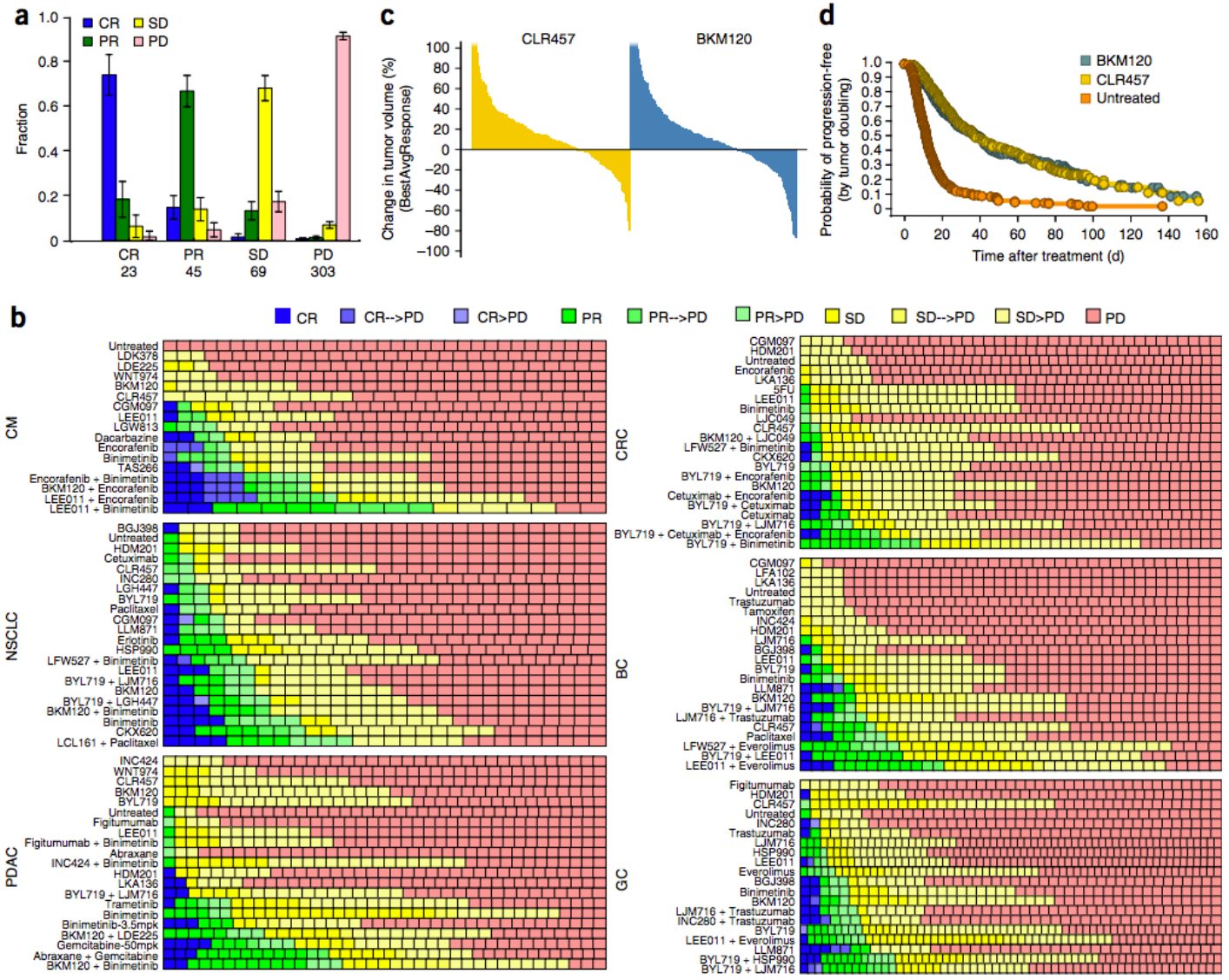

Figure 2 Systematic approach for *in vivo* compound profiling using PDXs (PCT), and its reproducibility. (**a**) Feasibility assessment of 1 × 1 × 1 PCT approach by Pearson correlation analysis. *x* axis, number of majority response from each response category; *y* axis, fraction of individual animal response relative to the majority (average ± s.e.m.). A total of 2,138 single-animal response data were collected and categorized from 440 unique treatment models (Online Methods). CR: complete response; PR: partial response; SD: stable disease; PD: progressive disease. (**b**) Summary of compound sensitivity in the PCTs. The BestAvgResponse was used to make response calls (Online Methods), and each square represents a PDX. A total of 62 treatment groups were tested in 277 PDXs across six indications (BRCA (breast cancer, $n = 43$), CM (cutaneous melanoma, $n = 33$), CRC (colorectal carcinoma, $n = 59$), GC (gastric cancer, $n = 64$), NSCLC (non-small cell lung carcinoma, $n = 36$) and PDAC (pancreatic ductal adenocarcinoma, $n = 42$)). Arrow (CR→PD, PR→PD, SD→PD, and CR>PD, PR>PD, SD>PD) indicates disease progression; > indicates progression seen after 64 d; > pindicates progression in <64 d. (**c**) Waterfall plot of responses to the PI3K inhibitors CLR457 ($n = 205$) and BKM120 ($n = 213$) across all indications; each bar represents an individual PDX. (**d**) Kaplan-Meier progression-free survival curve of PDXs treated with CLR457 ($n = 205$) and BKM120 ($n = 213$) across all indications.

Immunotherapy in Cancer Treatment

Cancer immunotherapy:Monoclonal antibodies[14][19]

Antibody	Brand name	Type	Target	Approval date	Approved treatment(s)
Alemtuzumab	Campath	humanized	CD52	2001	B-cell chronic lymphocytic leukemia (CLL)[20]
Atezolizumab	Tecentriq	humanized	PD-L1	2016	bladder cancer [21]
Ipilimumab	Yervoy	human	CTLA4	2011	metastatic melanoma[22]
Ofatumumab	Arzerra	human	CD20	2009	refractory CLL[23]
Nivolumab	Opdivo	human	ligand activation of the programmed cell death 1 (PD-1) receptor on activated T cells	2014	unresectable or metastatic melanoma, squamous non-small cell lung cancer[24]
Pembrolizumab	Keytruda	humanized	programmed cell death 1 (PD-1) receptor	2014	metastatic melanoma[24]
Rituximab	Rituxan, Mabthera	chimeric	CD20	1997	non-Hodgkin lymphoma[25]
				2010	CLL[26]

Immunotherapy in Cancer Treatment

FDA Approves Merck's KEYTRUDA® (pembrolizumab) in Metastatic NSCLC for First-Line Treatment of Patients Whose Tumors Have High PD-L1 Expression (Tumor Proportion Score [TPS] of 50 Percent or More) With No EGFR or ALK Genomic Tumor Aberrations

KEYTRUDA is the Only Anti-PD-1 Therapy Approved in First-Line Treatment of Metastatic NSCLC; KEYTRUDA Demonstrated Superior Progression-Free and Overall Survival Compared to Chemotherapy in Patients Whose Tumors Expressed High Levels of PD-L1

FDA Also Approves a Labeling Update for KEYTRUDA for the Treatment of Patients with Metastatic NSCLC Whose Tumors Express PD-L1 (TPS of One Percent or More) With Disease Progression On or After Platinum-Containing Chemotherapy; Patients With EGFR or ALK Genomic Tumor Aberrations Should Have Disease Progression On FDA-Approved Therapy for These Aberrations Prior to Receiving KEYTRUDA

Monday, October 24, 2016 6:04 pm EDT

Efficacy Results from KEYNOTE-024

Endpoint	KEYTRUDA 200 mg every 3 weeks (n=154)	Chemotherapy (n=151)
PFS		
Number (%) of patients with event	73 (47%)	116 (77%)
Median in months (95% CI)	10.3 (6.7, NR)	6.0 (4.2, 6.2)
Hazard ratio* (95% CI)	0.50 (0.37, 0.68)	
p-Value (stratified log-rank)	<0.001	
OS		
Number (%) of patients with event	44 (29%)	64 (42%)
Median in months (95% CI)	NR (NR, NR)	NR (9.4, NR)
Hazard ratio* (95% CI)	0.60 (0.41, 0.89)	
p-Value (stratified log-rank)	0.005†	
Objective Response Rate		
ORR % (95% CI)	45% (37, 53)	28% (21, 36)
Complete response %	4%	1%
Partial response %	41%	27%
p-Value (Miettenen-Nurminen)	0.001	
Median duration of response in months (range)	NR (1.9+, 14.5+)	6.3 (2.1+, 12.6+)

* Based on the stratified Cox proportional hazard model

† P-value is compared with 0.0118 of the allocated alpha for this interim analysis

NR = not reached

XactMice

eNews | *June 24, 2015*

THE XACTMICE YOU NEED FOR A TUMOR MICROENVIRONMENT

By Brian Soper, Ph.D.

Human immune cells and the tumor microenvironment

Exciting progress is being made in the development of mice that support tumor growth in the presence of a human immune system. A new publication in *Oncogene* (Morton et al., 2015) demonstrates the importance of human immune cells in maintaining the microenvironment of patient derived xenografts (PDX). The human immune cells infiltrate the tumor, stimulate lymphangiogenesis, and help to maintain the original genetic expression profile of the PDX. These observations highlight the complex interactions between tumors and the immune system and demonstrate the importance of these interactions in maintaining original tumor fidelity. Maintaining all aspects of human tumor growth in a mouse may enable identification of new treatment strategies that more accurately translate into clinical applications.

XactMice

Oncogene (2016) **35,** 290–300

www.nature.com/onc

ORIGINAL ARTICLE

XactMice: humanizing mouse bone marrow enables microenvironment reconstitution in a patient-derived xenograft model of head and neck cancer

JJ Morton[1,8], G Bird[2,8], SB Keysar[1], DP Astling[1,3], TR Lyons[1], RT Anderson[1], MJ Glogowska[1], P Estes[2], JR Eagles[1], PN Le[1], G Gan[4], B McGettigan[1], P Fernandez[5], N Padilla-Just[1], M Varella-Garcia[1], JI Song[6], DW Bowles[1], P Schedin[1], A-C Tan[1,3], DR Roop[2,7], X-J Wang[5,7], Y Refaeli[2,7] and A Jimeno[1,6,7]

The limitations of cancer cell lines have led to the development of direct patient-derived xenograft models. However, the interplay between the implanted human cancer cells and recruited mouse stromal and immune cells alters the tumor microenvironment and limits the value of these models. To overcome these constraints, we have developed a technique to expand human hematopoietic stem and progenitor cells (HSPCs) and use them to reconstitute the radiation-depleted bone marrow of a NOD/SCID/IL2rg$^{-/-}$ (NSG) mouse on which a patient's tumor is then transplanted (XactMice). The human HSPCs produce immune cells that home into the tumor and help replicate its natural microenvironment. Despite previous passage on nude mice, the expression of epithelial, stromal and immune genes in XactMice tumors aligns more closely to that of the patient tumor than to those grown in non-humanized mice—an effect partially facilitated by human cytokines expressed by both the HSPC progeny and the tumor cells. The human immune and stromal cells produced in the XactMice can help recapitulate the microenvironment of an implanted xenograft, reverse the initial genetic drift seen after passage on non-humanized mice and provide a more accurate tumor model to guide patient treatment.

Oncogene (2016) **35,** 290–300; doi:10.1038/onc.2015.94; published online 20 April 2015

XactMice

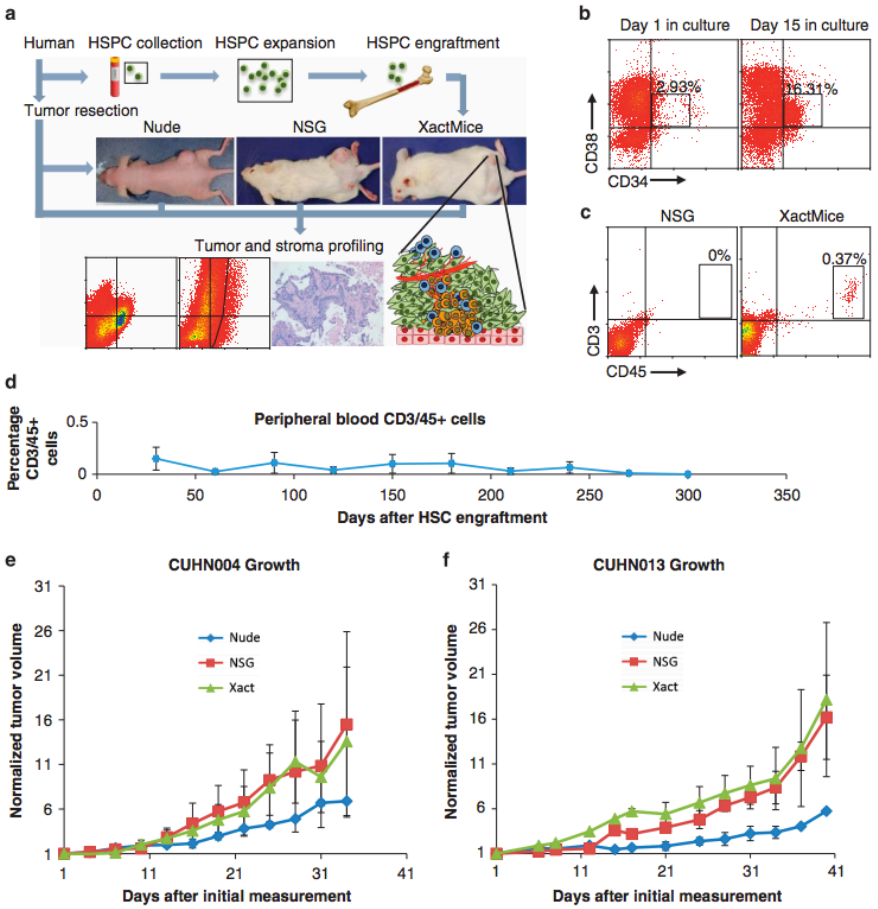

Figure 1. Overview and characterization of XactMice. (**a**) Schematic describing the generation of XactMice from human HSPCs, whose progeny migrate into the xenograft and differentiate into stromal cells. The growth and composition of tumors can be compared in nude, NSG and XactMice. (**b**) Flow cytometry measuring the expansion of HSPCs *in vitro* by the percentage of CD34/CD38+ cells. (**c**) Flow cytometry detecting human hematopoietic CD3/CD45+ cells in peripheral XactMice but not NSG blood, indicating that the HSPCs have successfully engrafted and are generating circulating lymphocytes. (**d**) The average percentage of human CD3/CD45+ cells in the peripheral blood of XactMice, as determined by flow cytometry, over the course of 7 months after engraftment. (**e**, **f**) There were no significant differences in either CUHN004 or CUHN013 tumor growth rates between nude, NSG and XactMice. Tumor measurements ($W \times W \times H$)/2 were recorded from all mouse strains in three separate experiments. Although tumors seem to grow faster in the NSG and XactMice, no statistical difference was observed in growth between the three strains in these experiments. Average tumor volumes (mm^3) with the standard errors were used to create the recorded growth curves.

Humanized Mice

ARTICLES

nature biotechnology

Development and function of human innate immune cells in a humanized mouse model

Anthony Rongvaux[1,10], Tim Willinger[1,10], Jan Martinek[2,3], Till Strowig[1,9], Sofia V Gearty[1], Lino L Teichmann[4,5], Yasuyuki Saito[6], Florentina Marches[2], Stephanie Halene[7], A Karolina Palucka[2], Markus G Manz[6] & Richard A Flavell[1,8]

Mice repopulated with human hematopoietic cells are a powerful tool for the study of human hematopoiesis and immune function *in vivo*. However, existing humanized mouse models cannot support development of human innate immune cells, including myeloid cells and natural killer (NK) cells. Here we describe two mouse strains called MITRG and MISTRG, in which human versions of four genes encoding cytokines important for innate immune cell development are knocked into their respective mouse loci. The human cytokines support the development and function of monocytes, macrophages and NK cells derived from human fetal liver or adult CD34$^+$ progenitor cells injected into the mice. Human macrophages infiltrated a human tumor xenograft in MITRG and MISTRG mice in a manner resembling that observed in tumors obtained from human patients. This humanized mouse model may be used to model the human immune system in scenarios of health and pathology, and may enable evaluation of therapeutic candidates in an *in vivo* setting relevant to human physiology.

Lessons Learned

DOI:10.1093/jnci/djt209
Advance Access publication September 19, 2013

REVIEWS

From Bench to Bedside: Lessons Learned in Translating Preclinical Studies in Cancer Drug Development

Christopher H. Lieu, Aik-Choon Tan, Stephen Leong, Jennifer R. Diamond, S. Gail Eckhardt

Manuscript received August 5, 2012; revised June 12, 2013; accepted June 17, 2013.

Correspondence to: Christopher H. Lieu, MD, Division of Medical Oncology, University of Colorado, MS 8117, 12801 E 17th Ave, Aurora, CO 80045 (e-mail: christopher.lieu@ucdenver.edu).

The development of targeted agents in oncology has rapidly expanded over the past 2 decades and has led to clinically significant improvements in the treatment of numerous cancers. Unfortunately, not all success at the bench in preclinical experiments has translated to success at the bedside. As preclinical studies shift toward defining proof of mechanism, patient selection, and rational drug combinations, it is critical to understand the lessons learned from prior translational studies to gain an understanding of prior drug development successes and failures. By learning from prior drug development, future translational studies will provide more clinically relevant data, and the underlying hope is that the clinical success rate will improve and the treatment of patients with ineffective targeted therapy will be limited.

J Natl Cancer Inst;2013;105:1441–1456

Take Home Message

- Cancer cell lines capture the genomic features of human cancers
- Comprehensive characterization of the cancer cell lines served as rich resources for studying human cancer biology
- Pharmacogenomics profiling in cancer cell may identify putative biomarkers of drug response for future validation